

UC Santa Cruz

UC Santa Cruz Electronic Theses and Dissertations

Title

Ontogenetic Allometry Underlies Life History Patterns of Cleaning Behavior

Permalink

<https://escholarship.org/uc/item/5vb6q7cf>

Author

Baliga, Vikram B.

Publication Date

2016

Peer reviewed|Thesis/dissertation

UNIVERSITY OF CALIFORNIA
SANTA CRUZ

**ONTOGENETIC ALLOMETRY UNDERLIES LIFE HISTORY PATTERNS
OF CLEANING BEHAVIOR**

A dissertation submitted in partial satisfaction
of the requirements for the degree of

DOCTOR OF PHILOSOPHY

in

Ecology and Evolutionary Biology

by

Vikram B. Baliga

June 2016

The Dissertation of Vikram B. Baliga is
approved:

Professor Rita S. Mehta, Chair

Professor Peter T. Raimondi

Professor Bruce E. Lyon

Tyrus Miller
Vice Provost and Dean of Graduate Studies

Copyright © by
Vikram B. Baliga
2016

Table of Contents

List of Figures and Tables	iv - vii
Abstract	viii - ix
Acknowledgements	x - xii
Statement of Contribution	xiii - xiv
Introduction	1
Chapter 1	11
Linking Cranial Morphology to Prey Capture Kinematics in Three Cleaner Wrasses: <i>Labroides dimidiatus</i> , <i>Larabicus quadrilineatus</i> , and <i>Thalassoma lutescens</i>	
Chapter 2	28
Size and shape in independent evolutions of cleaning in the Labridae and Gobiidae	
Chapter 3	81
An evolutionary approach to scaling: Phylo-allometric analyses indicate concordance between morphology and the ontogeny of cleaning behavior in wrasses	
Conclusions	129
Appendix	134
A.1 Tables S2.1 – S2.5	135 – 160
A.2 Permission for Published Material	161

List of Tables and Figures in this Dissertation

Figure i.1	4
The diversity of marine cleaner fishes	
Figure 1.1	13
Landmarks used during kinematic analyses	
Figure 1.2	15
Photographs of the external cranial morphology of three cleaner wrasses	
Figure 1.3	16
Lateral and ventral views of cranial morphology of three cleaner wrasses	
Figure 1.4	17
Lateral views of key ligaments in the feeding apparatus of three cleaner wrasses	
Table 1.1	18
Mean values for morphological data in three cleaner fishes	
Table 1.2	19
Mean values for timing variables in kinematic analyses in three cleaner fishes	
Table 1.3	19
Mean values for excursion distances and rotations in kinematic analyses in three cleaner fishes	
Figure 1.5	20
Kinematic profiles of three cleaner fishes feeding on attached invertebrates	
Table 1.4	21
PCA on kinematic variables reveals axes of variation in the feeding behaviors of three cleaner fishes	
Table 1.5	21
Hypothesis testing of all pairs of species-treatment means via MANOVA	
Figure 1.6	21
Axes of kinematic variation in prey capture as revealed by PCA for three cleaner fish species	
Figure S1.1	26
Setup for each feeding treatment	

Figure S1.2	26
Quantifying cranial elevation and girdle retraction	
Figure S1.3	27
Quantifying body orientation angle	
Figure S1.4	27
Caniniform tooth at the distal end of the alveolar process in <i>Labroides dimidiatus</i> and <i>Larabicus quadrilineatus</i>	
Figure 2.1	31
Geographic distributions of obligate cleaner fishes	
Table 1.2	37
Information on model selection for each gene region in two phylogenetic analyses	
Table 2.2	38
Fossil and biogeographic information used for divergence time estimation in BEAST	
Figure 2.2	43
Landmarks used during geometric morphometric analyses	
Figure 2.3	48
The evolution of obligate cleaning	
Table 2.3	51
Parameter estimates for models fit to log-transformed total length	
Figure 2.4	53
Distributions of the likelihood ratio statistic for evolutionary model comparisons	
Figure 2.5	55
Phenograms of body size evolution in gobiids and labrids	
Figure 2.6	57
Phylomorphospace of Western Atlantic gobies	
Figure 2.7	59
Phylomorphospace of labrids	
Figure 2.8	61
Combined phylomorphospace of gobiid and labrid taxa	
Table 2.4	63
Metrics of convergence among cleaners within each phylomorphospace	

Figure 2.9	65
Group-specific misclassifications	
Table 2.5	67
Loadings of PC axes in pFDA	
Figure 2.10	69
Phylogenetical Flexible Discriminant Analysis of geometric morphometric data	
Figure 3.1	87
Phylogenetic relationships between species sampled in the present study	
Figure 3.2	88
Measurements used in the present study	
Figure 3.3	96
Juvenile phylomorphospace	
Figure 3.4	98
Phylo-allometric space for 33 species of wrasses	
Table 3.1	99
Loadings of traits in the juvenile morphospace	
Table 3.2	99
Loadings of traits in phylo-allometric space	
Figure 3.5	101
Discriminant axes for 33 species of wrasses	
Table 3.3	102
Confusion matrix from pFDA performed on ontogenetic scaling vectors	
Table S3.1	117
Specimens in the present study	
Table S3.2	119
Traits measured on specimens in the present study	
Table S3.3	121
Loadings of traits in the adult morphospace	
Table S3.4	122
P-values from phylogenetically-informed ANOVAs	

Table S3.5	123
Coefficients from pFDA performed on ontogenetic scaling vectors	
Table S3.6	124
Phylogenetically-informed MANOVA of pFDA scores	
Table S3.7	126
Slopes from Standardized Major Axis regressions of each trait vs. standard length	
Table S2.1	135
GenBank Accession IDs of sequences used in this study for 45 gobiid species	
Table S2.2	139
GenBank Accession IDs of sequences used in this study for 10 gobiid outgroup species	
Table S2.3	140
GenBank Accession IDs of sequences used in this study for 320 labrid species	
Table S2.4	158
GenBank Accession IDs of sequences used in this study for 20 species set as outgroup to the labrids	
Table S2.5	160
GenBank Accession IDs of sequences used in this study for 5 species set as outgroup to the gobiids and labrids	

Abstract

ONTOGENETIC ALLOMETRY UNDERLIES LIFE HISTORY PATTERNS OF CLEANING BEHAVIOR

Vikram B. Baliga

Studies have shown that ontogenetic shifts in ecology often drive adaptive changes in the scaling of musculoskeletal systems, resulting in differential performance. These support the idea that allometric changes in morphology often co-occur with changes in feeding strategies, locomotor behavior or habitat use. Fewer studies, however, have compared the ontogenetic trajectories of functional traits across closely related species to better understand the extent to which such patterns of scaling may be specifically adaptive during a particular life history stage. A confound, however, is that phylogenetic information is inherently present in development; phenotypic evolution occurs via modification of ancestral development patterns. Thus, a phylogenetically-informed approach that makes comparisons among species' ontogenetic scaling patterns can make important contributions to our understanding of morphological diversity among species. Presently, studies using such an approach are absent in the literature. I use the evolution of cleaning behavior as a model system to understand how ontogenetic scaling patterns contribute to macroevolutionary patterns of morphological and ecological diversity. I first identify general head and body characteristics that were associated with the evolution of

cleaning: an elongate body paired with an elongate head, and a terminal mouth that allows jaws with low mobility to bite rapidly on individually-targeted prey items. My “phylo-allometric” analyses then enable me to show evidence that the repeated evolution of facultative and obligate cleaning (in which taxa continue to clean as adults) is associated with the maintenance of characters over ontogeny that are conducive to cleaning in the juvenile phase. On the other hand, taxa that transition away from cleaning during ontogeny do not maintain such characters, and exhibit phenotypic trajectories that are distinct from those of other wrasses. This indicates that the recurring evolution of juvenile cleaning behavior in the Labridae has involved similar effects on developmental scaling patterns. The repeated evolution of each of these patterns shows that labrid scaling trajectories are fundamentally labile and appear to evolve adaptively to changing ecological pressures over ontogeny.

Acknowledgements

I thank my advisor, Dr. Rita S. Mehta, for her support throughout my graduate career. I am truly honored to be her first doctoral student. Rita's dedication to her students has been exceptional, as she offers immense support and encouragement not only for academic pursuits, but also for our personal goals. Throughout my time as a graduate student in her lab, Rita has brought unique and creative insights to our discussions, which tremendously influenced the trajectory of my research.

I also thank members of my dissertation reading committee: Dr. Peter T. Raimondi and Dr. Bruce E. Lyon. Both Pete and Bruce offered extremely valuable guidance in methodological aspects, and helped me frame some of my work in a way that would be broadly accessible. In addition, Dr. Peter C. Wainwright provided tremendous insights on reef fish evolution, morphological and functional diversity, and macroevolutionary methods during my advancement to candidacy and in several additional conversations over the years.

I am deeply indebted to several undergraduates, high school students, and teachers who assisted me in collecting data over the years. In no particular order, I thank: Michellé Mac, Katheryn Pelon, Kate Galloway, Tiffany Portulano, Sarah Baumgart, Burnne Yew, Satina Ciandro, Dan Johnston, Elora Pradhan, O'Brian Santos, Shannon Templeton, and Andrea Longoria.

A large proportion of morphological specimens featured in Chapters 2 and 3 were obtained thanks to loans from museum collections managers. Often, my sampling entailed dissection and/or clearing & staining of specimens, both of which are forms of ‘destructive’ sampling. I am thus extremely thankful for the contributions these collections managers made in support of my research: Jeff Williams (Smithsonian National Museum of Natural History), Rick Feeny (LA County Museum of Natural History), Dave Catania (California Academy of Sciences), and G Zora (Paris Museum of Natural History).

A majority of my research was conducted thanks to financial support from the following awards: the Rosemary Grant Award for Graduate Student Research from the Society for the Study of Evolution; the Society for Integrative and Comparative Biology (SICB) Grant-in-Aid of Research Award; the Friends of the Long Marine Lab Student Research and Education Award; the Dr. Earl H. Myers & Ethel M. Myers Oceanographic & Marine Biology Trust Award; the UC Santa Cruz Graduate Student Association Travel Grant; and the UCSC Outstanding Teaching Assistant Award Ecology and Evolutionary Biology.

I want to thank all of the members of the Mehta Lab, past and present. Dr. Dave Collar and Dr. Josh Reece, as postdoctoral researchers in the lab, provided me with extremely valuable guidance during my first few years of graduate school. In addition to the numerous undergraduate research assistants I thanked above, I want to acknowledge two additional undergraduates who made my graduate tenure all the

more fun: Leith Miller and Jacob Harrison. The two of you will go on to do extraordinary things. My fellow graduate students Ben Higgins, Chris Law, and Sarah Kienle have been amazing peers and really made the lab a fun, collegial, and often silly place. I hope you guys keep toasting with gummy bears anytime there is reason to celebrate. May the tradition live on!

I thank many friends and family who gave me emotional and/or financial support over the years. My parents' attitudes towards education and intellectual pursuits have been vital to the formation of my own values as an adult. I thank them for their support and encouragement during my time in grad school. A number of fellow grad students made working at LML a blast: Gary Longo, Brent Hughes, Claudio Rojas-Leyton, Ben Weitzman, Sarah Peterson, Kristin de Nesnera, Max Tarjan, Caleb Bryce, Jimmy O'Donnell, Justin Cummings, and many others. A few of my peers in the Economics program, Arseni Skaperdas, Cheyney O'Fallon, and Matt Baumer, and our brother in Physics, Angelo Monteaux, really made my time in Santa Cruz special.

And finally, I want to express deep gratitude to Juliet Oshiro. I often tell people that attending grad school was the best decision I ever made. Frankly, that's because doing so brought you (and Chewie!) into my life. I cannot imagine how I'd have gotten through all this without you. I am thankful for the many adventures we've had thus far, and I am looking forward to whatever the next chapter brings.

Statement of Contribution

The text of this dissertation includes reprints of the following previously published material:

Chapter 1:

Baliga VB and Mehta RS. 2015. Linking Cranial Morphology to Prey Capture Kinematics in Three Cleaner Wrasses: *Labroides dimidiatus*, *Larabicus quadrilineatus*, and *Thalassoma lutescens*. *Journal of Morphology*. 276, 1377–91. doi:10.1002/jmor.20425.

For this chapter, I was responsible for the majority of the laboratory work, data analyses, manuscript preparation, and submission. The co-author listed in this publication, Rita Mehta, directed and supervised the research which forms the basis for the dissertation.

In addition, the Introduction and Conclusion contain segments of text from the following previously published work:

Baliga VB and Mehta RS. 2014. Scaling patterns inform ontogenetic transitions away from cleaning in *Thalassoma* wrasses. *The Journal of Experimental Biology*. 217, 3597-3606. doi:10.1242/jeb.107680.

Baliga VB and Law CJ. 2016. Cleaners among wrasses: Phylogenetics and evolutionary patterns of cleaning behavior within Labridae. *Molecular Phylogenetics and Evolution*. 94A, 424-435. doi:10.1016/j.ympev.2015.09.006.

In Baliga and Mehta (2014), I was responsible for the majority of the laboratory work, data analyses, manuscript preparation, and submission. The co-author listed in

this publication, Rita Mehta, directed and supervised the research which forms the basis for the dissertation.

In Baliga and Law (2016), I was responsible for the majority of the laboratory work, data analyses, manuscript preparation, and submission. The co-author listed in this publication, Chris Law, assisted with data analyses. A signed statement of permission from my collaborator is available in the Appendix (section A.2).

Introduction

Across the Tree of Life, there is remarkable disparity among clades in both species richness and morphological diversity. A central goal of evolutionary morphology is to understand why some groups of species are phenotypically constrained while others are more variegated. Studies of ecomorphology provide valuable insights on the relationships among morphology, performance, and ecology in species, which in turn help us understand the generation and maintenance of diversity (Bock and Van Walhert 1965; Arnold 1983; Wainwright and Reilly 1994).

Prey acquisition is a critical animal behavior, as vertebrate organisms must apprehend and consume food to survive. Through studies of ecomorphology, it is clear that the functional demands of feeding affect the evolution of diversity in the vertebrate skull (Bock 1977; Liem 1980; Wainwright and Reilly 1994; Herrel et al. 1998; Santana and Dumont 2009; Collar et al. 2014). Additionally, the consequences of overall size on the structure and function of organismal systems are pervasive (McMahon 1984; Schmidt-Nielson 1984) and influence trophic niche. For example, in the North American fresh water clade, Centrarchidae, piscivory constrains morphological diversification of the skull while highly piscivorous fishes exhibit some of the largest maximum body sizes within the Centrarchidae. Therefore, it is not surprising that a central focus of functional morphology studies is to understand how the scaling of the musculoskeletal system influences the scaling of functional traits, such as the feeding apparatus, across ontogeny.

Several studies have argued that ontogenetic shifts in ecology often drive adaptive changes in the scaling of musculoskeletal systems, resulting in differential performance (McMahon 1984; Richard and Wainwright 1995; Deban and O'Reilly 2005; Herrel and Gibb 2006; Pfaller et al. 2011). These studies, in turn, support the idea that allometric changes in morphology often co-occur with changes in feeding strategies, locomotor behavior or habitat use. Fewer studies, however, have compared the ontogenetic trajectories of functional traits across closely related species to better understand the extent to which such patterns of scaling may be specifically adaptive during a particular life history stage (but see Mitteroecker et al. 2004; Herrel and O'Reilly 2006; Frédérick and Sheets 2009; Wilson and Sánchez-Villagra 2010).

A confound, however, is that phylogenetic information is inherently present in development; phenotypic evolution occurs via modification of ancestral development patterns (Gould 1977). Thus, a phylogenetically-informed approach that makes comparisons among species' ontogenetic scaling patterns can make important contributions to our understanding of morphological diversity among species. Presently, studies using such an approach are absent in the literature and a central goal of this dissertation is to provide a framework in which both ontogeny and phylogeny are incorporated upon examining behavioral innovations.

I use the evolution of cleaning behavior as a model system to understand how ontogenetic scaling patterns contribute to macroevolutionary patterns of morphological and ecological diversity. Cleaning behavior, otherwise known as “ectoparasitivory”, provides us with the opportunity to examine both the patterns of

scaling of phenotypic traits and shifts in feeding ecology within clades of fishes. In fishes, cleaning is a mutualistic behavior wherein an individual consumes ectoparasites (generally juvenile gnathiid or cymothoid isopods) off other organisms. The presence of cleaners in a habitat can have tremendous ecological consequences. For instance, experimental removal of the bluestreak cleaner wrasse (*Labroides dimidiatus*) has been shown to affect the behavior, recruitment dynamics, and sizes of client fishes (Waldie et al. 2011). This behavior not only relies on the ability of client species to recognize cleaners but also requires that cleaners possess morphological, functional and behavioral traits that are necessary to find and remove ectoparasites.

Cleaner fishes can be categorized by whether they perform the behavior 1) predominately as juveniles, 2) facultatively throughout ontogeny, or 3) obligately (Côté 2000). Over two-thirds of fishes that clean do so predominately as juveniles (Côté 2000), exhibiting ontogenetic transitions away from cleaning behavior (Fig i.1). While these species are referred to as ‘facultative (juvenile) cleaners’ in the literature (e.g. Côté 2000), for simplicity I hereafter refer to these species as ‘juvenile’ cleaners.

Obligate cleaners are more conspicuous (although infrequent from an evolutionary perspective) and most of what is known about cleaning behavior has been determined through observing species in the obligate cleaner genus *Labroides*. For example, *L. dimidiatus* commonly maintains “cleaning stations”, small areas that attract visiting “client” organisms (Youngbluth 1968). In *L. dimidiatus*, cleaning interactions often begin with the cleaner fish approaching a potential client and presenting itself by swimming in a vertical oscillatory pattern (Randall 1958; Gorlick

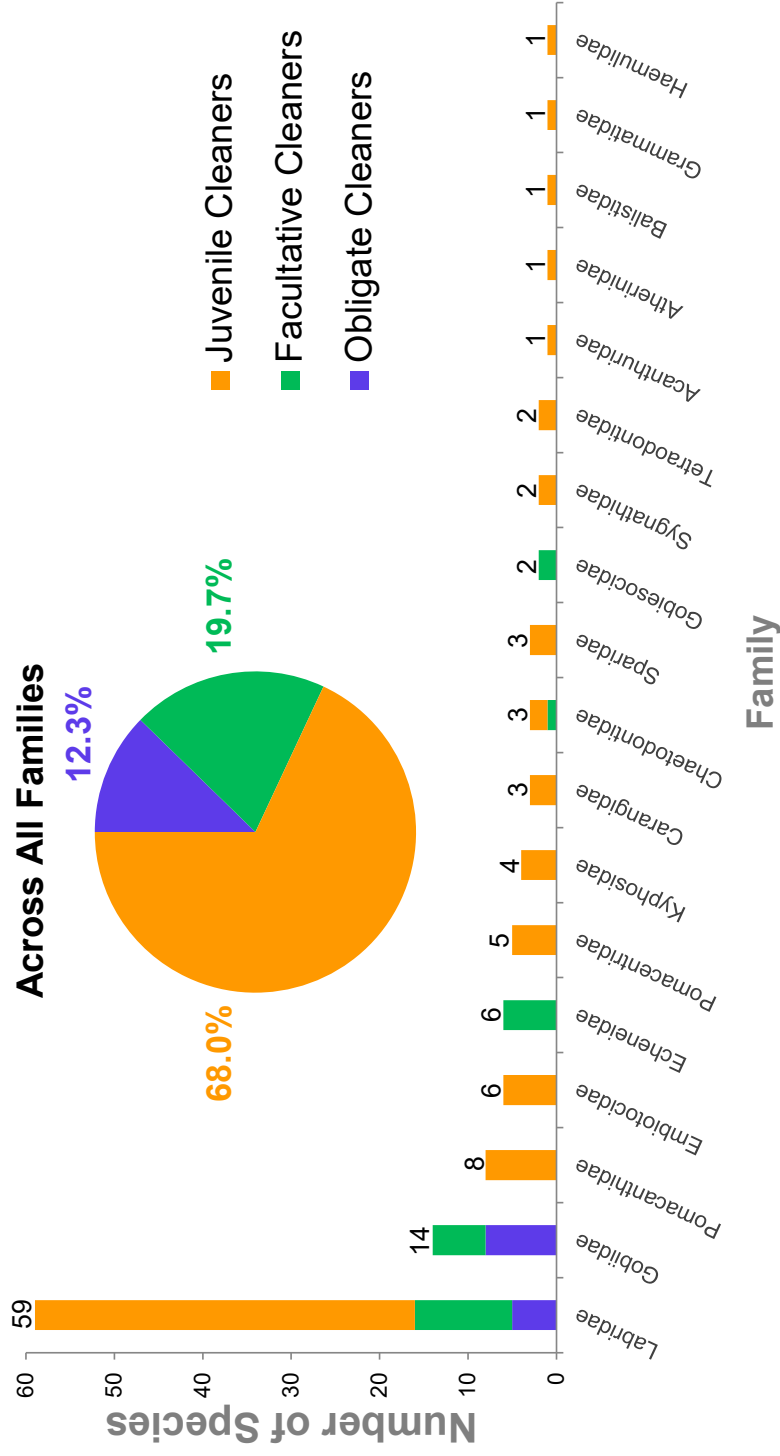


Fig. i.1 – The Diversity of Marine Cleaner Fishes. The number of cleaner fishes within families of marine fishes is shown. Data are taken from Côté (2000) and Baliaga and Law (2016). The pie chart (insert) depicts the proportions of juvenile, facultative and obligate cleaners when all cleaner species in all families are pooled. Colors correspond to dietary categories: orange – juvenile cleaner; green – facultative cleaner; purple – obligate cleaner.

et al. 1978). A receptive client will then pose to solicit cleaning by holding still in the water column, spreading its pectoral and pelvic fins, opening its jaws, and flaring its opercula laterally (Losey 1972; Côté et al. 1998). The cleaner will dart around the client's body as it picks off ectoparasites, most commonly gnathiid isopod larvae (Grutter 1996) that may be embedded in the fins, gills, buccal cavity, and pharyngeal chamber of the client (Grutter 1996; Côté 2000; Grutter 2010).

Cleaning is not exclusive to labrids; in fact, at least 18 marine families of fishes include at least one member that cleans (Fig i.1). Côté (2000) provides an extensive list of cleaner fishes. Baliga and Law (2016) found 59 species of labrids engage in cleaning. This is four times as many species as in the next highest group the Gobiidae, within which 14 species of cleaners are recognized. This suggests cleaner fish species richness is not directly proportional to clade diversity, especially when considering the Gobiidae has close to 2,000 extant members. Furthermore, of the various groups of marine fishes in which cleaning is found, the overwhelming majority contain five or fewer species that clean (Côté, 2000). These metrics underscore the exceptional diversity of labrid cleaners, marking labrids as a model clade within which to explore the evolution of cleaning.

In order to answer the question of how ecological (e.g. dietary) shifts can influence the evolution of scaling patterns, an informative suite of traits first needs to be determined. After all, the measure of a species' ontogenetic trajectory is defined by the traits from which it is composed. While cleaner fishes have been examined as model system in behavioral economics and ecology, little is known about the

functional morphology of feeding in these species. Additionally, the topological and temporal patterns of cleaner evolution need to be established. In this dissertation, I employ studies of functional and evolutionary morphology and to ultimately carry out macroevolutionary comparisons of the evolution of scaling patterns.

In my first chapter, I investigate the cranial morphology and kinematics of feeding in three species of labrid cleaner fishes. This investigation, which is the first to document the functional morphology of feeding in cleaners, provides an understanding of the characters associated with ectoparasitivism. The species investigated are *Labroides dimidiatus* (obligate cleaner), *Larabicus quadrilineatus* (juvenile cleaner), and *Thalassoma lucasanum* (juvenile cleaner). Through high-speed videography, I recorded prey capture in these taxa using two feeding treatments: 1) suspended client fishes and 2) attached invertebrates.

My second chapter takes a macroevolutionary approach to examine shape diversity across cleaner fishes. In this chapter I compare shape evolution in members in the Labridae and Gobiidae. Labrids and gobiids provide an excellent comparison as these clades contain the only known evolutions of obligate cleaning. I first use Bayesian methods to infer a phylogeny for a clade of Western Atlantic gobies, and then using stochastic character mapping methods, I infer transitions in the evolution of cleaning behavior. Phylogenetic inference of taxonomic relationships between the Labridae, as well as inferences of the temporal and topological aspects of cleaning evolution, are covered in Baliga and Law (2016), which produced valuable phylogenetic background for this dissertation chapter. Some of the analyses in Baliga

and Law (2016), however, have been revised in this chapter in light of new information on labrid cleaners. I then use Bayesian methods to infer a single phylogeny for the Western Atlantic gobies and a group of 320 labrid fishes in order to aid me in analyses of gobiid and labrid morphology. Through geometric morphometrics, I quantify body shape in both gobiid and labrid taxa. I then use the gobiid and labrid phylogeny, along with the morphometric data, to generate a combined phylomorphospace for both families, along with separate, family-specific phylomorphospaces. Finally, I examine the extent of convergence among cleaners within and across each of these families.

My third chapter provides methods for examining ontogenetic trajectories in a phylogenetically-informed framework. Using the evolution of labrid cleaning as a case study, I collect ontogenetic series of specimens for 33 labrids (18 cleaners and 15 closely-related non-cleaners). Informed by the patterns I uncovered in Chapters 1 and 2, I measure morphological traits of the body, fins, and cranial skeleton in each ontogenetic series. I then generate a phylogenetically-informed allometric space, or “phylo-allometric space”, that captures the diversity of ontogenetic trajectories while accounting for relationships between taxa. I also use phylogenetic discriminant analysis to understand whether the trajectories of obligate cleaners, facultative cleaners, juvenile cleaners, and non-cleaners can be discerned from each other. These comparative methods ultimately allow me to assess whether the ontogeny of cleaning behavior in wrasses is concordant with ontogenetic patterns of morphology.

1.2 References

- Arnold S.J. 1983. Morphology, performance and fitness. *Am. Zool.* 23: 347-361.
- Baliga V.B., Law C.J. 2016. Cleaners among wrasses: Phylogenetics and evolutionary patterns of cleaning behavior within Labridae. *Mol. Phyl. Evol.* 94, 424-435. (doi:10.1016/j.ympev.2015.09.006)
- Bock W. 1977. Toward an ecological morphology. *Vogelwarte* 29: 127-135.
- Bock W., Van Walhert J. 1965. The role of adaptive mechanisms in the origin of higher levels of organisation. *Sys. Biol.* 14(4): 272-287.
- Collar D.C., Quintero M., Buttler B., Ward A.B., Mehta RS. 2016. Body shape transformation along a shared axis of anatomical evolution in labyrinth fishes (Anabantoidei). *Evolution.* 70:555-67.
- Côté I.M. 2000. Evolution and Ecology of Cleaning Symbioses in the Sea. *Oceanogr. Mar. Biol. Annu. Rev.* 38, 311–355.
- Côté, I.M., Arnal C., Reynolds J.D. 1998. Variation in posing behaviour among fish species visiting cleaning stations. *J Fish Biol.* 53, Suppl. A, 256-266.
- Deban S.M., O'Reilly J.C. 2005. The ontogeny of feeding kinematics in the giant salamander *Cryptobranchus alleganiensis*: does current function or phylogenetic relatedness predict the scaling patterns of movement? *Zool.* 108: 155-167.
- Frédérich B., Sheets H.D. 2009. Evolution of ontogenetic allometry shaping giant species: a case study from the damselfish genus *Daschyllus* (Pomacentridae). *Bio. J. Linn. Soc.* 99, 99-117. (doi:10.1111/j.1095-8312.2009.01336.x)
- Gorlick D.L., Atkins P.D., Losey G.S. 1978. Cleaning stations as watering holes, garbage dumps, and sites for the evolution of reciprocal altruism? *Am. Nat.* 112: 341-353.
- Gould S.J. 1977. *Ontogeny and Phylogeny*. Cambridge, Massachusetts: The Belknap Press of Harvard University Press. ISBN 0-674-63940-5.
- Grutter A.S. 1996. Parasite removal rates by the cleaner wrasse *Labroides dimidiatus*. *Mar. Ecol. Prog. Ser.* 130, 61–70.
- Grutter A.S. 2010. Cleaner fish. *Curr. Biol.* 20, 547–549. doi:10.1016/j.cub.2010.04.013
- Herrel A., Aerts P., De Vree F. 1998. Ecomorphology of the lizard feeding apparatus: a modelling approach. *Neth. J. Zool.* 48(1): 1-25.

- Herrel A., Gibb A.C. 2006. Ontogeny of performance in vertebrates. *Physiol. Biochem. Zool.* 79, 1-6.
- Herrel A., O'Reilly J.C. 2006. Ontogenetic scaling of bite force in lizards and turtles. *Physiol Biochem. Zool.* 79, 31-42. (doi:10.1086/498193)
- Liem K.F. 1980. Adaptive significance of intra- and interspecific differences in the feeding repertoires of cichlid fishes. *Am. Zool.* 20: 295-314.
- Losey G.S. 1972. The Ecological Importance of Cleaning Symbiosis. *Copeia* 1972(4), 820–833.
- McMahon T.A. 1984. *Muscles, Reflexes, and Locomotion*. Princeton: Princeton University Press.
- Mitteroecker P., Gunz P., Bernhard M., Shaefer K., Bookstein F.L. 2004. Comparison of cranial ontogenetic trajectories among great apes and humans. *J. Hum. Evol.* 46, 679-698. (doi:10.1016/j.jhevol.2004.03.006)
- Pfaller J.B., Gignac P.M., Erickson G.M. 2011. Ontogenetic changes in jaw-muscle architecture facilitate durophagy in the turtle *Sternotherus minor*. *J. Exp. Biol.* 214(Pt 10), 1655–1667.
- Randall J.E. 1958. A Review of the Labrid Fish Genus *Labroides*, with Descriptions of Two New Species and Notes on Ecology. *Pac. Sci.* 12, 327–347.
- Richard B.A., Wainwright P.C. 1995. Scaling the feeding mechanism of largemouth bass (*Micropterus salmoides*): kinematics of prey capture. *J. Exp. Biol.*, 198, 419–433.
- Santana S.E., Dumont E.R. 2009. Connecting behaviour and performance: The evolution of biting behaviour and bite performance in bats. *J Evol. Biol.* 22 (11): 2131-2145.
- Schmidt-Nielson K. 1984. *Scaling: Why is Animal Size so Important?* Cambridge: Cambridge University Press.
- Wainwright P.C., Reilly S.M. 1994. (editors) *Ecological morphology: integrative organismal biology*. Chicago, University of Chicago Press.
- Waldie P.A., Blomberg S.P., Cheney K.L., Goldizen A.W., Grutter A.S. 2011. Long-Term Effects of the Cleaner Fish *Labroides dimidiatus* on Coral Reef Fish Communities. *PLoS ONE* 6(6): e21201. doi:10.1371/journal.pone.0021201
- Wilson L.A.B., Sánchez-Villagra M.R. 2010. Diversity trends and their ontogenetic basis: an exploration of allometric disparity in rodents. *Proc. R. Soc. B.* 277, 1227-1234. (doi:10.1098/rspb.2009.1958)

Youngbluth M.J. 1968. Aspects of the ecology and ethology of the cleaning fish,
Labroides phthirophagus Randall. Z. Tierpsychol. 25, 915-932.

Chapter 1

Linking Cranial Morphology to Prey Capture Kinematics in Three Cleaner Wrasses: *Labroides dimidiatus*, *Larabicus quadrilineatus*, and *Thalassoma lutescens*

Vikram B. Baliga* and Rita S. Mehta

Department of Ecology and Evolutionary Biology, Long Marine Laboratory, University of California Santa Cruz, Santa Cruz, California 95060

ABSTRACT Cleaner fishes are well known for removing and consuming ectoparasites off other taxa. Observers have noted that cleaners continuously “pick” ectoparasites from the bodies of their respective client organisms, but little is known about the kinematics of cleaning. While a recent study described the jaw morphology of cleaners as having small jaw-closing muscles and weak bite forces, it is unknown how these traits translate into jaw movements during feeding to capture and remove ectoparasites embedded in their clients. Here, we describe cranial morphology and kinematic patterns of feeding for three species of cleaner wrasses. Through high-speed videography of cleaner fishes feeding in two experimental treatments, we document prey capture kinematic profiles for *Labroides dimidiatus*, *Larabicus quadrilineatus*, and *Thalassoma lutescens*. Our results indicate that cleaning in labrids may be associated with the ability to perform low-displacement, fast jaw movements that allow for rapid and multiple gape cycles on individually targeted items. Finally, while the feeding kinematics of cleaners show notable similarities to those of “picker” cyprinodontiforms, we find key differences in the timing of events. In fact, cleaners generally seem to be able to capture prey twice as fast as cyprinodontiforms. We thus suggest that the kinematic patterns exhibited by cleaners are indicative of picking behavior, but that “pickers” may be more kinematically diverse than previously thought. *J. Morphol.* 276:1377–1391, 2015. © 2015 Wiley Periodicals, Inc.

KEY WORDS: cleaner fish; kinematics; morphology; cleaning behavior; picking

INTRODUCTION

In fishes, cleaning behavior is a mutualistic service that involves the consumption of ectoparasites off other taxa. Over 120 species of teleost fishes exhibit cleaning behavior, and cleaners are spread across 18 marine families (Côté, 2000; Froese and Pauly, 2015). The majority of cleaner fishes (at least 75 species) exhibit cleaning behavior predominately as juveniles, transitioning from this feeding strategy over ontogeny (Côté, 2000; Froese and Pauly, 2015).

Why certain species clean as juveniles while others do not is poorly understood. A recent study

that examined cleaners and non-cleaning close relatives revealed that as juveniles, cleaners possess weak jaws with low mobility, among other traits. As cleaner fishes grow, they show positive allometry for many traits functionally related to feeding, which may facilitate transitions away from cleaning into adulthood (Baliga and Mehta, 2014).

How distinct the prey capture kinematics of cleaning are from other well-documented prey capture behaviors in fishes is not clear. We predict cleaners to possess not only morphological adaptations, but also specialized jaw movements during feeding to capture and remove ectoparasites embedded in their clients. Workers have informally described cleaners as continuously “picking” ectoparasites from the bodies of their respective client organisms (Darcy et al., 1974; Losey et al., 1994). The functional morphology of cleaning, however, has not been systematically studied, and kinematic details of prey acquisition have yet to be uncovered.

Others have used the term “picking” to describe a form of manipulation in some cichlids (Liem, 1979), or a form of prey capture by biting in embiotocids and labrids (Horn and Ferry-Graham, 2006). Here, a predator’s precise and repeated movements of its upper jaws allow protruding teeth to be used as a prehensile tool used to dislodge small, sessile prey from a substrate (Liem,

Additional supporting information may be found in the online version of this article.

*Correspondence to: Vikram B. Baliga; 150B Center for Ocean Health, Long Marine Laboratory, Santa Cruz, CA 95060. E-mail: vbaliga@ucsc.edu

Conflict of Interest: The authors have no conflicts of interest to declare.

Received 6 March 2015; Revised 3 June 2015; Accepted 11 July 2015.

Published online 12 August 2015 in Wiley Online Library (wileyonlinelibrary.com). DOI 10.1002/jmor.20425

1979). In Cyprinodontiformes, “picking” is also used to describe precisely controlled and coordinated “forceps-like” movements of the upper and lower jaws (Ferry-Graham et al., 2008; Hernandez et al., 2009). In contrast to other forms of biting, cyprinodontiform picking involves the selective acquisition of individual prey items (small invertebrate prey) from the substrate or water column, while other items are left behind (Hernandez et al., 2008). The fine-tuned precise movements underlying the picking behavior in cyprinodontiform taxa are associated with a morphological novelty in the premaxillomandibular ligament connecting the upper and lower jaws (Hernandez et al., 2008).

Whether picking in cleaner fishes is similar to the picking behavior observed in other taxa is unknown and can only be determined through kinematic studies. We hypothesize that cleaner fishes employ a similar feeding strategy, using precise, coordinated movements of the jaws, leading to the removal of targeted items from a client’s body while leaving little room for error in haphazardly biting into the client itself. Whether morphological novelties have evolved in association with cleaning has not been determined.

The mostly coral reef-associated clade Labridae (wrasses and parrotfishes) contains more known cleaner fish species than in any other group (Côté, 2000; Froese and Pauly, 2015). We report on the cranial morphology and kinematic patterns of feeding of three labrids: *Labroides dimidiatus* (Valenciennes, 1839), *Larabicus quadrilineatus* (Rüppell, 1835), and *Thalassoma lutescens* (Lay and Bennet, 1839). Of these three species, only *L. dimidiatus* is described as an obligate cleaner fish; it is known to clean throughout ontogeny, and obtains >85% of its dietary items through cleaning (Côté, 2000). The monotypic *L. quadrilineatus* is a close relative of *L. dimidiatus*; as shown in Cowman and Bellwood (2011), this species is immediately sister to the monophyletic group containing all the *Labroides* taxa. Unlike its close relatives in *Labroides*, *Larabicus* is reported to be a facultative (juvenile) cleaner (Côté, 2000), and has been shown to undergo an ontogenetic transition away from cleaning as it enters adulthood (Randall and Springer, 1975; Randall, 1986). The size at which this shift occurs is not precisely known. Cole (2010) found that in the closely related *Diproctacanthus xanthurus* and *Labropsis alleni*, a precipitous decrease in cleaning occurs when these species reach approximately 35 and 45 mm standard length, respectively. Given that *Larabicus*, *Diproctacanthus*, and *Labropsis* all transition away from cleaning to obligate corallivory in adulthood, and each attains a similar maximum adult size, it is reasonable to assume that the transition away from cleaning also occurs around 35–45 mm standard length in *Larabicus*. Similarly, *T. lutescens* is a facultative (juvenile) cleaner (Côté, 2000). This species is more distantly

related to the other taxa in this study, and is one of several *Thalassoma* species that cleans facultatively (Côté, 2000; Baliga and Mehta, 2014). *T. lutescens* exhibits a dietary shift away from cleaning as it enters adulthood (McCourt, 1984), which was recently found to be at approximately 85-mm standard length (Baliga and Mehta, 2014).

While the cranial morphology of the obligate cleaner *L. dimidiatus* has been described previously (Tedman, 1980a,b), a more generalized view of cleaner fish morphology is lacking. Furthermore, it has not been established how the morphology of cleaner fishes relates to the kinematic patterns they exhibit. Our goals were thus to 1) describe the morphology of cleaner fishes in Labridae and 2) document the kinematics of feeding in these taxa.

MATERIALS AND METHODS

Species

We gathered all data from juvenile individuals of three cleaner fishes in the Labridae: *L. dimidiatus* (Valenciennes, 1839) (standard length [SL] = 40.25–60.12 mm), *L. quadrilineatus* (Rüppell, 1835) (SL = 36.12–52.42 mm), and *T. lutescens* (Lay and Bennet, 1839) (SL = 50.20–83.98 mm). We examined juvenile individuals (identified by size and coloration pattern) because two of the species of interest clean facultatively as juveniles, while *L. dimidiatus* is an obligate cleaner, cleaning throughout its life history. We obtained all individuals ($n = 5$ per species, 15 individuals total) through the aquarium trade. We housed and filmed animals at the Long Marine Laboratory, University of California, Santa Cruz (IACUC #1009).

Collection of Kinematic Data

We used a Photron FASTCAM SA3 high-speed video camera (Photron, Tokyo) fitted with a macro lens to record each individual’s feeding behaviors at 1,000 frames/sec in $1,024 \times 1,024$ resolution. All individuals were subject to each of two feeding treatments: 1) suspended client fishes and 2) attached invertebrates. We recorded feeding behaviors only after individuals were fully accustomed to feeding in each treatment type (typically 2–4 days). After each feeding trial, we recorded a still image of a ruler placed in the water column, for scale, without adjusting the camera’s position, focus, or zoom level.

For the suspended client fishes treatment, we first euthanized individuals of *Chromis viridis* and *Dascyllus reticulatus* purchased from the aquarium trade, and wild-caught *Oxyjulis californica*. We then immediately froze them to preserve the mucus coating and/or ectoparasite loads on these potential client fishes. During feeding trials, we randomly selected a potential client and suspended it in the water column using a wire (Supporting Information S-Fig. 1A). Over the course of our study, we presented each individual cleaner fish with at least three individuals of each species of client fish. We presented each suspended client to the cleaner for no more than 7 min in order to mimic a typical maximum duration of such interactions in the wild (Hobson, 1971; Grutter, 1995; Grutter, 1996; Cole, 2010).

For the attached invertebrates treatment, we fed all individuals a mix of bloodworms and mysis shrimp attached to a substrate. We combined thawed mixtures of these prey items and then manually embedded the prey onto a wire mesh. We then suspended this wire mesh into the water column for feeding (Supporting Information S-Fig. 1B).

We digitized a total of 138 feeding sequences using the program Tracker 4.87 (Brown, 2009). For the attached

invertebrates treatment, we analyzed a total of 90 sequences (six sequences per individual fish). For the suspended client fishes treatment, we analyzed a total of 48 sequences (six sequences per individual fish), because not every individual cleaner fish engaged in cleaning during these trials. We only analyzed sequences in which 1) a successful strike occurred, 2) we were able to capture a completely lateral view of the feeding event, and 3) the fish's cranial axis was perpendicular to the camera. We considered trials successful when a fish removed an ectoparasite, scale, or some detritus from the suspended client, or a piece of bloodworm or shrimp from the wire mesh. We defined time zero (t_0) as the onset of the strike: the frame previous to that which showed initial jaw opening. We defined the end of the strike as the frame in which the jaws returned to their initial, prefeeding positions.

To quantify kinematic variables, we used seven landmarks on the external anatomy of the fish, following a slight modification of the procedure used by Ferry-Graham et al. (2002) on other labrids. These homologous landmarks (Fig. 1) were: 1) the anterior tip of the premaxilla, 2) the posterior margin of the nasal bone, 3) the (approximate) point of articulation between the hyomandibula and the neurocranium, 4) the dorsal margin of the insertion of the pelvic fin, 5) the anteroventral protrusion of the hyoid, 6) the (approximate) articulation of the lower jaw with the quadrate (i.e., the jaw joint), and 7) the anterior tip of the dentary (lower jaw). Using automated object tracking in Tracker (which we manually checked for error), we then used changes in the positions of these landmarks to gather data for three displacement variables, three angular variables, and eight timing variables. We digitized landmarks in every frame, and thus, we calculated all variables at every 1-ms interval.

The displacement variables we calculated were gape distance, premaxillary protrusion, and hyoid depression (all to the nearest 0.01 mm). We defined gape distance as the estimated distance between upper and lower jaw tips (Points 1 and 7 in Fig. 1). We calculated premaxillary protrusion as the net change in straight-line distance between the upper jaw tip and the posterior margin of the nasal bone (Points 1 and 2 in Fig. 1). We calculated hyoid displacement as the net change in straight-line distance between the anteroventral protrusion of the hyoid and the approximate point of articulation of the hyomandibula with the neurocranium (Points 3 and 5 in Fig. 1).

We calculated the three angular variables (in degrees): lower jaw rotation, cranial elevation, and girdle rotation. We defined each of these variables as the net change in an angle relative to its starting position at time t_0 . Because there was minimal rotation in Point 3, we used it as a reference point. The angle we used to calculate lower jaw rotation was measured using Points 3, 6 (vertex), and 7 (Fig. 1). For cranial elevation, we calculated the angular rotation of Point 2 with respect to Point 3. We defined girdle rotation as the angular rotation of Point 4 with respect to Point 3 (Supporting Information S-Fig. 2). In calculating both cranial elevation and girdle rotation, we used an additional point to define the angular rotations. This additional point did not correspond to a discrete landmark. Rather, it varied across videos, but was chosen to be a point on the fish's body that 1) did not rotate, and 2) we could reliably find in each frame of the video. While we were interested in capturing the degree of pectoral girdle retraction, we found that the flapping of the pectoral fins often obscured the positions of features on the pectoral girdle. Only in a subset of our videos ($n = 17$; seven for *L. dimidiatus*, five for *Larabicus*, five for *T. lutescens*) did the pectoral girdle's position remain clear throughout the feeding strike. We found that in these videos, the rotation of the pectoral girdle was remarkably correlated with the rotation of the pelvic fin insertion point within each species, as well as overall ($R^2 = 0.96$, slope = 1.003). We, therefore, chose to use the dorsal margin of the insertion of the pelvic fin (Point 4) as a proxy for the position of the pectoral girdle.

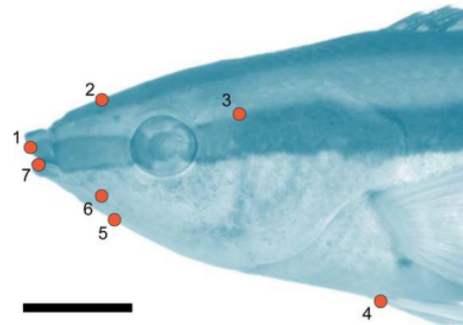


Fig. 1. Landmarks used during kinematic analyses. This lateral photograph of *L. dimidiatus* is faded for ease of viewing the following landmarks: 1) the anterior tip of the premaxilla, 2) the posterior margin of the nasal bone, 3) the (approximate) point of articulation between of the hyomandibula and the neurocranium, 4) the dorsal margin of the insertion of the pelvic fin (a reference point), 5) the anteroventral protrusion of the hyoid, 6) the (approximate) articulation of the lower jaw with the quadrate (i.e., the jaw joint), and 7) the anterior tip of the dentary (lower jaw). Scale bar = 5 mm.

The timing variables (ms) were: 1) time to peak gape, 2) time to peak premaxillary protrusion, 3) time to peak lower jaw rotation, 4) time to peak cranial elevation, 5) time to peak hyoid displacement, 6) time to prey contact (adduction of the jaws), 7) time to peak girdle rotation, and 8) time to full jaw retraction (i.e., the end of the strike).

In addition, we measured the body orientation angle at the onset of the strike by measuring the angle between the midline of the fish's cranium and the surface of the suspended wire mesh or client fish, with the vertex defined at the point where the strike occurred (Supporting Information S-Fig. 3).

Comparisons of Feeding Kinematics

In order to further explore the diversity of kinematic patterns shown by cleaners, we used a principal components analysis (PCA). For the PCA, we used 13 kinematic variables: (timing): time to peak gape, time to peak premaxillary protrusion, time to peak lower jaw rotation, time to peak cranial elevation, time to peak hyoid displacement, and time to complete jaw retraction; (displacement): peak gape distance, peak premaxillary protrusion distance, peak lower jaw rotation, peak cranial elevation, peak girdle rotation, peak hyoid displacement, and body orientation angle. We used each individual fish's mean data for all of these variables from each treatment. Because the data set comprised timing variables, linear measurements, and angles, we factored the correlation matrix of the variables in the PCA.

Following Jolicoeur (1963), when a PCA is computed using a nonsize-corrected data set, the first principal component (PC1) represents the line of best fit to the multivariate data (Pearson, 1901), and size is considered a latent variable that affects all variables simultaneously. We thus considered PC1 to capture the effects of body size on kinematics, while subsequent PCs capture other aspects of kinematic variation. We report only the PCs that cumulatively accounted for up to 95% of the total variation. We did not seek to incorporate phylogenetic information into the PCA, given that we were interested in exploring intraspecific variation.

To test for differences in mean kinematic profiles between species-treatment combinations, we conducted a multivariate analysis of variance (MANOVA) using scores from PCs 2–4 as the dependent variables. Using these scores allowed us to

conduct our comparative analyses in a manner that minimized the effects of predator body size. We defined groups as data belonging to distinct feeding treatments within species, wherever possible. We then conducted a series of pairwise comparisons of group means, and evaluated significance based on Hotelling's T-Square values and *P*-values.

Collection of Morphological Data

After videography, we euthanized all specimens via an overdose of MS-222 (IACUC protocol 1006) and fixed them in 10% buffered formalin for 10–14 days before transferring them to 70% ethanol for short-term storage.

We followed Winterbottom (1974) for muscle identification and descriptions. We removed two muscles from each preserved fish: the mm. adductor mandibulae (AM), and the mm. sternohyoideus (SH). The AM complex is a set of muscles that is responsible for generating the force involved in powering the closing of the jaws during biting. The SH depresses the hyoid bar, causing buccal expansion, which in turn aids in the generation of suction forces (Lauder et al., 1986; Westneat, 1990). Contraction of the SH also places tension on the interopercular-mandibular ligament, which connects the anterior aspect of the interoperculum with the posteroventral portion of the articular, thus contributing to depressing the dentary. We weighed each muscle to the nearest 0.0001 g using a Secura 213-1S precision balance (Sartorius Stedim Biotech GmbH, Germany). We removed all sections of the AM from one side of the specimen except section A₆ (Winterbottom, 1974), and then weighed each section independently.

Following muscle dissections, we cleared and double-stained specimens for bone and cartilage following Dingerkus and Uhler (1977). We used cleared and double-stained specimens to make osteological descriptions, and our terminology follows Gregory (1933) and Tedman (1980a,b).

In wrasses, a four-bar linkage system in the anterior jaws guides the rotation of the maxilla and the protrusion of the premaxilla as the mandible is depressed (Westneat, 1990; Westneat, 1994). The maxillary kinematic transmission coefficient (KT) for this linkage system relates the amount of maxillary rotation produced by a given amount of lower jaw rotation. This ratio is analogous to the inverse of the mechanical advantage of simple lever systems. Following Westneat (1990), we calculated maxillary KT as the ratio between the degrees of maxillary rotation and the degrees of lower jaw rotation for each specimen, which results in a dimensionless number. Since the assessment of maxillary KT is sensitive to the starting position of the system (Hulse and Wainwright, 2002), we measured all starting angles with the jaws closed. We then rotated the lower jaw into a fully depressed position to quantify the changes in the angles associated with the input and output to the four-bar system.

We measured three additional traits on cleared and stained specimens: vertical gape distance, premaxillary protrusion distance, and basihyal length. We used these morphological variables to normalize their corresponding kinematic variables (vertical gape distance, premaxillary protrusion distance, and hyoid displacement, respectively) when plotting kinematic profiles. Vertical gape distance was measured as the distance between each of the most anterior canine teeth on the upper and lower jaws when the mouth was fully open. Premaxillary protrusion distance was measured as the excursion distance of the anteriormost canine tooth on the premaxilla as the upper jaw travels rostrally when the lower jaw is depressed. For each of these measurements, we rotated the lower jaw into a fully depressed position without forcing it beyond natural extension. Basihyal length was measured as the anterior to posterior distance along the midline of the basihyal. Measurements were recorded to the nearest 0.01 mm using the program ImageJ 1.47 (Rasband, 2014).

Journal of Morphology

RESULTS

Morphology of Labrid Cleaners

External features. All three species feature an elongate, fusiform body shape. While describing the external features of these species in detail is not a focus of this study, we do note, however, that both *L. dimidiatus* and its close relative *Larabicus* feature fleshy, tube-shaped lips (Fig. 2). Additionally, the lower lip of each of these species features a short cleft along the midline. This split in the lip effectively creates two distinct lobes, each of which is immediately anterior to a large canine tooth. Unlike these species, *T. lutescens* lacks fleshy lips and has no midline split.

Jaws. The three cleaner fishes show a diversity of jaw shape, particularly in the paired premaxillae. A notable feature of both *L. dimidiatus* and *Larabicus* is the ventrally oriented curvature of the alveolar process of the premaxilla (Fig. 3A,C). All teeth are located on the paired premaxillae and dentary. The anterior tips of each premaxilla and each dentary feature a single, large caniniform tooth that is slightly recurved. Between each of these anterior caniniform teeth and extending caudally lie several rows of smaller villiform teeth. These teeth only occupy an anterior portion of each premaxilla and dentary, over a region that extends no more than approximately one-third the length of each bone. Both species also have a single caniniform tooth located on the ateromedial face of the distal end of each alveolar process. These tusk-like teeth are of similar size to those found on the anterior tips of the jaws. These teeth do not appear to have a cutting edge (Supporting Information S-Fig. 4).

Unlike the condition seen in *L. dimidiatus* and *Larabicus*, *T. lutescens* has premaxillae that feature relatively straight alveolar processes with no caniniform teeth at the distal ends (Fig. 3E). Also, while both the premaxilla and the dentary are lined with caniniform teeth; no villiform teeth are present. The largest teeth in *T. lutescens* occupy the most anterior portions of the upper and lower jaws, and feature a slightly recurved shape. Toward the posterior portions of these bones, the teeth become smaller, less recurved, and more rounded. Some of this roundedness could be blunting, possibly due to wear.

In all three species, the ascending process of the premaxilla slides over the premaxillary condyle of the maxilla as the jaws open and close. While the thickness of this ascending process tapers evenly in *L. dimidiatus* and *Larabicus*, there is a distinct protuberance toward the base of the ventral side of this process in *T. lutescens*. In all three species, the ascending process curves slightly ventrally at the distal end. A palatopremaxillary ligament (Tedman, 1980b; Fig. 4) joins the medial side of the palatine to the dorsal side of the ascending

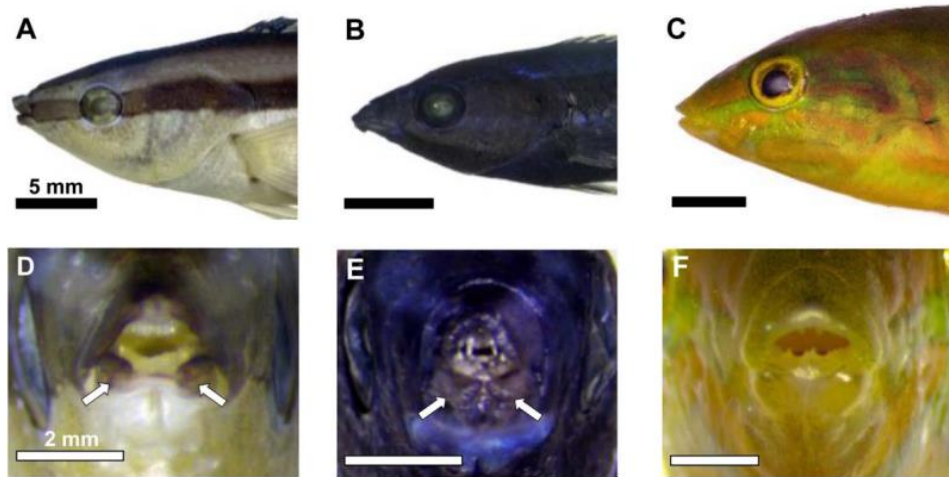


Fig. 2. Photographs of the external cranial morphology of three cleaner wrasses. Lateral photographs of *L. dimidiatus*, (A) *L. quadrilineatus*, (B) and *T. lutescens*; (C) black scale bars = 5 mm. (D–F) Anterior views of the lips and oral jaws of these species; white scale bars = 2 mm. *L. dimidiatus* (D) and *L. quadrilineatus* (E) each feature tube-shaped lips, with a vertical split in the lower lip along the midline. In D and E, white arrows point to distinct lobes on the lower lip, separated by the midline split. *T. lutescens* (F) lacks fleshy lips and has no midline split.

process of the premaxilla. A thick ligament, which we term the “quadrato-maxillary ligament,” connects the anterior portion of the quadrate to the maxillary head (Fig. 4). As the jaws open, this ligament stabilizes the rotation of the maxilla, and appears to be the limiting factor in the extent of this rotation.

In all three species, the dentary articulates snugly with the horizontal process of the articular bone, and there is little to no flexion between the bones (Tedman, 1980a). As noted in other wrasses, an interoperculoarticular ligament connects the anterior edge of the interopercular to the posteroventral edge of the articular (Anker, 1986; Westneat, 1990).

In labrids, a set of ligaments connects the distal end of the maxillary arm, the alveolar process of the premaxilla, and the ascending process of the dentary, which Tedman (1980b) terms the “maxillo-dento-premaxillary complex.” Anker (1986) specifies names for these ligaments, and Westneat (1990) describes them further. A premaxilla-maxillary ligament tethers the alveolar process of the premaxilla to the anterior edge of the distal end of the maxillary arm. A mandibular-maxillary ligament connects the distal end of the maxillary arm to the ascending process of the dentary. These ligaments, depicted in Figure 4, are present in all three cleaner fish species, attaching at similar points on their respective bones.

Maxillary KT. We found the maxillary KT of *L. dimidiatus* and *Larabicus* to be similar (0.70

and 0.62, respectively), while that of *T. lutescens* was slightly higher (0.99). We report species mean \pm SD for this trait in Table 1.

Hyoid. The hyoid apparatus consists of paired interhyals, epihyals, ceratohyals, hypohyals, and an unpaired basihyal and urohyal (Fig. 3). Unlike Tedman’s (1980a) description of a single hypohyal bone in *L. dimidiatus*, we find two distinct bones: the hypohyal and the basihyal (Fig. 3B). The hypohyals are paired bones, short and rounded in appearance. The basihyal is the anteriormost bone in the hyoid apparatus, and takes the form of an elongate bar. This bone is relatively shorter in *L. dimidiatus* than in the other two taxa. In *T. lutescens*, the anterior tip of the basihyal is more broad and flat than that of the other two species.

The hyoid apparatus also supports the branchiostegal rays. *Larabicus* and *L. dimidiatus* each have five pairs of branchiostegal rays; *T. lutescens* has six. The first two pairs of branchiostegal rays are found on each medial face of the ceratohyals. All subsequent rays articulate with the lateral surfaces of the ceratohyals and epihyals.

Myology. We highlight the characteristics of the mm. AM and mm. SH muscles: The AM complex in labrids is composed of four muscles: A1, A2, A3, and A ω , which is also called the intramandibularis (Winterbottom, 1974; Tedman, 1980b). The intramandibularis originates on the medial face of the coronoid process of the articular and inserts on the ascending process of the dentary as well as the horizontal process of the articular

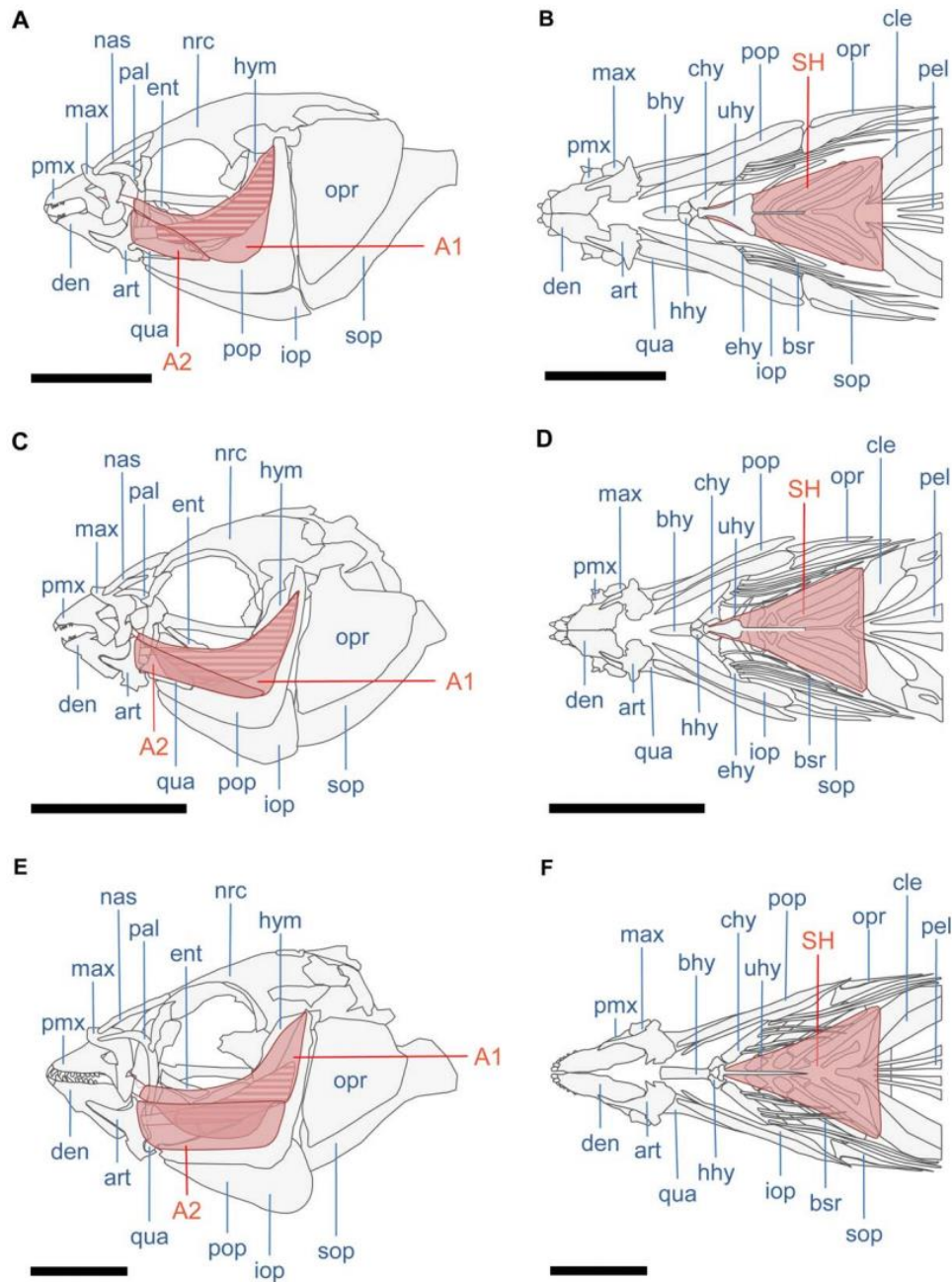
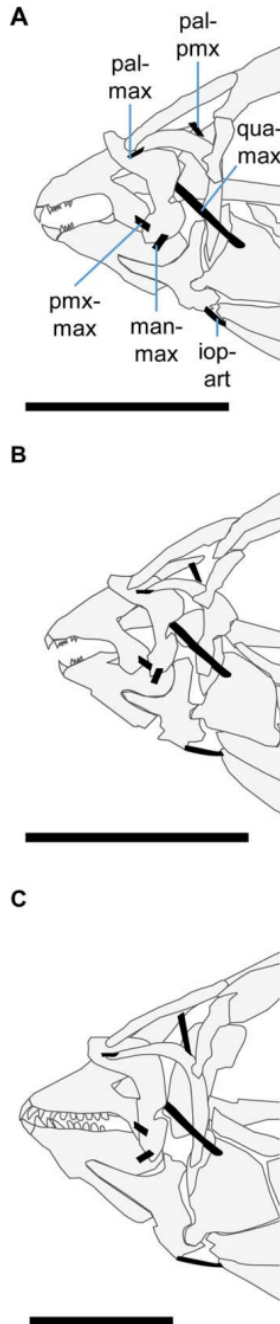


Fig. 3. Lateral and ventral views of cranial morphology of three cleaner wrasses. (A, B) *L. dimidiatus*; (C, D) *L. quadrilineatus*; (E, F) *T. lutescens*. Scale bars = 5 mm. AM muscles (A1, A2, A3) and SH muscles are also shown. AM muscles A1 and A2 overlie the more medial A3 (striped, unlabeled). Bone name abbreviations: art, articular; bhy, basihyal; bsr, branchiostegal rays; chy, ceratohyal; cle, cleithrum; den, dentary; ent, entopterygoid; hhy, hypohyal; hym, hyomandibula; iop, interopercle; max, maxilla; nas, nasal; nrc, neurocranium; opr, opercle; pal, palatine; pel, pelvis; pmx, premaxilla; qua, quadrate; sop, subopercle; uhy, urohyal.

(Tedman, 1980b). Due to its small size, especially in small juvenile fishes, we did not dissect out this muscle. All other muscle masses are reported in Table 1.



Following Winterbottom (1974), the defining characteristic of the A1 is that it inserts on the maxilla. In labrids, the A1 originates on the preopercle and quadrate bones and inserts on the premaxillary condyle of the maxilla via a long tendon and aponeurosis (Tedman, 1980b). It is of similar shape and relative size in all of the present taxa (Fig. 3, Table 1).

The A2 subdivision is the most superficial of the AM subdivisions (Fig. 3). Its origin is on the ventrolateral face of the quadrate and the anterolateral edge of the preopercle, in a more ventral location than that of the A1. It inserts onto the medial face of the coronoid process of the articular bone. In *L. dimidiatus*, the A2 is notably smaller (Table 1), and its origin is restricted to the quadrate.

The A3 is the most medial subdivision of the AM complex, covered predominantly by (A1 and partially by A2; Fig. 3). The A3 has two parts, as noted by Tedman (1980b). One part has a wide origin on the anterolateral edge of the preopercle, the hyomandibula, the metapterygoid, and the symplectic. The other part more narrowly originates on the hyomandibula and metapterygoid. Both parts join together via an aponeurosis, which leads to a well-developed tendon (Tedman, 1980b). This large tendon inserts onto the medial surface of the articular. The A3 is similarly shaped in all three species (Fig. 3), although in *T. lutescens* it is disproportionately smaller by mass (Table 1).

The SH broadly originates on the cleithrum, with both the right and left sides tapering toward their anterior insertions on the urohyal (Winterbottom, 1974). This tapering gives the SH a roughly triangular shape in all three species (Fig. 3). We find, however, differences in muscle size; it appears to be substantially smaller in *L. dimidiatus*, while large in the sister species *Larabicus* when corrected for body size (Table 1).

Feeding Kinematics of Cleaners

During feeding trials in which we presented euthanized suspended client fishes to cleaners, not every cleaner fish interacted with the client. The largest two individuals of *Larabicus* (49.33 and 52.42 mm standard length) and all five individuals of *T. lutescens* consistently showed no interest in cleaning the variety of clients we presented throughout the study.

We thus report data from feeding behaviors of five *L. dimidiatus* and three *Larabicus* individuals.

Fig. 4. Lateral views of key ligaments in the feeding apparatus of three cleaner wrasses. (A) *L. dimidiatus*; (B) *L. quadrilineatus*; (C) *T. lutescens*. Scale bars = 5 mm. Ligament name abbreviations: iop-art, interopercular-articular; man-max, mandibular-maxillary; pal-max, palatomaxillary; pal-pmx, palatopremaxillary; pmx-max, premaxilla-maxillary; qua-max, quadrato-maxillary.

TABLE 1. Mean values for morphological data in three cleaner fishes

Species (# of individuals)	Standard length (mm)	A1 mass (g)	A2 mass (g)	A3 mass (g)	Total AM mass (g)	SH mass (g)	Maxillary KT	Vertical gape distance (mm)	Premaxillary protrusion distance (mm)	Basihyal length (mm)
<i>Labroides dimidiatus</i> (n = 5)	50.73 (8.20)	0.0045 (0.0012)	0.0024 (0.0005)	0.0047 (0.0011)	0.0116 (0.0026)	0.0065 (0.0036)	0.70 (0.06)	2.94 (0.20)	1.12 (0.15)	1.04 (0.17)
<i>Larabicus quadrlineatus</i> (n = 5)	42.86 (7.47)	0.0032 (0.0020)	0.0017 (0.0011)	0.0033 (0.0022)	0.0082 (0.0052)	0.0177 (0.0053)	0.62 (0.04)	2.49 (0.19)	0.71 (0.11)	1.00 (0.21)
<i>Thalassoma lutescens</i> (n = 5)	68.18 (12.88)	0.0184 (0.0103)	0.0091 (0.0047)	0.0077 (0.0038)	0.0352 (0.0187)	0.0391 (0.0225)	0.99 (0.05)	3.70 (0.27)	2.95 (0.33)	2.32 (0.24)

Mean values and standard deviations (in parentheses) are reported. Values for Maxillary KT, Vertical Gape Distance, Premaxillary Protrusion Distance, and Basihyal Length were measured on cleared and stained specimens. Maxillary KT is a dimensionless ratio (see Methods). AM: Adductor Mandibulae; KT: Kinematic Transmission Coefficient; SH: Sternohyoideus.

These individuals showed immediate interest in the client fish upon presentation, making repeated feeding strikes upon the client's body within the first few minutes. Individuals from both species consistently showed the ability to feed on suspended clients from a variety of positions, including those in which the predator was completely inverted (Supporting Information S-Fig. 2D). Generally, each cleaner fish lost interest in the suspended client after 3–5 min of interaction. We present prey capture kinematics for these cleaner fishes in Tables 2 and 3.

In contrast to the behaviors, we observed during the suspended client fishes treatment, all individuals readily fed on attached invertebrates. Here, every individual captured prey via biting; in each video, the oral jaws made direct contact with the prey item. Fishes from all three species showed rapid and multiple gape cycles in which individual invertebrates were targeted (Tables 2 and 3; Fig. 5).

Comparisons of Prey Capture Kinematics.

We used data from six feeding strikes per feeding treatment, per individual. Through PCA, we found that four axes of variation cumulatively accounted for 95% of the total variance in the dataset (Table 4). All 13 variables loaded strongly onto PC1, and the eigenvectors were all in the same direction. This result fits Jolicoeur's characterization of the "size axis," wherein size is a latent factor that affects all variables (Jolicoeur, 1963).

We found that PCs 2 through 4 capture the majority of kinematic variation unrelated to size. Notably, all timing variables loaded negatively on all three of these axes. On PC2, which accounted for 16.52% of total variation, peak hyoid displacement, body orientation angle, and peak girdle rotation loaded strongly and positively. A variety of other traits loaded negatively on this axis, albeit weakly, including peak lower jaw rotation, and peak premaxillary protrusion distance. It is along this axis that species were generally separated (Fig. 6). On PC3 (3.83%), peak gape distance and body orientation angle loaded the most strongly. This axis revealed some sources of intraspecific variation, as indicated by the spread of individuals (especially in *T. lutescens*) in Figure 6.

Our MANOVA confirmed that groups within PCs 2–4 generally showed statistically significant differences in mean values (Wilk's $\lambda = 0.007$, $F_{12,42} = 20.015$, P -value < 0.001). An all-pairs comparison, however, revealed that not all pairs of groups showed significant differences (Table 5). Comparisons between feeding treatments within both *L. dimidiatus* and *Larabicus* did not show significant differences. All other pairs of species-treatment groups showed significant differences in means (all P -values < 0.003).

Kinematics of Prey Capture on Suspended Client Fishes. In *L. dimidiatus*, we found prey

TABLE 2. Mean values for timing variables in kinematic analyses in three cleaner fishes

Treatment Species (# of individuals)	Time to peak gape (ms)	Time to peak premaxillary protrusion (ms)	Time to peak lower jaw rotation (ms)	Time to peak hyoid displacement (ms)	Time to peak cranial elevation (ms)	Time to prey bite (ms)	Time to peak girdle rotation (ms)	Time to jaw retraction (ms)
Suspended clients								
<i>Labroides dimidiatus</i> (n = 5)	10.40 (0.20)	11.23 (0.33)	10.40 (0.20)	14.16 (0.52)	14.67 (0.63)	19.47 (0.76)	19.86 (1.34)	30.23 (2.00)
<i>Larabicus quadrilineatus</i> (n = 3)	11.17 (0.21)	11.00 (0.57)	11.17 (0.27)	16.28 (0.29)	16.28 (0.19)	24.01 (0.52)	21.37 (1.07)	31.50 (1.89)
Attached invertebrates								
<i>Labroides dimidiatus</i> (n = 5)	10.27 (0.24)	11.28 (0.11)	10.27 (0.24)	14.37 (0.71)	15.00 (0.67)	20.02 (0.53)	20.08 (1.23)	30.27 (1.89)
<i>Larabicus quadrilineatus</i> (n = 5)	11.17 (0.19)	11.00 (0.62)	11.17 (0.19)	16.20 (0.22)	16.20 (0.22)	23.78 (0.19)	21.76 (0.99)	32.28 (1.15)
<i>Thalassoma lutescens</i> (n = 5)	14.78 (0.18)	21.76 (0.38)	20.32 (0.17)	25.48 (0.37)	25.54 (0.82)	24.48 (0.29)	36.34 (2.45)	57.90 (2.60)

Mean values and standard errors (in parentheses) are reported for each kinematic variable related to timing within each treatment.

TABLE 3. Mean values for excursion distances and rotations in kinematic analyses in three cleaner fishes

Treatment Species (# of individuals)	Peak gape distance (mm)	Peak premaxillary protrusion distance (mm)	Peak hyoid displacement (mm)	Peak lower jaw rotation (°)	Peak cranial elevation (°)	Peak girdle rotation (°)	Body orientation angle (°)
Suspended clients							
<i>Labroides dimidiatus</i> (n = 5)	1.27 (0.05)	0.67 (0.06)	0.15 (0.01)	13.33 (0.28)	2.86 (0.35)	2.16 (0.33)	45.25 (0.28)
<i>Larabicus quadrilineatus</i> (n = 3)	1.42 (0.12)	0.32 (0.09)	0.26 (0.03)	11.54 (0.33)	4.17 (0.27)	2.87 (0.31)	63.02 (0.52)
Attached invertebrates							
<i>Labroides dimidiatus</i> (n = 5)	1.26 (0.08)	0.67 (0.06)	0.16 (0.01)	13.02 (0.42)	2.52 (0.23)	2.17 (0.26)	58.29 (0.63)
<i>Larabicus quadrilineatus</i> (n = 5)	1.41 (0.18)	0.33 (0.08)	0.26 (0.02)	11.69 (0.19)	3.24 (0.34)	3.42 (0.27)	64.14 (0.75)
<i>Thalassoma lutescens</i> (n = 5)	3.11 (0.54)	2.36 (0.36)	0.25 (0.01)	25.88 (0.43)	5.34 (0.20)	2.78 (0.26)	70.02 (1.24)

Mean values and standard errors (in parentheses) are reported for each kinematic variable related to excursion distance or rotation within each treatment.

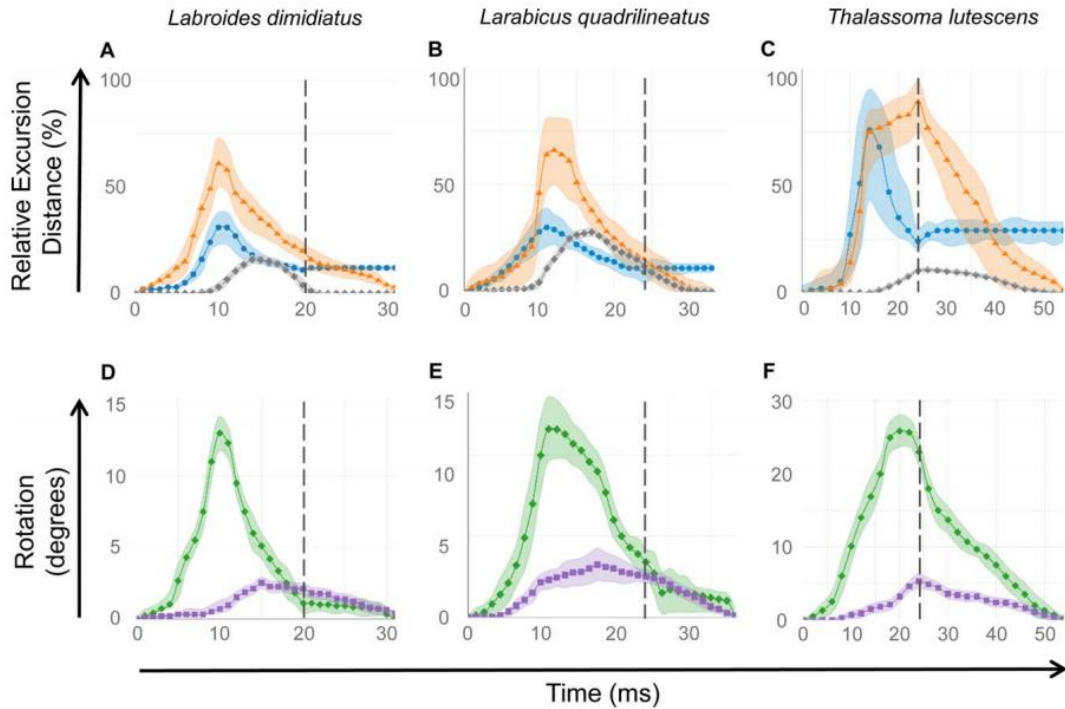


Fig. 5. Kinematic profiles of three cleaner fishes feeding on attached invertebrates. Profiles illustrate kinematics of (A, D) *L. dimidiatus*, (B, E) *L. quadrilineatus*, and (C, F) *T. lutescens*. All profiles depict mean \pm s.e. values after adjusting for size. Data are from the embedded invertebrates treatment, across all individuals within a species. Dashed vertical lines show the mean time at which prey capture occurred via biting. In A–C, blue circles indicate data for gape excursion, orange triangles indicate data for premaxillary protrusion distance, and gray diamonds indicate data for hyoid displacement. These kinematic variables are normalized by their corresponding morphological variables, (measured on cleared and stained specimens): vertical gape distance, premaxillary protrusion distance, and basihyal length, respectively. We calculated gape excursion as the gape distance at time t minus the initial gape distance. This accounts for the space between the jaws before the onset of the strike, and represents the actual distance the jaws travel. Standard error in hyoid displacements is relatively small (see Table 3); thus, errors (shading) are not fully visible. In D–F, green diamonds indicate data for lower jaw rotation, and purple squares for cranial rotation.

capture events were rapid, with gape cycles (i.e., the time between jaw opening and full jaw retraction) lasting 30.2 ± 2.00 ms s.e. (Table 2). Individuals of this species showed modest excursion distances (Table 3) for peak gape (1.27 ± 0.05 mm s.e.), peak premaxillary protrusion (0.67 ± 0.06 mm s.e.), and also extremely small excursions for peak hyoid displacement (0.15 ± 0.01 mm s.e.). These low-displacement events were coupled with modest rotations; peak jaw rotation was $13.33 \pm 0.28^\circ$ s.e., peak cranial rotation was $2.86 \pm 0.35^\circ$ s.e., and peak girdle rotation was $2.16 \pm 0.33^\circ$ s.e. The timing of peak jaw rotation was synchronous with peak gape excursion in every video we analyzed (Supporting Information S-Video 1). During prey capture events, *L. dimidiatus* individuals maintained an acute body orientation angle ($45.25 \pm 0.28^\circ$ s.e.).

In *Larabicus*, we also found prey capture events to be rapid, with gape cycles lasting 31.5 ± 1.89

ms s.e. (Table 2). Individuals of this species showed modest excursion distances (Table 3) for peak gape (1.42 ± 0.12 mm s.e.), peak premaxillary protrusion (0.32 ± 0.09 mm s.e.). Peak hyoid displacement, however, was higher (0.26 ± 0.03 mm s.e.) than that shown in *L. dimidiatus*. Again, the low-displacement events were coupled with modest rotations; peak jaw rotation was $11.54 \pm 0.33^\circ$ s.e., peak cranial rotation was $4.17 \pm 0.27^\circ$ s.e., and peak girdle rotation was $2.87 \pm 0.31^\circ$ s.e. As in *L. dimidiatus*, the timing of peak jaw rotation was synchronous with peak gape excursion in every video we analyzed (Supporting Information S-Video 2). During prey capture events, *Larabicus* individuals maintained an acute body orientation angle ($63.02 \pm 0.52^\circ$ s.e.).

Kinematics of Feeding on Attached Invertebrates. In this treatment, we identified a clearer role of suction in prey capture in *L. dimidiatus* and *Larabicus*. As the jaws opened, we

TABLE 4. PCA on kinematic variables reveals axes of variation in the feeding behaviors of three cleaner fishes

Principal component (% variance)	PC 1 (72.20%)	PC 2 (16.52%)	PC 3 (3.83%)	PC 4 (3.08%)
Time to peak gape	0.975	-0.027	-0.013	-0.046
Time to peak premaxillary protrusion	0.960	-0.242	-0.076	-0.035
Time to peak lower jaw rotation	0.984	-0.125	-0.033	-0.063
Time to peak cranial elevation	0.971	-0.076	-0.161	-0.053
Time to peak hyoid displacement	0.973	-0.028	-0.161	-0.092
Time to complete jaw retraction	0.960	-0.122	-0.034	-0.139
Peak gape distance	0.868	0.048	0.425	0.368
Peak premaxillary protrusion distance	0.893	-0.282	0.261	0.270
Peak hyoid displacement	0.471	0.777	0.023	-0.023
Peak lower jaw rotation	0.924	-0.314	-0.025	0.025
Peak cranial elevation	0.785	0.171	0.222	-0.137
Peak girdle rotation	0.423	0.863	0.299	-0.181
Body orientation angle	0.457	0.750	-0.441	0.263

We used each individual fish's mean data from each treatment in the PCA. Only the first four principal components are described here. Table entries are the loadings for variables (i.e., correlations between each variable and each principal component). Loadings in bold are strong (i.e., |loading| > 0.4).

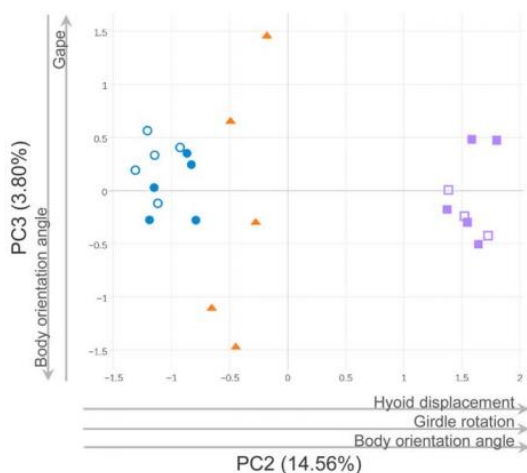


Fig. 6. Axes of kinematic variation in prey capture as revealed by PCA for three cleaner fish species. Symbols on the scatterplot represent five individuals per species. Blue circles represent *L. dimidiatus* individuals, orange diamonds represent *T. lutescens* individuals, and purple squares represent *L. quadrilineatus* individuals. Open symbols correspond to data from the suspended clients treatment, while filled symbols depict data from the attached invertebrates treatment. Variables that loaded strongly on each axis are represented by arrows that indicate the direction in which the variables increase along the axis. See Table 4 for additional information on loadings and text for discussion.

inferred suction generation by each of these species by noting that the invertebrate prey were immediately pulled toward the mouth of the predator. This suction force was rarely sufficient to overcome the prey's attachment to the wire mesh apparatus. In order to maintain consistency, we gathered kinematic data only from videos in which biting was employed to capture prey.

TABLE 5. Hypothesis testing of all pairs of species-treatment means via MANOVA

Group _i	Group _j	Hotelling's T-square	P-value
Lab dim AI	Lab dim SC	4.462	0.212
Lab dim AI	Tha lut AI	32.922	<0.003
Lab dim AI	Lar qua AI	653.623	<0.001
Lab dim AI	Lar qua SC	481.155	<0.001
Lab dim SC	Tha lut AI	60.951	<0.001
Lab dim SC	Lar qua AI	761.039	<0.001
Lab dim SC	Lar qua SC	561.491	<0.001
Tha lut AI	Lar qua AI	393.894	<0.001
Tha lut AI	Lar qua SC	288.122	<0.001
Lar qua AI	Lar qua SC*	0.255	0.901

For the MANOVA, we used scores from principal components 2, 3, and 4 as the dependent variables. We defined groups as data belonging to distinct feeding treatments within species. Group names use the first three letters of the genus and species name (e.g. *Labroides dimidiatus* = Lab dim), followed by an abbreviation for the treatment (AI: Attached Invertebrates; SC: Suspended Clients). Each group thus contained data from five individuals of the species, except the group marked (*), which contained data from three individuals. We obtained Hotelling's T-Square values and P-values via an all-pairs comparison of group means. Significant differences ($\alpha = 0.05$; P-value ≤ 0.05) between group means are indicated by bold P-values.

In both of these taxa, we found the kinematic patterns to be similar to those in the suspended client fishes treatment (Supporting Information S-Video 3, 4). These species again achieved prey capture through low-displacement events (Table 3; Fig. 5A,B). Peak gape was 1.26 ± 0.08 mm s.e. and peak jaw protrusion was 0.67 ± 0.06 mm s.e. in *L. dimidiatus*. In *Larabicus*, peak gape was $(1.41 \pm 0.18$ mm s.e.) and peak jaw protrusion was 0.33 ± 0.08 mm s.e.). These low-displacement events again were coupled with small rotations in the lower jaw and cranial skeleton (Fig. 5D,E). Peak jaw rotation was $13.02 \pm 0.42^\circ$ s.e., peak cranial rotation was $2.16 \pm 0.33^\circ$ s.e., and peak girdle rotation was $2.17 \pm 0.26^\circ$ s.e. in *L. dimidiatus*. In *Larabicus*, peak jaw

rotation was $11.69 \pm 0.19^\circ$ s.e., peak cranial rotation was $3.24 \pm 0.34^\circ$ s.e., and peak girdle rotation was $3.42 \pm 0.27^\circ$ s.e. These species also showed acute body orientation angles during prey capture; *L. dimidiatus*: $58.29 \pm 0.63^\circ$ s.e., *Larabicus*: $64.14 \pm 0.75^\circ$ s.e.

While also successfully targeting individual invertebrate prey, *T. lutescens* exhibited a kinematic pattern divergent from that of the other cleaners (Fig. 5C,F). Jaw movements were generally slower in *T. lutescens*, with time to peak gape occurring at 14.78 ± 0.18 ms s.e., and time to peak premaxillary protrusion occurring at 21.76 ± 0.38 ms s.e. (Table 2). Unlike in the other taxa, the timing of peak jaw rotation in *T. lutescens* was not synchronous with peak gape excursion, but rather showed synchrony with the time to peak premaxillary protrusion (Supporting Information S-Video 5). The excursion distances of peak gape (3.11 ± 0.54 mm s.e.) and peak premaxillary protrusion (2.36 ± 0.36 mm s.e.) were higher than those seen in the other cleaners, in part due to the larger body size of the *T. lutescens* individuals in this study (Table 3). This species also showed larger rotation values; peak jaw rotation was $25.88 \pm 0.43^\circ$ s.e., peak cranial rotation was $5.34 \pm 0.20^\circ$ s.e., and peak girdle rotation was $2.78 \pm 0.26^\circ$ s.e. These larger values for kinematic traits correspond to the higher maxillary KT values we found for *T. lutescens* (Table 1). Finally, *T. lutescens* did not exhibit as acute body orientation angles ($70.02 \pm 1.24^\circ$ s.e.) as the other species.

DISCUSSION

The kinematic patterns we quantified inform our understanding of the functional morphology of cleaners. In each feeding event, only single prey items (e.g., a single bloodworm, ectoparasite, or fish scale) were targeted, although often many were present. We find that all individuals in our study predominately captured prey via biting; in nearly every video, the upper and lower jaws made direct contact with the prey item (Alfaro et al., 2001).

Larabicus and *L. dimidiatus* show similarity in kinematic profiles, perhaps in part due to their close relatedness. In these species, individuals used the smaller, anteromedial villiform teeth to bite into the prey, rather than the larger anterior canines. The relatively acute body orientation angles (see Table 3) these species exhibited during prey capture allow the anteromedial teeth of the lower jaw to contact the prey via the split in the lower lip. Interestingly, individuals of *L. dimidiatus* approached suspended clients at slightly more acute body orientation angles than they did the wire mesh with attached invertebrates.

Journal of Morphology

The curve of the alveolar process of the premaxillae in *L. dimidiatus* and *Larabicus* ensures that only the anteriormost teeth make contact with prey, confining the bite to a reduced area. We interpret the function of these jaw-closing kinematics to be analogous to using forceps, where one exerts precise and localized force to remove an object (Ferry-Graham et al., 2008). Once captured, the prey item occupies the space left open by the split in the lower lip. From our videos, the single caniform tooth at the distal end of each alveolar process of the paired premaxillae does not appear to contact prey. Whether this tooth plays a functional role in feeding in these species remains unclear.

In *T. lutescens*, individuals captured prey using only the anteriormost caniform teeth, which are relatively large and somewhat recurved. Although teeth occupy a larger proportion of the alveolar process length in this species, only the anteriormost teeth came into contact with prey. Perhaps because this species lacks small villiform teeth and tube-shaped lips, *T. lutescens* is less likely to exhibit an acute body orientation angle.

In all three species, the lower jaw acts as one functional unit, and no intramandibular joint (IMJ; Konow and Bellwood, 2005; Konow et al., 2008; Ferry-Graham and Konow, 2010; Konow and Bellwood, 2011) is present. The relationship between cleaning and bearing an IMJ is not straightforward. IMJs generally augment vertical gape expansion during biting. The only group within the Labridae with IMJs (scarids) contains no known cleaners. On the other hand, pomacanthid IMJs restrict the extent of the gape (Konow et al., 2008), and some pomacanthids clean, such as the emperor angelfish (*Pomacanthus imperator*; Kuitert, 1996; Konow et al., 2006). Given that cleaners exhibit small gapes (this study; Wainwright et al., 2004; Baliga and Mehta, 2014) it is possible that this gape-restricting mechanism plays an important role in the functional morphology of cleaning in pomacanthids.

In each species, suction generation also seems to play an important role in prey capture, often helping to orient the prey item toward the buccal cavity. In cases where the prey is weakly attached to a substrate, suction alone could be sufficient for capture. However, in cases where the prey remains strongly attached, the predator uses the anteriormost portion of its oral jaws to bite into and pull off the prey item. While we did not explicitly quantify suction forces, we suspect that *Larabicus* possesses greater suction capability than the other two species we examined. *Larabicus* has a relatively large SH, the bony elements of the hyoid in this species are well developed, and there is a substantial peak hyoid displacement during prey capture. Furthermore, *Larabicus* (regardless of feeding treatment) had the highest positive scores

on PC2 of our PCA. Peak hyoid displacement and peak girdle rotation both load strongly and positively on this axis, while all timing variables load negatively (albeit weakly). Since predators with enhanced suction capability are expected to show greater hyoid displacements and a higher velocity of cranial expansion (Gibb and Ferry-Graham, 2005), the loadings on PC2 lead us to characterize it as a “relative suction capability” axis. High positive scores for *Larabicus* on this axis reflect its underlying ability to generate enhanced suction.

Our three species of cleaner fishes show small jaw displacements during feeding. Our results correspond with our finding relatively low maxillary KT values for these species. The mean maxillary KT for *L. dimidiatus* in our study was 0.70. This measurement is close to that found in larger individuals of this species by Wainwright et al. (2004), a study focused on labrids around the Great Barrier Reef. When we compare across the 104 wrasses in the Wainwright et al. (2004) dataset, we find that *L. dimidiatus* is ranked in the lower quartile for maxillary KT. *Larabicus*, which is not present in the Wainwright et al. (2004) dataset, exhibits an even lower maxillary KT than *L. dimidiatus*. In addition, while we here find the maxillary KT of *T. lutescens* (0.99) to be higher than those of our other two cleaner species, this KT is far lower than those of similarly sized noncleaner congeners (Baliga and Mehta, 2014). In this study, we find that the low maxillary KT of our three species is associated with reduced displacement of the jaws (small gape, little premaxillary protrusion) during feeding.

These low-displacement events are coupled with fast timing values for all the variables we measured. Together, these findings indicate that the evolution of cleaning in labrids may be associated with selection toward the ability to perform low-displacement, fast jaw movements that allow for rapid gape cycles on individually targeted items. Given that cleaners consume prey that are embedded into a substrate (skin between scales), it may not only be advantageous, but also necessary to take multiple quick bites in order to dislodge prey. Bites that are too forceful (i.e., abrasive) could dissuade client fishes to wait around in time for the cleaner to consume prey. We find support for this hypothesis in our assessment of the morphology of the present cleaner wrasses. Juvenile *Larabicus* and *L. dimidiatus* possess small jaw-closing muscles, low kinematic transmission, and small premaxillary protrusion. Previous work has shown that juvenile *T. lutescens* (among other *Thalassoma* cleaners) also have small jaw-closing muscles and exhibit relatively weak bite forces when compared to juvenile noncleaner congeners (Baliga and Mehta, 2014).

The kinematic patterns in both *L. dimidiatus* and *Larabicus* were remarkably similar across

feeding treatments, and the kinematics (timing, angular excursions, and displacements) were consistent across feeding strategies. Simply put, distinct feeding treatments within species did not lead to significant distinctions in feeding kinematics. While we were unable to solicit cleaning behavior from *T. lutescens*, we argue that the kinematic pattern that this species exhibits during our attached invertebrate feeding treatment could serve as a reasonable proxy; in both treatments, in this study, prey are attached to a substrate. Curiously, the two largest specimens of *Larabicus* (standard lengths 49.33 and 52.42 mm) also showed no interest in cleaning euthanized clients. While we have a low sample size in this study ($n = 5$), our findings confirm our assertion that the transition away from cleaning in this species likely occurs at a small size, probably around 45-mm standard length.

Picking

As documented by Ferry-Graham et al. (2008), cyprinodontiform taxa exhibit the ability to “pick” individual prey items from a substrate or water column. This is achieved through an unusual premaxillary protrusion mechanism, wherein the alveolar process of the premaxilla does not rotate anteriorly to occlude the sides of the open mouth during prey capture. Occluding the lateral sides of the mouth is considered to be important for generating suction (Ferry-Graham and Lauder, 2001; Day et al., 2005). Instead, a premaxillomandibular ligament restricts alveolar rotation, and the premaxilla slides anteroventrally along the length of its ascending process (Alexander, 1967; Hernandez et al., 2008).

In wrasses, a four-bar linkage system governs the movements of jaw opening and closing (Westneat, 1990; Westneat, 1994). While the premaxilla is not explicitly modeled as a component of this linkage system, its movements are guided by the rotation of the maxilla. Here, the alveolar process of the premaxilla typically rotates anteriorly during mouth opening due to the connection it shares with the alveolar process of the maxilla (the premaxilla-maxillary ligament; Fig. 4). The extent of this rotation varies as a function of each species’ maxillary KT; in species with a larger maxillary KT value, the maxilla (and thus the premaxilla) exhibits greater rotation. However, similar to the condition seen in cyprinodontiforms, the alveolar process of the premaxilla is effectively pinned to the alveolar process of the maxilla. Because of this connection, the premaxilla acts as a sliding element that descends along the length of its ascending process during prey capture. While this mechanism of premaxillary protrusion is present in the three cleaner fish species in this study, it is also a feature of the majority of wrasses, and thus

is not exclusive to cleaners (Westneat, 1990; Westneat, 1994).

Another key aspect of picking observed in cyprinodontiforms is the apparent trade-off between the speed and the precision of the bite. Ferry-Graham et al. (2008) note that the precise picking behavior of taxa in their study requires slow, controlled jaw movements. The authors further argue that these features may be traded off for some aspects of suction-feeding performance, such as jaw-opening speed and protrusion distance. We converted the following approximate time to peak gape times from their study to ms: 20–30 ms in *Fundulus rubrifrons* and *Kryptolebias marmoratus* and 40–50 ms in *Poecilia sphenops* and *Gambusia affinis*. The kinematic profiles for these “picker” species also indicate the mean total strike time ranges from approximately 55 ms (in *Fundulus*) to approximately 145 ms (in *Gambusia*). These timing values are markedly slower than those seen in three species of percomorphs (*Betta splendens*, *Chaetodon xanthurus*, and *Syngnathus leptorhynchus*) highlighted in their study, results which the authors use to postulate that dexterity requires slow, precisely controlled jaw movements.

In this study, no such trade-off exists. Cleaners are fast, precise pickers that are capable of obtaining individual prey items. We find that while exhibiting excursions of a similar magnitude to those seen in cyprinodontiforms, cleaners achieve peak gape in 10–17 ms, and a full gape cycle between 32–55 ms. Effectively, all jaw movements of cleaner fishes are twice as fast as those seen in cyprinodontiform pickers. Suction generation also seems to play an important role in prey capture, and cleaner fishes appear to be capable of both speed and dexterity. Cleaners in our study were consistent in the timing of kinematic events, regardless of size or species identity (indicated by weak loadings of these variables on PCs 2–4). Cleaners are capable of fast jaw opening and fast jaw occlusion, which facilitates obtaining individual prey items embedded in a client.

CONCLUSION

The kinematic basis of cleaning behavior appears to be in rapid, low-displacement jaw movements. While notable suction forces are generated as the jaws open, the capture of securely attached prey relies on a biting behavior in which only the anterior tips of the jaws contact the prey. These mouth movements allow cleaners to selectively grasp individual prey items, akin to the “picking” seen in cyprinodontiform taxa. While the feeding styles of cleaners show notable similarity to those of cyprinodontiforms, we find key differences between these taxa in the timing of kinematic events. In fact, cleaners generally seem to be able to capture prey twice as fast as cyprinodontiforms.

Journal of Morphology

We thus suggest that the kinematic patterns exhibited by cleaners are indicative of picking behavior, but that “pickers” may be more kinematically diverse in timing than previously thought. Perhaps unsurprisingly, the closely related *L. dimidiatus* and *L. quadrilineatus* showed a high degree of similarity in traits. It is likely that studies on the morphology and feeding kinematics of cleaners in other labrid genera (e.g., *Symphodus*, *Halichoeres*, *Bodianus*, and *Coris*) will shed further light on the diversity of picking behaviors.

ACKNOWLEDGMENTS

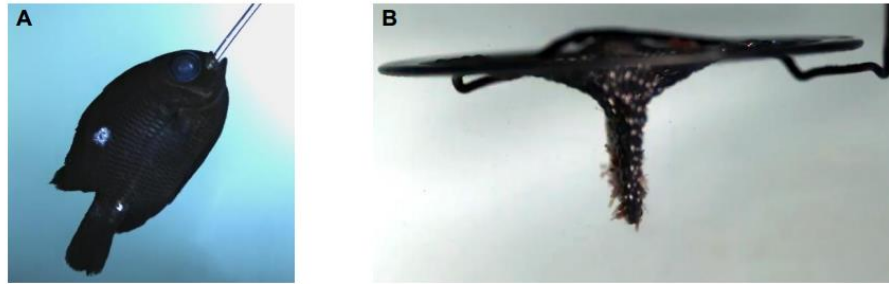
The authors thank T. Portulano for help with digitizing landmarks on videos, and M. Mac for assistance with muscle dissections and some portions of the clearing & staining process. C.J. Law provided helpful discussion on the manuscript. The authors also thank two reviewers for their very insightful comments and helpful suggestions.

LITERATURE CITED

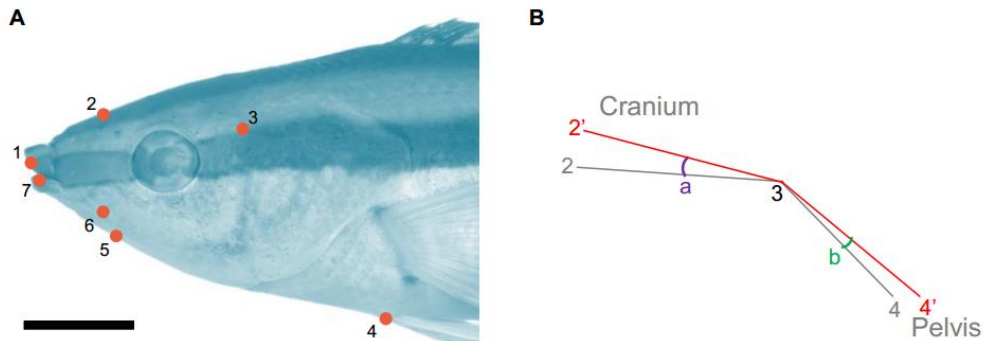
- Alexander RMcN. 1967. The functions and mechanics of the protrusible upper jaws of some acanthopterygian fish. *J Zool* 151:43–64.
- Alfaro ME, Janovetz J, Westneat MW. 2001. Motor control across trophic strategies: Muscle activity of biting and suction feeding fishes. *Am Zool* 41:1266–1279.
- Anker GCh. 1986. The morphology of joints and ligaments in the head of a generalized Haplochromis species: *H. elegans* Trewavas 1933 (Teleostei, Cichlidae). *Neth J Zool* 36:499–530.
- Baliga VB, Mehta RS. 2014. Scaling patterns inform ontogenetic transitions away from cleaning in *Thalassoma* wrasses. *J Exp Biol* 217:3597–3606.
- Brown D. 2009. Tracker Video Analysis and Modeling Tool (Version 4.87) [Computer software]. Retrieved Jan 2, 2015, Available at: <http://www.cabrillo.edu/~dbrown/tracker/>.
- Cole AJ. 2010. Cleaning to corallivory: Ontogenetic shifts in feeding ecology of tubelip wrasse. *Coral Reefs* 29:125–129.
- Coté IM. 2000. Evolution and ecology of cleaning symbioses in the sea. *Oceanogr Mar Biol* 38:311–355.
- Cowman PF, Bellwood DR. 2011. Coral reefs as drivers of cladogenesis: Expanding coral reefs, cryptic extinction events, and the development of biodiversity hotspots. *J Evol Biol* 24:2543–2562.
- Darcy GH, Maisel E, Ogden TC. 1974. Cleaning preferences of the gobies *Gobiosoma evelynae* and *G. prochilos* and the juvenile wrasse *Thalassoma bifasciatum*. *Copeia* 1974:375–379.
- Day SW, Higham TE, Cheer AY, Wainwright PC. 2005. Spatial and temporal flow patterns during suction feeding of bluegill sunfish (*Lepomis macrochirus*) by Particle Image Velocimetry. *J Exp Biol* 208:2661–2671.
- Dingerkus G, Uhler DL. 1977. Enzyme clearing of Alcian blue-stained whole small vertebrates for demonstration of cartilage. *Stain Technol* 32:229–231.
- Ferry-Graham LA, Konow N. 2010. The intramandibular joint in *Girella*: A mechanism for increased force production? *J Morphol* 271:271–279.
- Ferry-Graham LA, Lauder GV. 2001. Aquatic prey capture in Ray-finned fishes: A century of progress and new directions. *J Morphol* 248:99–119.
- Ferry-Graham LA, Wainwright PC, Westneat MW, Bellwood DR. 2002. Mechanisms of benthic prey capture in wrasses (Labridae). *Mar Biol* 41:819–830.
- Ferry-Graham LA, Gibb AC, Hernandez LP. 2008. Premaxillary movements in cyprinodontiform fishes: An unusual protrusion

- mechanism facilitates “picking” prey capture. *Zoology* 111: 455–466.
- Froese R, Pauly D, editors. 2015. FishBase. World Wide Web electronic Publication, Kiel, Germany. Available at: www.fishbase.org, version (1/2015).
- Gibb AC, Ferry-Graham L. 2005. Cranial movements during suction feeding in teleost fishes: Are they modified to enhance suction production? *Zoology* 108:141–153. (2015):
- Gregory WK. 1933. Fish skulls: A study of the evolution of natural mechanisms. *Trans Am Philos Soc* 23:481 p.
- Grutter AS. 1995. Relationship between cleaning rates and ectoparasite loads in coral reef fishes. *Mar Ecol Prog Ser* 118: 51–58.
- Grutter AS. 1996. Parasite removal rates by the cleaner wrasse *Labroides dimidiatus*. *Mar Ecol Prog Ser* 130:61–70.
- Hernandez LP, Ferry-Graham LA, Gibb AC. 2008. Morphology of a picky eater: A novel mechanism underlies premaxillary protrusion and retraction within cyprinodontiforms. *Zoology* 111:442–454.
- Hernandez LP, Gibb AC, Ferry-Graham LA. 2009. Trophic apparatus in cyprinodontiform fishes: Functional specializations for picking and scraping behaviors. *J. Morphol* 270:645–661.
- Hobson ES. 1971. Cleaning symbioses among California inshore fishes. *Fish Bull* 69:491–523.
- Horn MH, Ferry-Graham LA. 2006. Feeding mechanisms and trophic interactions. In: Allen LG, Pondella DJ, Horn MH, editors. *The Ecology of Marine Fishes: California and Adjacent Waters*. Berkeley: University of California Press. pp 397–410.
- Hulsey CD, Wainwright PC. 2002. Projecting mechanics into morphospace: Disparity in the feeding system of labrid fishes. *Proc R Soc B* 269:317–326.
- Jolicoeur P. 1963. The multivariate generalization of the allometry equation. *Biometrics* 19:497–499.
- Konow N, Bellwood DR. 2005. Prey-capture in *Pomacanthus semicirculatus* (Teleostei, Pomacanthidae): Functional implications of intramandibular joints in marine angelfishes. *J Exp Biol* 208:1421–1433.
- Konow N, Bellwood DR. 2011. Evolution of high trophic diversity based on limited functional disparity in the feeding apparatus of marine angelfishes (f. Pomacanthidae). *PLoS One* 6: e24113.
- Konow N, Fitzpatrick R, Barnett A. 2006. Adult Emperor angelfish (*Pomacanthus imperator*) clean Giant sunfishes (*Mola mola*) at Nusa Lembongan, Indonesia. *Coral Reefs* 25: 208–208.
- Konow N, Bellwood DR, Wainwright PC, Kerr AM. 2008. Evolution of novel jaw joints promote trophic diversity in coral reef fishes. *Biol J Linn Soc* 93:545–555.
- Kuiter RH. 1996. *Guide to the Sea Fishes of Australia*. Sydney: New Holland.
- Lauder GV, Wainwright PC, Findeis E. 1986. Physiological mechanisms of aquatic prey capture in sunfishes: Functional determinants of buccal pressure changes. *Comp Biochem Physiol* 84A:729–734.
- Liem KF. 1979. Modulatory multiplicity in the feeding mechanism in cichlid fishes, as exemplified by the invertebrate pickers of Lake Tanganyika. *J Zool Lond* 189:93–125.
- Losey GS, Balazs GH, Privitera LA. 1994. Cleaning symbiosis between the wrasse, *Thalassoma duperrey*, and the green turtle, *Chelonia mydas*. *Copeia* 684–690.
- McCourt RM, Thomson DA. 1984. Cleaning behavior of the juvenile Panamic sergeant major, *Abudefduf troschelii* (Gill), with a resume of cleaning associations in the Gulf of California and adjacent waters. *California Fish Game* 70:234–239.
- Pearson K. 1901. On lines and planes of closest fit to systems of points in space. *Philos Mag* 2:559–572.
- Rasband WS. 2014. ImageJ. U. S. National Institutes of Health, Bethesda, Maryland, USA. Available at: <http://imagej.nih.gov/ij/>, version 1.49.
- Randall JE. 1986. *Red Sea Reef Fishes*. London: Immel Publishing, 192 p.
- Randall JE, Springer VG. 1975. The monotypic Indo-Pacific labrid fish genera *Labrichthys* and *Diproctacanthus* with description of a new related genus, *Larabicus*. *Proc Biol Soc Wash* 86:279–298.
- Tedman RA. 1980a. Comparative study of the cranial morphology of the labrids *Choerodon venustus* and *Labroides dimidiatus* and the scarid *Scarus fasciatus* (Pisces: Perciformes) I. Head skeleton. *Aust J Mar Freshwater Res* 31:337–49.
- Tedman RA. 1980b. Comparative study of the cranial morphology of the labrids *Choerodon venustus* and *Labroides dimidiatus* and the scarid *Scarus fasciatus* (Pisces: Perciformes) II. Cranial myology and feeding mechanisms. *Aust J Mar Freshwater Res* 31:351–72.
- Wainwright PC, Bellwood DR, Westneat MW, Grubich JR, Hoey AS. 2004. A functional morphospace for the skull of labrid fishes: Patterns of diversity in a complex biomechanical system. *Bio J Linn Soc Lond* 82:1–25.
- Westneat MW. 1990. Feeding mechanics of teleost fishes (Labridae; Perciformes): A test of four-bar linkage models. *J Morphol* 205:269–295.
- Westneat MW. 1994. Transmission of force and velocity in the feeding mechanisms of labrid fishes (Teleostei, Perciformes). *Zoomorphology* 114:103–118.
- Winterbottom R. 1974. A descriptive synonymy of the striated muscles of the Teleostei. *Proc Acad Natl Sci Phila* 125:225–317.

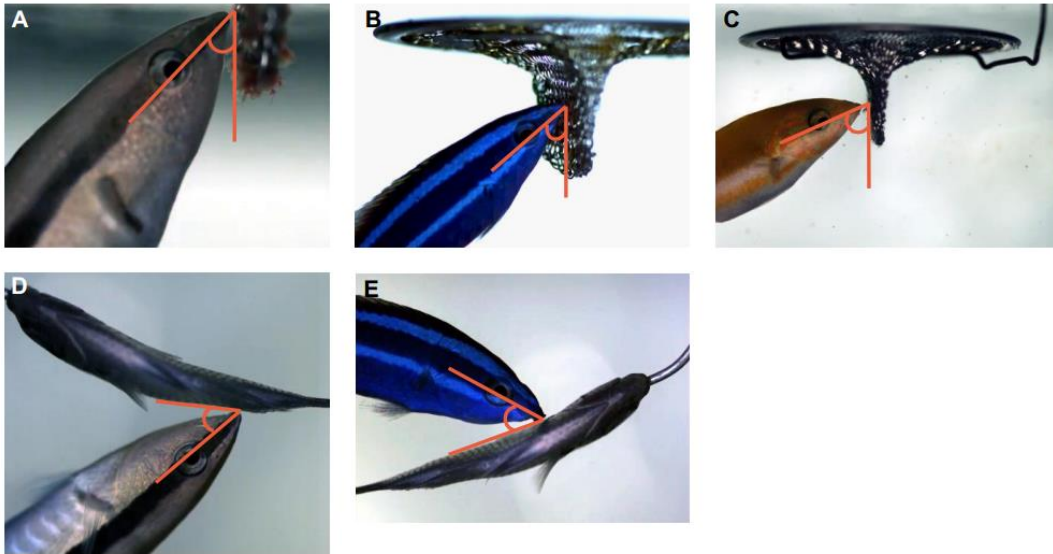
Supporting Information (Figures) for
Linking Cranial Morphology to Prey Capture Kinematics in Three Cleaner Wrasses: *Labroides*
dimidiatus, *Larabicus quadrilineatus*, and *Thalassoma lutescens*
 Vikram B. Baliga & Rita S. Mehta



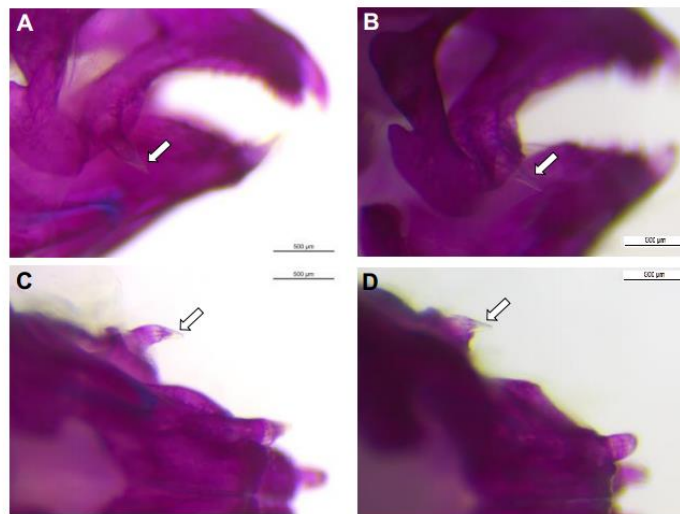
Supporting Information Fig. 1 - Setup for each feeding treatment. (A) The “suspended clients” treatment: we randomly selected a potential client (here, a specimen of *Dascyllus reticulatus*) and suspended it in the water column using a wire; (B) The “attached invertebrates” treatment: we combined thawed mixtures of bloodworms and mysis shrimp and then manually embedded the prey onto a wire mesh. We suspended the wire mesh into the water column for feeding.



Supporting Information Fig. 2 – Quantifying cranial elevation and girdle retraction. (A) is identical to Fig. 1 of the main text, and is here for reference. (B) depiction of cranial elevation and girdle retraction ($^{\circ}$). In B, the positions of all points and lines (and thus, sizes of angles) are exaggerated. Here, points 2, 3 and 4 indicate initial positions, and 2', 3' and 4' indicate positions during peak rotations. Because there is minimal rotation in point 3, we used it as a point of reference. We define cranial rotation as the angular rotation of point 2 with respect to point 3 (angle a), and girdle rotation as the angular rotation of point 4 with respect to point 3 (angle b).



Supporting Information Fig. 3 - Quantifying body orientation angle. (A-C) Cleaner fishes feeding during the attached invertebrates treatment; (D-E) Cleaner fishes feeding during the suspended clients treatment (here, specimens of *Chromis viridis*). (A,D) *Labroides dimidiatus*; (B,E) *Larabicus quadrilineatus*; (C) *Thalassoma lutescens*. We measured the body orientation angle at the onset of the strike by measuring the angle between the midline of the fish's cranium and the surface of the suspended wire mesh or client fish, with the vertex defined at the point where the strike occurred.



Supporting Information Fig. 4 - Caniform tooth at the distal end of the alveolar process in *Labroides dimidiatus* and *Larabicus quadrilineatus*. (A,C) Lateral and ventral views of the jaws of *Labroides dimidiatus* (B,D) Lateral and ventral views of the jaws of *Larabicus quadrilineatus*. Specimens in these photos were cleared & double-stained (see Methods) prior to photographing. In all photos, a white arrow points towards the caniform tooth of interest. We did not find these teeth to possess a cutting edge.

Chapter 2 – Size and shape in independent evolutions of cleaning in the Labridae and Gobiidae

Vikram B. Baliga^a

^aDepartment of Ecology and Evolutionary Biology, Long Marine Laboratory,
University of California Santa Cruz, 100 Shaffer Road, Santa Cruz, CA 95060, USA

Abstract:

Both body shape and size affect the locomotor behavior of organisms, but how these relate to other functional systems such as feeding requires an approach where independent origins of a trophic specialization can be examined. I use the evolution of cleaning behavior in clades within two marine fish families, Gobiidae and Labridae, to explore the extent to which specialization in this trophic strategy is associated with phenotypic evolution. While inference of how and when cleaning evolved in the Labridae has been established previously, I use similar methods to infer the temporal and topological trends of cleaning evolution in the Gobiidae. Curiously, I find that obligate cleaning in these families appears to have evolved contemporaneously (8 – 11 MYA) in separate geographic regions. Through fitting evolutionary models, I explore the extent to which the evolution of cleaning has affected body size in these families, and find that certain smaller-bodied lineages within these families may have been historically “pre-adapted” to clean. I also infer a phylogeny for both families to generate a combined phylomorphospace of body shape using geometric morphometrics. Obligate cleaners exhibit significant morphological convergence in this phylomorphospace, while facultative and juvenile cleaner taxa show more varied patterns. Overall, the evolution of cleaning is associated with not just small body size but a reduction in body depth, elongation of the head, and a more terminal orientation of the mouth. These traits are presumed to enhance a cleaner’s ability to remove ectoparasites that inhabit tightly-confined places such as the gills and oral cavity of their clientele.

2.1 Introduction

Body shape plays a crucial role in the movement of organisms. In the aquatic environment, the shape of the body, fins, and the underlying axial skeleton reflect the ability of organisms to propel and maneuver through water. Since body shape and size affects locomotor behavior, which is central to an organism's ecology, they can strongly influence other functional systems such as feeding (Rice and Westneat 2005; Higham et al. 2007; Collar et al. 2008). An integrated perspective on shape, size and feeding may be especially insightful for feeding specializations that are novel or restricted to particular life history stages.

Obligate cleaner fishes are exclusively found in the labrid genus *Labroides* (5 species, all obligate cleaners) and gobiid genus *Elacatinus* (6 species of obligate cleaners among 19 total) (Côté 2000; Baliga and Law 2016). These genera occupy geographically non-overlapping regions; *Labroides* species are found in the Red Sea, Indian Ocean, and Indo-Pacific, while *Elacatinus* species are exclusively Caribbean (Fig 2.1). Within each region, congeners within these genera overlap in range (GBIF 2016), indicating that species may compete with each other for available parasite prey. Together, these patterns suggest that competition among obligate cleaners within geographic areas could promote morphological divergence as congeners partition niches. Alternatively, obligate cleaners may still exhibit phenotypic convergence as their fundamental niches (i.e. the reliance on ectoparasitivism) are inherently similar, indicating that these taxa may share similar functional constraints

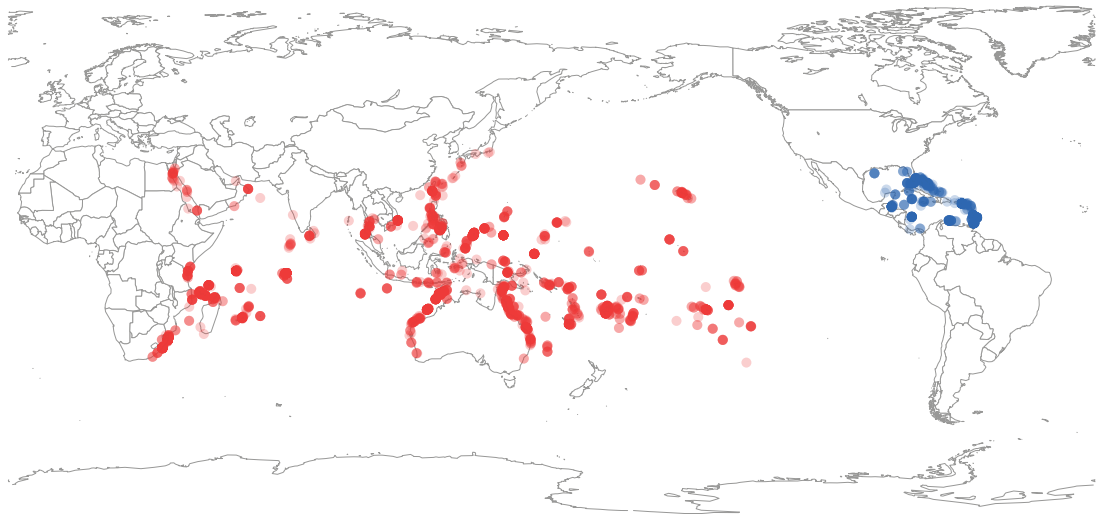


Fig. 2.1 – Geographic distributions of obligate cleaner fishes. Observational data for obligate cleaners in *Elacatinus* (blue; 6 species) and *Labroides* (red; 5 species) were acquired from the Global Biodiversity Information Facility (GBIF 2016). Each point represents a single observation of an individual within a species; within genera, species' distributions are pooled. Distributions for the two genera are non-overlapping: *Elacatinus* sp. are found in the Caribbean, whereas *Labroides* sp. are found in the Red Sea, Indian Ocean, and Indo-Pacific.

related to feeding and locomotion (e.g. traits that are necessary for the detection and capture of ectoparasites).

Moreover, the observation that cleaning behavior is non-uniform in the extent to which taxa engage in the behavior begs the question of how convergent cleaner fishes are in overall size and shape. While we might anticipate obligate cleaners to show higher levels of phenotypic convergence, the evolution of cleaners that do not exclusively rely on parasites for food, facultative and/or juvenile cleaning, suggests imperfect convergence may be at play (Collar et al. 2014). While it may be expected that increased reliance on a particular feeding strategy may promote the evolution of a particular morphological “specialization”, ecomorphological studies of the Labridae indicate a loose relationship between morphology and diet (Wainwright et al. 2004; Bellwood et al. 2006). In fact, morphological specialization in labrids not necessarily equating to trophic specialization might be crucial to supporting their biodiversity on coral reefs (Bellwood et al 2006). Of particular note, however, is Bellwood et al. (2006)’s finding that morphological disparity is lower in the more extreme labrid dietary groups, including obligate cleaner fishes. This indicates that some trophic groups, including those that are more “specialized” in diet, might actually be functionally constrained to exhibit a particular phenotype thus possibly contributing to lineage-specific constraints.

Client taxa (generally other fishes) often allow cleaners to remove ectoparasites that may occupy vulnerable, tightly-confined, and hard to reach places, such as the gills and the oral cavity (Grutter 1996; Côté 2000; Grutter 2010). Furthermore, some

taxa, such as the obligate cleaner *Labroides dimidiatus*, often perform an oscillatory swimming “dance” to signal their presence to potential clientele (Randall 1958; Gorlick et al. 1978). More recently, it has been shown that a relatively low moment of inertia in the vertebral skeleton of cleaners gives them relatively lithe, flexible bodies when compared to non-cleaning congeners (Baliga and Mehta *in review*). Together, these observations imply that the evolution of cleaning may be associated with a particular body shape: one that is small, relatively elongate, and promotes flexibility.

Previous efforts have suggested that there is a relationship between cleaning and body size. Feder (1966) may have been the first to observe that cleaner fishes tend to be small. Côté (2000) provided evidence that within the gobiid genus *Elacatinus*, cleaners were not significantly smaller than non-cleaner congeners, however this comparison did not consider relatedness among species as a phylogeny of the gobies was not available at the time. Using paired contrasts of maximum size in labrid juvenile cleaners and non-cleaner congeners, Côté (2000) also found that cleaners were significantly smaller than non-cleaners. Such comparisons are problematic, however, because these taxa clean predominately as juveniles. Thus, the effects of body size on cleaning are only comparable during the juvenile phase. Additionally, maximum adult size may not necessarily reflect maximum size in the juvenile phase. While maximal juvenile sizes are not readily available, a phylogenetically-informed analysis of facultative and obligate taxa in both families (i.e. cleaners who engage in the behavior throughout ontogeny) could shed light on the importance of body size in cleaning.

Here, I take a comparative approach in assessing the phenotypes of cleaners in the Gobiidae and Labridae. While a previous study has explored the topological and temporal patterns of cleaning evolution in the Labridae (Baliga and Law 2016), similar efforts have been largely absent in the Gobiidae (but see Côté and Soares 2011), and are thus necessary to understand another independent evolution of obligate cleaning. Additionally, placing gobiid and labrid species in a common phylomorphospace (*sensu* Sidlauskas et al. 2008) would help assess whether similar morphological changes occur in the independent evolutions of cleaning. Such an effort, however, requires phylogenetic inference of both families combined. Once a common phylomorphospace is generated, the extent of convergence among gobiid and labrid cleaners can be quantified.

My goals were to use a phylogenetically-informed framework to assess whether: 1) the evolution of cleaning is associated with a reduction in body size, 2) cleaner fishes share a particular body shape, and 3) cleaner fishes, particularly obligate species, are convergent in phenotype.

2.2 Methods

2.2.1 Tree Inference

Two sets of phylogenies were inferred in this study: one for a Western Atlantic clade of gobies, and the other for a combined labrid and Western Atlantic goby genetic dataset. For each analysis, gene sequences were obtained from GenBank.

For the Western Atlantic goby phylogeny, I obtained gene sequences for species of *Elacatinus* and close allies following Taylor and Hellberg (2005). Forty-four species were selected for the in-group, while the outgroup, comprising 10 species, incorporated various other goby lineages. Gene sequences were obtained for four mitochondrial (12S, COI, cytb, and trnT) and four nuclear (GPR85, RAG1, RHOD, and ZIC1) genes (see Tables S2.1-S2.5 in the Appendix for accession numbers), and the overall coverage was 49.32%.

For the combined labrid and Western Atlantic goby phylogeny, sequences for 320 labrids and 44 Western Atlantic gobies were obtained. Selection of the 320 labrids follows Baliga and Law (2016) while the 44 gobies follow specifications listed above. Additionally, several other taxa were included as outgroups to each specific ingroup. A set of 20 perciform taxa were included to serve as an immediate outgroup to the labrids. Two gobies, *Microgobius microlepis* and *Zosterissor ophiocephalus*, were specified as outgroup to the Western Atlantic goby clade. Finally, an additional set of 5 taxa from toadfish, goatfish, and cardinalfish lineages were specified as members of an outgroup to all other taxa. Thus, a total of 391 species were included. Each outgroup specification follows the topological trends shown by previous phylogenies for gobies (Taylor and Hellberg 2005), labrids (Cowman and Bellwood 2011) and extensive teleost fish phylogenies (Near et al. 2013; Rabosky et al. 2013). In order to optimize the coverage of gene sequences for taxa, I used a set of sequences that differed from that which was used by Baliga and Law (2016) and the Western Atlantic goby phylogeny (above). Here, four mitochondrial (12S, 16S, COI and

CYTB) and three nuclear (RAG1, RAG2, and ZIC1) were used to attain an overall coverage of 50.57%.

For each analysis, each gene was aligned separately using Geneious 4.8.5. Models of evolution for each gene were then fit and compared using jModelTest 2.0 (Darriba et al. 2012). For each gene, the best-fit model (assessed via AIC and BIC) was found to be GTR+I+ Γ or a close variant thereof (see Table 2.1 for more). Gene sequences were then concatenated using SequenceMatrix 1.7.8 (Vaidya et al. 2011).

I then simultaneously estimated topology, branch lengths, and divergence times in a Bayesian framework for each phylogeny using BEAST 2.3.1 (Bouckaert et al. 2014). In each phylogenetic analysis, I employed a relaxed log normal clock model approach, partitioned the supermatrix by sequence, and fit a separate model for each partition based on the results from jModelTest. To estimate divergence times, I placed informative parametric priors on nodes of the tree (Table 2.2). I identified descendant members of each node based on the topology of Taylor and Hellberg (2005) and Baliga and Law (2016). These priors were informed by fossil data and historical biogeographical events that have been used by previous studies (Taylor and Hellberg 2005; Kazancıoğlu et al. 2009; Alfaro et al. 2009; Cowman and Bellwood 2011; Near et al. 2013; Thacker 2015; Baliga and Law 2016).

For each analysis, I conducted 10 separate runs (each from a different random starting point) in order to ensure that each BEAST MCMC sampling converged on the target distribution. I ran the MCMC sampler for the Western Atlantic goby tree

for 20 million generations, while the combined labrid and Western Atlantic goby tree was run for 200 million generations. I also ran a similar analysis in which each supermatrix was not partitioned, but found that the MCMC runs had great difficulty attaining stationarity. I assessed convergence via Tracer 1.6 (Rambaut et al. 2014) and used this tool to estimate the effective sample size (ESS) of each parameter.

Table 2.1 Information on model selection for each gene region in two phylogenetic analyses

Model parameters were chosen based on results from jModelTest based on both AIC and BIC (i.e. both methods returned the same model within 95%)

A) Model selection for the Western Atlantic gobiid phylogeny

Gene Name	Type	Length (bp)	% taxa sampled	AICc/BIC*
12s	mitochondrial	2151	49.06%	TIM2+I+G
COI	mitochondrial	661	64.15%	GTR+I+G
CYTB	mitochondrial	1135	69.81%	TrN+I+G
GPR85	nuclear	990	30.19%	GTR+I+G
RAG1	nuclear	1290	69.81%	TrN+I+G
ZIC1	nuclear	849	32.08%	GTR+I+G
RHO1	nuclear	796	66.04%	TPM1uf+I+G
TRNT	mitochondrial	537	28.30%	TPM2uf+G

* Both AIC and BIC returned the same model within 95% CI.

B) Model selection for the combined labrid and Western Atlantic gobiid phylogeny

Gene Name	Type	Length (bp)	% taxa sampled	AICc/BIC*
12S	mitochondrial	1010	68.54	GTR+I+G
16S	mitochondrial	665	80.81	TPM2uf+I+G
COI	mitochondrial	675	79.79	GTR+I+G
CYTB	mitochondrial	851	50.12	GTR +I+G
RAG1	nuclear	1370	17.90	TIM2ef+I+G
RAG2	nuclear	831	40.41	TPM1uf+I+G
ZIC1	nuclear	899	16.37	GTR+I+G

* Both AIC and BIC returned the same model within 95% CI.

Table 2.2 Fossil and biogeographic information used for divergence time estimation in BEAST

Group	Fossil or Event	Age (MY)	Distribution	Prior (5-95%)	Source
Root (crown Labridae)	K/T boundary	66.2*	Normal	62.2-70.3	Near et al. 2013
Hypsiogenyines	<i>Phyllopharyngodon longipinnis</i>	50†	Lognormal	51.5-63.1	Bellwood 1990
Labridae (-Hypsiogenyines)	<i>Eocoris bloti</i>	50†	Lognormal	51.5-63.1	Bannikov and Sorbini 1990
	<i>Bellwoodilabrus landinii</i>	50†	Lognormal	51.5-63.1	Bannikov and Carnevale 2010
<i>Pseudodax moluccanus</i> / <i>Achoerodus viridis</i>	<i>Trigondon jugleri</i>	14‡	Lognormal	15.1-44.0	Schultz and Bellwood 2004
<i>Calotomus Sparisoma</i>	<i>Calotomus preisli</i>	14‡	Lognormal	15.1-44.0	Bellwood and Schultz 1991
<i>Halichoeres dispilus/H. pictus</i>	Isthmus of Panama	9.5‡	Normal	3.1-15.9	Coates and Obando 1996; Barber and Bellwood 2005; Taylor and Hellberg 2005; Montes et al. 2015
<i>Elacatinus</i> (except <i>E. panamensis</i> and <i>E. rubrigenis</i>)					
<i>Bolbometopon muricatum</i> / <i>Cetoscarus bicolor</i>	<i>Bolbometopon</i> sp.	5†	Lognormal	6.1-11.1	Bellwood and Schultz 1991

* The K/T boundary is often used as a guide for the estimation of the age of the crown group; no fossil labrids have been found before this event

† Minimum age for the fossil

‡ Estimation for this biogeographic event incorporates information from traditional sources that estimate the closure of the Isthmus of Panama to have occurred 3.1-3.5 MYA as well as a recent study that presents evidence for the closure instead occurring 13-15 MYA.

Once I discarded the burn-in from each run (the first 15-20%), I combined runs via LogCombiner 2.3.1 and assembled the maximum clade credibility (MCC) tree in TreeAnnotator 2.3.1 (Bouckaert et al. 2014). Within each BEAST run, the ESS of all parameters were generally >200, with the lowest ESS still >100. After I discarded the burn-in and combined the results of all 10 runs, the ESS of all parameters for each analysis were >600, but the vast majority of parameters had ESS >3000.

I retained both the MCC tree as well as 100 trees from the posterior distribution from each analysis for use in the phenotypic analyses. For labrid-specific analyses, I obtained 100 trees from the posterior distribution of trees from Baliga and Law (2016).

2.2.2 *Inferring the evolutionary history of cleaning*

I categorized each species in the genetic datasets to one of four categories: 1) non-cleaner, 2) juvenile cleaner, 3) facultative cleaner, or 4) obligate cleaner. Juvenile cleaners are those that clean predominately as juveniles or sub-adults. Facultative cleaner species clean throughout ontogeny, although they do not rely on cleaning behavior as their sole means of food acquisition. Obligate cleaners depend on cleaning to obtain nearly all sources of food. These categories were designed to be discrete and non-overlapping.

Categorizations for gobies follow those made by Côté (2000) and White et al. (2006). Labrid categorizations follow Baliga & Law (2016), with two exceptions. Recent observations have shown *Thalassoma amblycephalum* to clean in the juvenile

phase (S. Gingins, personal communication). Additionally, while *T. klunzingeri* was listed as a juvenile cleaner in Baliga and Law (2016), its synonymy with *T. rueppellii* was missed. Thus, in the present analyses, both *T. amblycephalum* and *T. rueppellii* were re-categorized as juvenile cleaners.

I then employed stochastic character mapping (Nielsen 2002; Huelsenbeck et al. 2003; Bollback 2006) to simulate the evolutionary history of cleaning on gobiid and labrid phylogenies. I performed two separate sets of character mapping: one for the (44-taxon) Western Atlantic goby phylogenies and the other for (320-taxon) labrids (a re-analysis with updated information for *T. amblycephalum* and *T. rueppellii*). All outgroup taxa were pruned prior to mappings. Methods for stochastic character mapping largely followed those outlined in Baliga and Law (2016), however I sampled 100 stochastic character maps for each tree in each of the 100-tree posterior distribution sets. Thus a total of 20,000 character maps were sampled, 10,000 for each family.

I did not seek to perform stochastic character mapping for the combined labrid and gobiid phylogenies for a variety of reasons: 1) the unequal sampling of taxa (320 labrids vs 44 gobiids), 2) inherent differences between the families in life-history patterns of cleaning (there are no juvenile cleaners in Gobiidae), and thus 3) observed differences in the Markovian transition matrices for each family. These combined differences would increase the error of character transitions across the phylogeny.

2.2.3 Analyses of Size

Size data for all taxa were compiled from FishBase (Froese and Pauly 2016). The maximum total length (TL, in centimeters) was collected for each species on each phylogeny, wherever available. In (relatively uncommon) cases where only maximum standard length was available, the TL was approximated via species- or genus-specific morphometric coefficients.

To determine how the history of cleaning may have influenced body size evolution, I fit evolutionary models to the datasets using *OUwie* (Beaulieu et al. 2012). The ‘flexible’ Ornstein Uhlenbeck (OU) models available via *OUwie* allow for the testing of hypotheses related to state-dependent diversification. Here, each dietary category represents a regime that can influence body size evolution. Flexible OU models can distinguish between these scenarios by estimating three parameters: θ (the optimal trait value), α (the strength of selection towards the optima) and σ (the square root of the Brownian motion evolutionary rate parameter).

I fit evolutionary models to the evolution of TL separately for each family. To incorporate uncertainty from both stochastic character mapping and phylogeny, I fit models to each family’s 10,000 mapped trees (100 trees x 100 mappings). For each dataset, I fit four different models: two representing Brownian motion and two representing OU processes. The least complex model (BM1) fit a common σ for all lineages. A more complex model, BMS, allowed each dietary regime to have a separate σ . The more complex OU model (OUM) included separate optima for each dietary regime, while a single-optimum OU model (OU1) fit a common optimum for all dietary regimes. Other, more complex models (i.e. OUMV, OUMA, OUMVA)

were explored, but for these models eigendecomposition of the Hessian matrices yielded negative eigenvalues. Thus, I found the information in the datasets and phylogenies to be insufficient to fit these complex models. I also used functions in the *pmc* package (Boettiger et al. 2012) to estimate test power among models via parametric bootstrapping.

2.2.4 Analyses of Shape

I first collected lateral photographs for 1-10 specimens of 229 total species (188 labrids and 41 gobies) from various online repositories and/or photographs taken by the authors (see Table S6 in the Appendix). This sampling included 49 of 59 labrid and 12 of 13 gobiid cleaners, as well as closely-related non-cleaners. Because a majority of labrid cleaners show an ontogenetic transition away from cleaning as adults, I collected photographs of juvenile specimens only for all labrid species. On the other hand, all photographs of goby species were of the adult form. Assessments of juvenile vs. adult form followed descriptions of size and phase-specific coloration patterns (Burgess et al. 1991; Randall et al. 1997; Myers 1999).

I then used a geometric morphometric approach to analyses of body shape. I digitized 18 landmarks on each photograph (Figure 2.2) using *tpsDig2* (Rohlf 2006). After landmarks were placed, I included an additional 32 semi-landmarks to capture additional contours of body shape. Procrustes superimposition (Gower 1975) was used to account for size, location and rotational differences between specimen

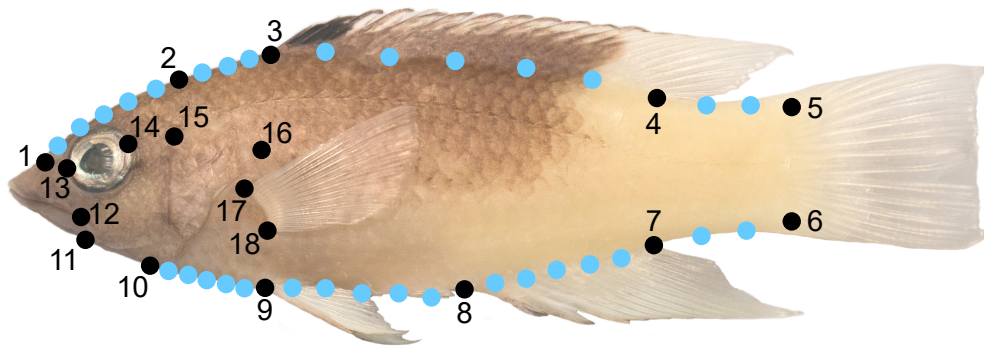


Fig. 2.2 – Landmarks used during geometric morphometric analyses. Eighteen landmarks (black, numbered) and 32 semi-landmarks (blue) were placed on each specimen in the present study. Landmark definitions: 1 – distal edge of the nasal bone; 2 – dorsal edge of the neurocranium (margin of epaxial muscle); 3 – insertion of the first dorsal fin ray; 4 – insertion of the last dorsal fin ray; 5 – dorsal edge of hypural; 6 – ventral edge of hypural; 7 – insertion of the last anal fin ray; 8 – vent; 9 – anterior insertion of the pelvic fin; 10 – ventral edge of skull (margin of hypaxial muscle); 11 – proximal tip of lower jaw; 12 – (approximate) corner of mouth; 13 – distal edge of prefrontal; 14 – distal edge of dermosphenotic; 15 – dorsal tip of hyomandibula; posterior tip of operculum; 17 – dorsal insertion of pectoral fin; 18 – ventral insertion of pectoral fin.

photographs. After superimposition, average shapes were computed within each species, and all subsequent analyses were performed on species' mean shapes.

I then used phylogenetic Principal Components Analysis (pPCA; Revell 2009) to find the major axes of variation among taxa after accounting for relationships among taxa. All pPCAs were performed using functions available in *phytools* (Revell 2012). Family-specific pPCAs were generated using the Western Atlantic gobiid MCC tree and the labrid MCC tree from Baliga and Law (2016), respectively. A combined labrid and gobiid pPCA was performed using the combined labrid and Western Atlantic gobiid MCC tree.

To interpret morphological variation along axes in phylomorphospace, I adopted an approach that differs from common practices in the geometric morphometric literature. The centroid of phylomorphospace is a point in which the value on each pPCA axis is zero. To generate loadings for the *i*th pPCA axis, the maximum (or minimum) score was used as the *i*th value of a vector, the length of which equaled the total number of pPCA axes. All other values in the vector were then set to zero, and all such vectors were concatenated into a matrix, *G*. This matrix was then used to generate shapes corresponding to the maxima (or minima) of axes:

$$P = G V^{-1} + A$$

where *P* is a matrix of shape coordinates for the maxima (or minima) of axes, *V* is the matrix of eigenvectors from the original phylogenetic PCA, and *A* is a “vector of

phylogenetic means” (a vector containing the estimated ancestral states for each of the traits; Revell 2009).

I then used the *plotRefToTarget()* function in *geomorph* to plot shape differences between the centroid of phylomorphospace and each pPCA axis’ maximum (or minimum) shape. Loadings were thus visualized as changes between the centroid and each maximum (or minimum) shape.

2.2.5 Testing for convergence

Convergence among cleaners was assessed using methods in Stayton (2015). Because obligate cleaners are monophyletic within each family, convergence between obligate taxa could only be assessed in a combined phylomorphospace for labrids and gobiids. Within the combined labrid and gobiid phylomorphospace, convergence among obligate taxa (in *Labroides* and *Elacatinus*) was measured using Stayton’s C_2 . Stayton’s C_2 quantifies the amount that lineages have evolved to become more similar. It is measured by subtracting D_{tip} (the distance, here Euclidean, between putatively convergent taxa in phenotypic space) from D_{max} (the maximum distance between any pair of taxa in the lineages). Larger values of C_2 thus indicate greater amounts of convergence. Convergence among all cleaner fishes (including juvenile and facultative cleaners) in this phylomorphospace was also assessed and tested. Tests of significance in convergence ($\alpha = 0.05$) were performed via functions available in *conveovl*, with 1000 simulations per test (Stayton 2014).

Additionally, convergence among cleaners was assessed within families. In each family-specific phylomorphospace, we employed Stayton's C_4 , which is Stayton's C_2 scaled by the total amount of evolution in the clade defined by the common ancestor to the putatively convergent taxa. This metric was chosen in order to make assessments of convergence comparable across analyses. Stayton's C_4 was measured at the following levels: 1) among all cleaners, 2) among facultative cleaners, 3) among juvenile cleaners (in the labrid dataset only). Convergence within families among obligate cleaners was not assessed, since obligate cleaning likely evolved only once in each family. Within each set of analyses for a particular phylomorphospace, p-values were adjusted for multiple hypothesis testing following Benjamini and Hochberg (1995).

To determine the sets of characteristics that might aid in discriminating between members of the dietary categories, we used phylogenetic Flexible Discriminant Analysis (pFDA; Motani and Schmitz 2011). In order to avoid over-parameterizing the discriminant function, we used an iterative procedure wherein the number of pPCA axes fed into the discriminant analysis ranged from 1 to all 100. In the simplest case, only the first PC was used in pFDA. In each subsequent case, the next PC was added as a predictor. I then assessed how misclassifications within each dietary category (as well as overall misclassifications) varied with the total number of PCs used to inform my selection of the final pFDA model. As no single set of PC axes minimized misclassifications in all dietary groups, I opted to use the smallest set of PCs in which all obligate cleaners could be discriminated from each of the other

groups. Once the final pFDA model was selected, the loadings of discriminant axes (i.e. the correlations between each discriminant axis and each original PC axis) were useful in identifying trait combinations that could be used to discriminate among dietary groups.

2.3 Results

2.3.1 Phylogenetic Inference and Mapping the Evolution of Cleaning

Bayesian analyses yielded a well-supported MCC phylogeny for the Western Atlantic gobies that was largely congruent with that produced by Taylor and Hellberg (2005). We found the origin of the ingroup to be approximately 46.45 MYA (95% HPD: 29.92 – 60.04 MYA), which is close to that found by Thacker (2015): 45.0 MYA (95% HPD: 41.1-49.4 MYA). The majority of nodes were well-supported, with 34 of 43 nodes showing Bayesian posterior probabilities above 0.90. The BEAST runs converged on a MRCA time for Western Atlantic *Elacatinus* species of 15.42 MYA (95% HPD: 11.17 – 19.85 MYA). Two other (non-cleaner) *Elacatinus* species (*E. rubrigenis* and *E. panamensis*) were generally found to clade with *Tigrigobius multifasciatus* and *T. harveyi*. The MCC phylogeny is shown in Figure 2.3A.

In stochastic character mappings performed on 100 posterior-distribution gobiid trees, I found that cleaning likely evolved from non-cleaning 3 separate times (Mean: 3.25, SD: 0.83) in Western Atlantic gobies (Figure 2.3A), with few secondary transitions back to non-cleaning (Mean: 2.29, SD: 0.91). In the majority of mappings, obligate cleaning evolved once within this group (Mean: 1.28; SD: 0.37), within a

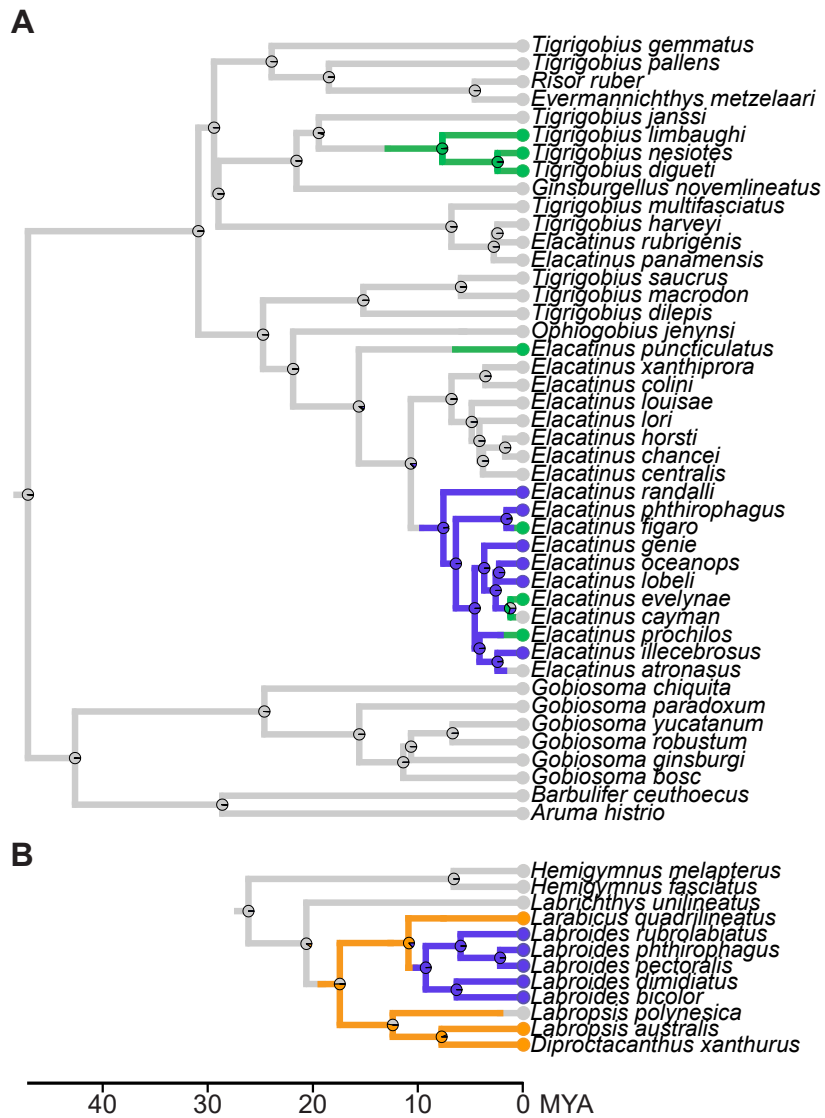


Fig. 2.3 – The evolution of obligate cleaning. A) MCC phylogeny from the Western Atlantic gobiid analyses. B) Labrichthyne (and close allies) clade, pruned from the MCC labrid phylogeny in Baliga and Law (2016). A single stochastic character map has been superimposed on each phylogeny, while pie charts on nodes indicate the distributions of states from 1000 stochastic character mappings performed on each MCC tree. Colors indicate dietary group: purple – obligate cleaner; green – facultative cleaner; orange – juvenile cleaner; grey – non-cleaner.

monophyletic subset of *Elacatinus*. Stochastic character mappings on labrid trees yielded similar results to those found by Baliga and Law (2016); cleaning was found to have evolved 27-31 times in the present study, compared to 26-30 times in Baliga and Law (2016). This slight deviation is likely due to the fact that the one of species that was re-classified as a juvenile cleaner *T. amblycephalum*, has sister taxa that are cleaners. Thus, cleaning in this species likely arose through evolutionary events already inferred in Baliga and Law (2016).

The combined labrid and goby MCC tree indicated a divergence time between labrid and gobies to be approximately 89.75 MYA (95% HPD: 73.15-107.65 MYA). This tree featured similar topology with each family compared to family-specific trees. Within the Western Atlantic goby portion, relationships among taxa, divergence times, and node support values were nearly identical those found in the goby-specific MCC phylogeny (see Figure S1 in the Appendix). Within the labrid portion, the topology...etc generally matched well against those found by previous studies (Westneat and Alfaro 2005; Kazancıoğlu et al. 2009; Alfaro et al. 2009; Cowman and Bellwood 2011; Baliga and Law 2016). Within clades, topologies and divergence times were fairly similar to those found by other studies, but the organization of major groups did differ, largely among the julidines (for more see Figure S2 in the Appendix).

2.3.2 Analyses of Maximum Body Size in Cleaner Fishes

In gobiid cleaner fishes, maximum body size was found to range from 3.30 to 5.53 cm TL. Gobiid non-cleaners ranged from 1.90 to 8.50 cm TL. In labrids, facultative and obligate cleaners ranged from 9.00 to 58.49 cm TL. One facultative species, however, presented as an extreme outlier: the maximum TL of *Labrus bergylta* (58.5 cm) was nearly double that of the next largest facultative cleaner *Thalassoma duperrey* (28.0 cm). Aside from *L. bergylta*, labrid facultative and obligate cleaners ranged from 9.0 to 28.0 cm TL. Non-cleaner labrids ranged from 4.10 to 229.0 cm TL.

In both the gobiid and labrid analyses, I found that Ornstein-Uhlenbeck models fit better than Brownian motion models (Table 2.3). In the gobiid analyses, $\Delta AICc$ scores for OU models were only slightly lower than those for BM models; AICc scores for all models were within 10 units of each other. In the labrid analyses, substantially more support for OU models was found, as BM models were found to have AIC scores that were 98.02 – 102.72 units higher than those of the OU models. Between the two OU models, a slight preference was found for OU1. Among OUM models, cleaners in the Gobiidae were found to have higher optima than non-cleaners (1.605 for facultative cleaners; 1.520 for obligate cleaners; 1.343 for non-cleaners; all SEMs <0.005). Among labrids, non-cleaners had the highest optima (3.162, SEM: 0.001), while facultatives (3.088, SEM: 0.024) and obligates (2.470, SEM 0.008) showed reductions in optima.

Phylogenetic Monte-Carlo analyses indicated that each phylogenetic dataset contained sufficient information to discriminate between BM and OU models (Figure

2.4). The datasets, however, did not provide sufficient power to distinguish between OUI and OUM models.

Table 2.3 Parameter estimates for models fit to log-transformed total length

Model	AICc	Δ AICc	Weight	σ^2 values	α	θ values
Gobiids						
BM1	39.74 (0.40)	7.62 (0.34)	0.06 (<0.001)	0.012 (<0.001)	-	-
BMS	41.71 (0.32)	9.58 (0.27)	0.03 (<0.001)	0.013, 0.016, 0.006 (all <0.002)	-	-
OUI	32.13 (0.08)	0 (0)	0.81 (<0.001)	0.088 (0.011)	0.347 (0.044)	1.367 (<0.001)
OUM	36.44 (0.09)	4.31 (0.02)	0.10 (<0.001)	0.087 (0.010)	0.347 (0.044)	1.343, 1.605, 1.520 (all <0.005)
Labrids						
BM1	654.75 (2.93)	102.60 (1.36)	<0.01 (<0.001)	0.034 (0.008)	-	-
BMS	654.87 (2.89)	102.72 (1.33)	<0.01 (<0.001)	0.035, 0.026, 0.004 (all < 0.001)	-	-
OUI	552.15 (1.57)	0 (0)	0.90 (<0.001)	0.078 (0.001)	0.083 (0.001)	3.157 (0.001)
OUM	556.73 (1.54)	4.59 (0.059)	0.10 (<0.001)	0.080 (0.001)	0.087 (0.001)	3.162, 3.088, 2.470 (0.001, 0.024, 0.008)

All models were fitted on 10000 stochastic character maps generated for each family using natural log-transformed total length data (see Methods). Within each cell, mean values are listed followed by standard errors in parentheses. Where multiple

parameter estimates are listed, values correspond to the dietary categories in the following order: non-cleaner, facultative cleaner, obligate cleaner. Parameter estimates for models with the lowest AICc scores are bolded.

Two phenograms (Evans et al. 2009) showcase the evolutionary history of maximum total length among taxa in the present study (Figure 2.5). Because OU models were found to fit each family's data better than BM models, ancestral character estimates in each family were inferred through an OU process (Revell 2012).

2.3.3 Analyses of Shape

In each family-specific phylomorphospace, elongation of the body was identified as a major axis of variation. Cleaner fishes generally tended to be more elongate than other non-cleaner taxa, but were not always the most elongate. Each family contained taxa that exhibited far more extreme elongation than the majority of other species. In the Gobiidae (Figure 2.6), *Evermannichthys metzelaari* showed extreme reductions in head, body and tail depth. This species also showed slight reductions in head length and an anterior shift in the insertion points of the pectoral fins. In the Labridae, (Figure 2.7) *Cheilio inermis*, *Oxyjulis californica*, *Coris julis*, and *Hologynmosus annulatus* each showed extreme elongation compared to the centroid shape. All four species showed large reductions in head, body, and tail depth, along with slight reductions in head length and an anterior shift in pectoral fin attachment points.

In the combined gobiid and labrid phylomorphospace (Figure 2.8), elongation was again found to be the major axis of variation among taxa; species with higher positive scores on PC1 tended to have bodies and heads that showed reduced depth, primarily

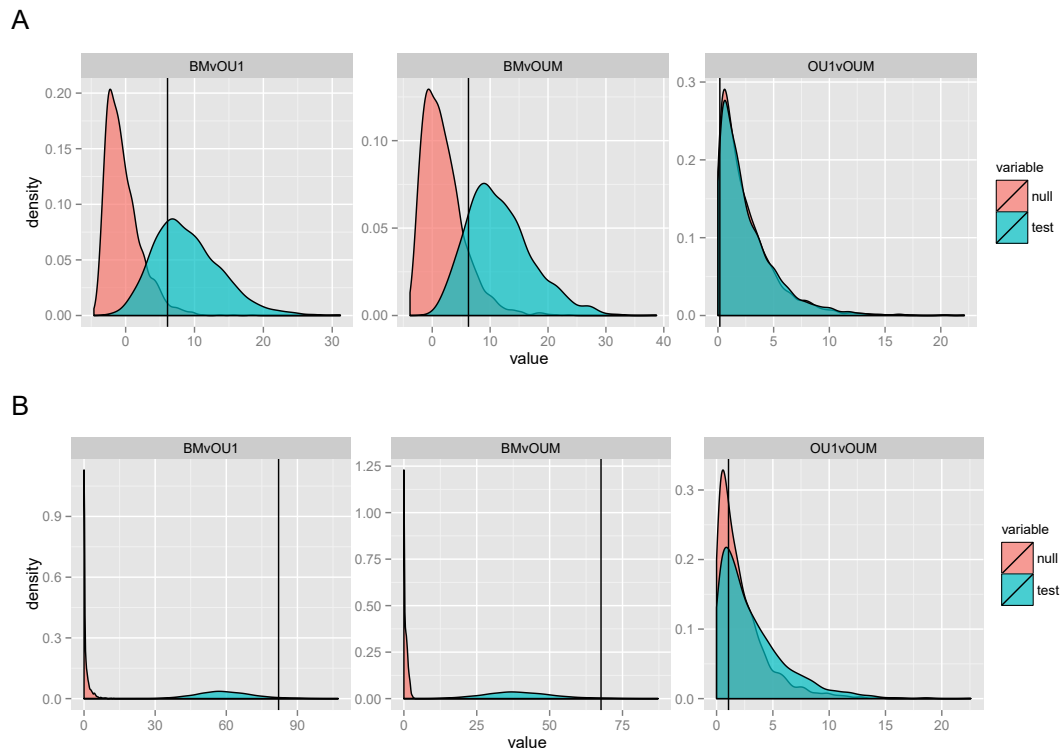


Fig. 2.4 – Distributions of the likelihood ratio statistic for evolutionary model comparisons. In each case, the red distribution shows the distribution of δ values obtained by bootstrapping under the simpler of the two models (treated as a “null”), while the teal distribution shows the distribution under the more complex of the two models. A total of 2000 replicates were used to generate each distribution. The vertical lines indicate the observed value of δ when the models are fit to their respective datasets. All distributions were generated via phylogenetic Monte Carlo-based methods (Boettiger et al. 2012) using A) the gobiid body size data, and B) the labrid body size data. In both A and B, Ornstein-Uhlenbeck models compare favorably over those involving Brownian motion, but each dataset has insufficient power to detect differences between Ornstein-Uhlenbeck models (i.e. OU1 vs OUM).

Fig. 2.5 – Phenograms of body size evolution in gobiids and labrids (on following page). Traitgrams (Evans et al. 2009) provide a projection of the phylogenetic tree in a space defined by the natural log of total length (y-axis) and time (x-axis). Body size evolution for Western Atlantic gobiids is shown in A, while labrid size evolution is shown in B. On each phylogeny, a single stochastic character map is superimposed. Because the maximum body size of juvenile cleaners was not examined, stochastic character maps have been altered to combine juvenile cleaner character states with those of the non-cleaners. As models indicated the body size of each family to be better-fit by Ornstein-Uhlenbeck models, the plotted ancestral body sizes here follow reconstructions via an OU (single-optimum) process. Colors indicate dietary group: purple – obligate cleaner; green – facultative cleaner; grey – juvenile cleaner or non-cleaner.

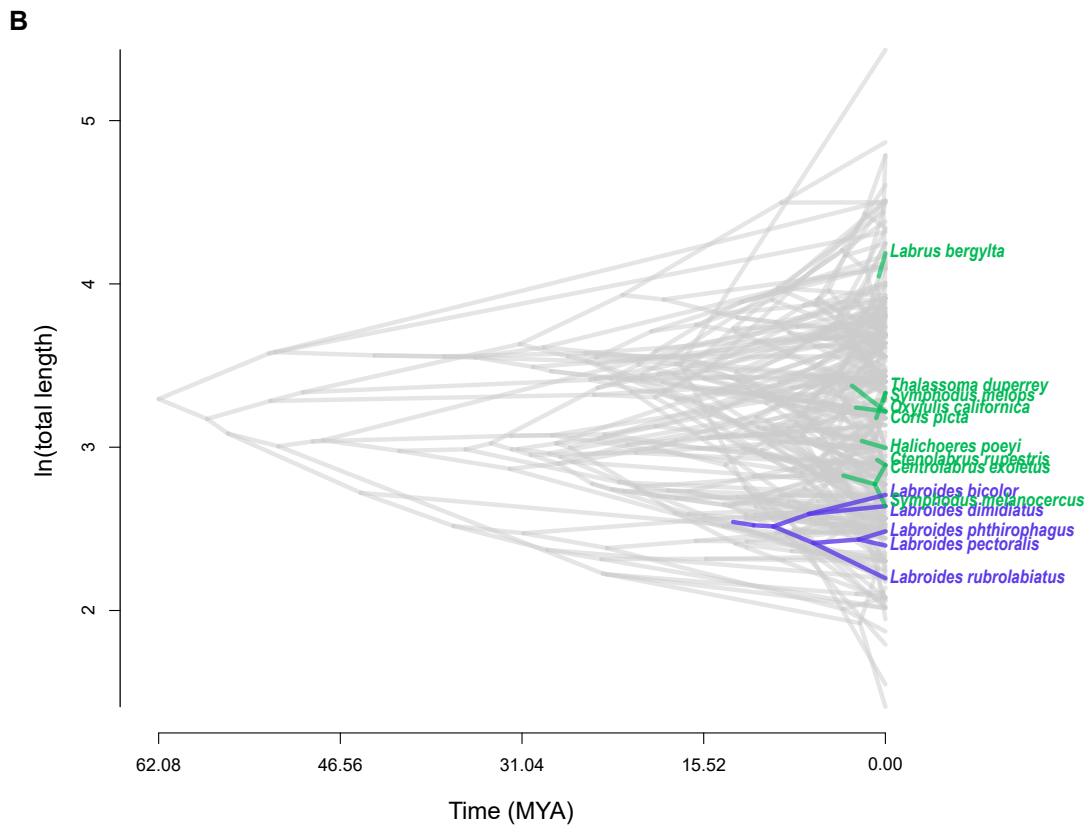
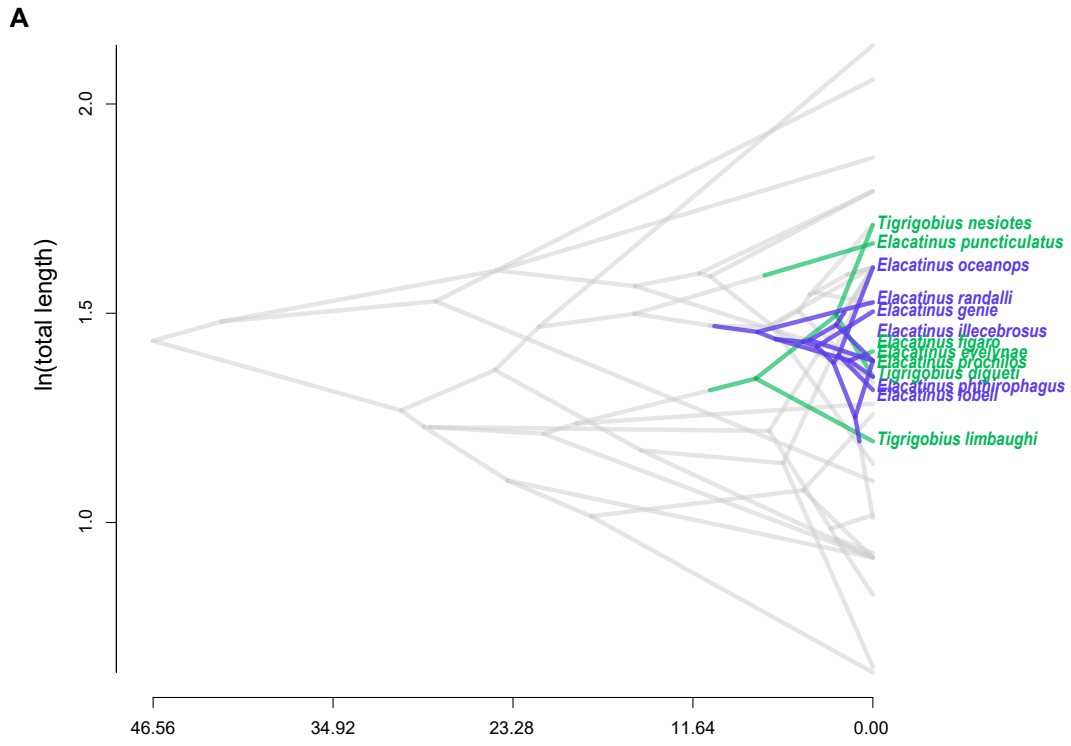


Fig. 2.6 – Phylomorphospace of Western Atlantic gobies (on following page). The first two principal components of a phylogenetic PCA (Revell 2009) are shown, with MCC phylogeny and inferred ancestral character states. Shapes along the ends of each axis indicate displacements of landmarks (i.e. loadings) along that axis (see Methods for more details). For clarity, only species in peripheral regions of the phylomorphospace are labeled. Colors indicate dietary group: purple – obligate cleaner; green – facultative cleaner; grey – non-cleaner.

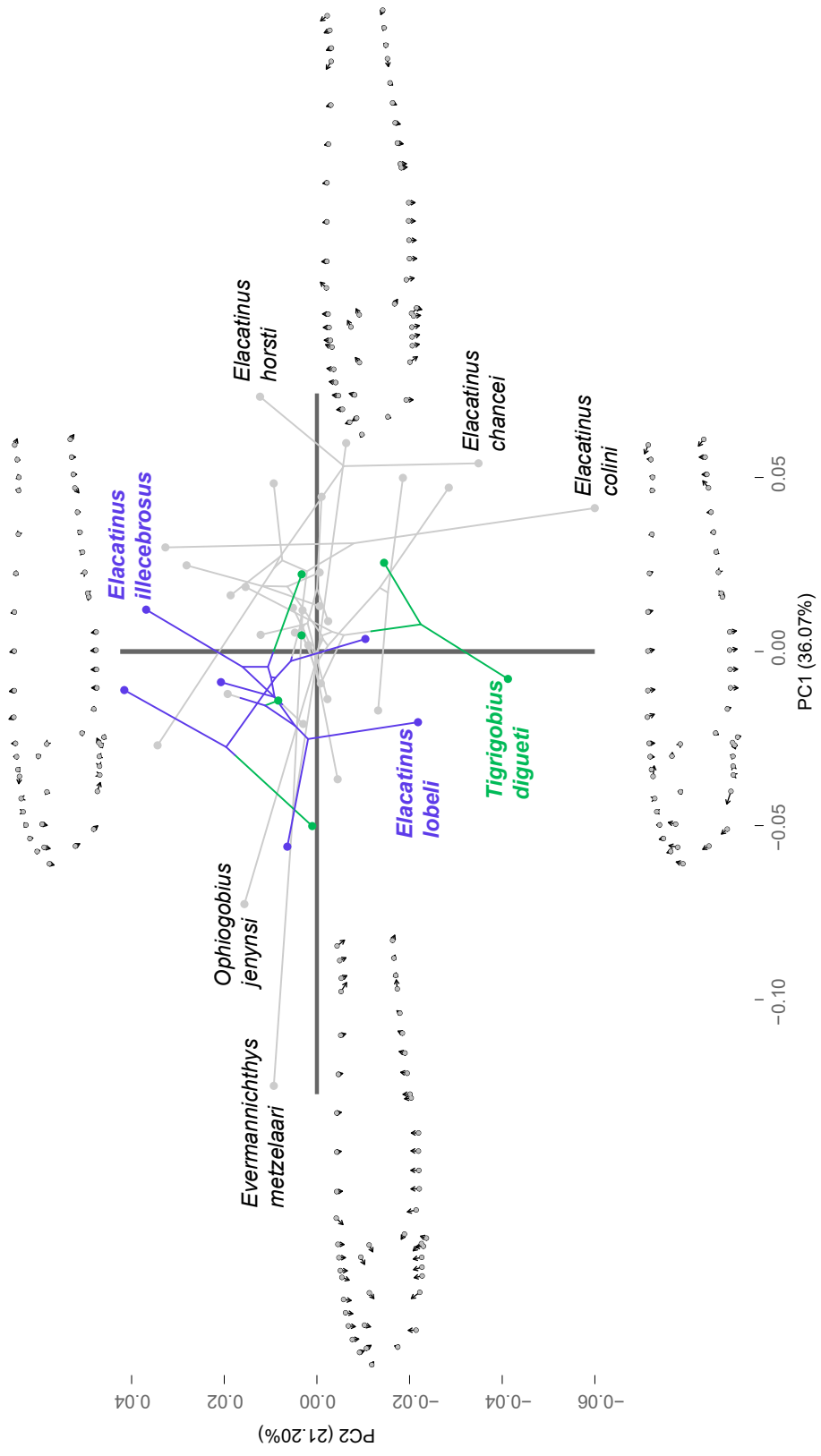


Fig. 2.7 – Phylomorphospace of labrids (on following page). The first two principal components of a phylogenetic PCA (Revell 2009) are shown, with MCC phylogeny and inferred ancestral character states. Shapes along the ends of each axis indicate displacements of landmarks (i.e. loadings) along that axis (see Methods for more details). For clarity, only species in peripheral regions of the phylomorphospace are labeled. Colors indicate dietary group: purple – obligate cleaner; green – facultative cleaner; orange – juvenile cleaner; grey – non-cleaner.

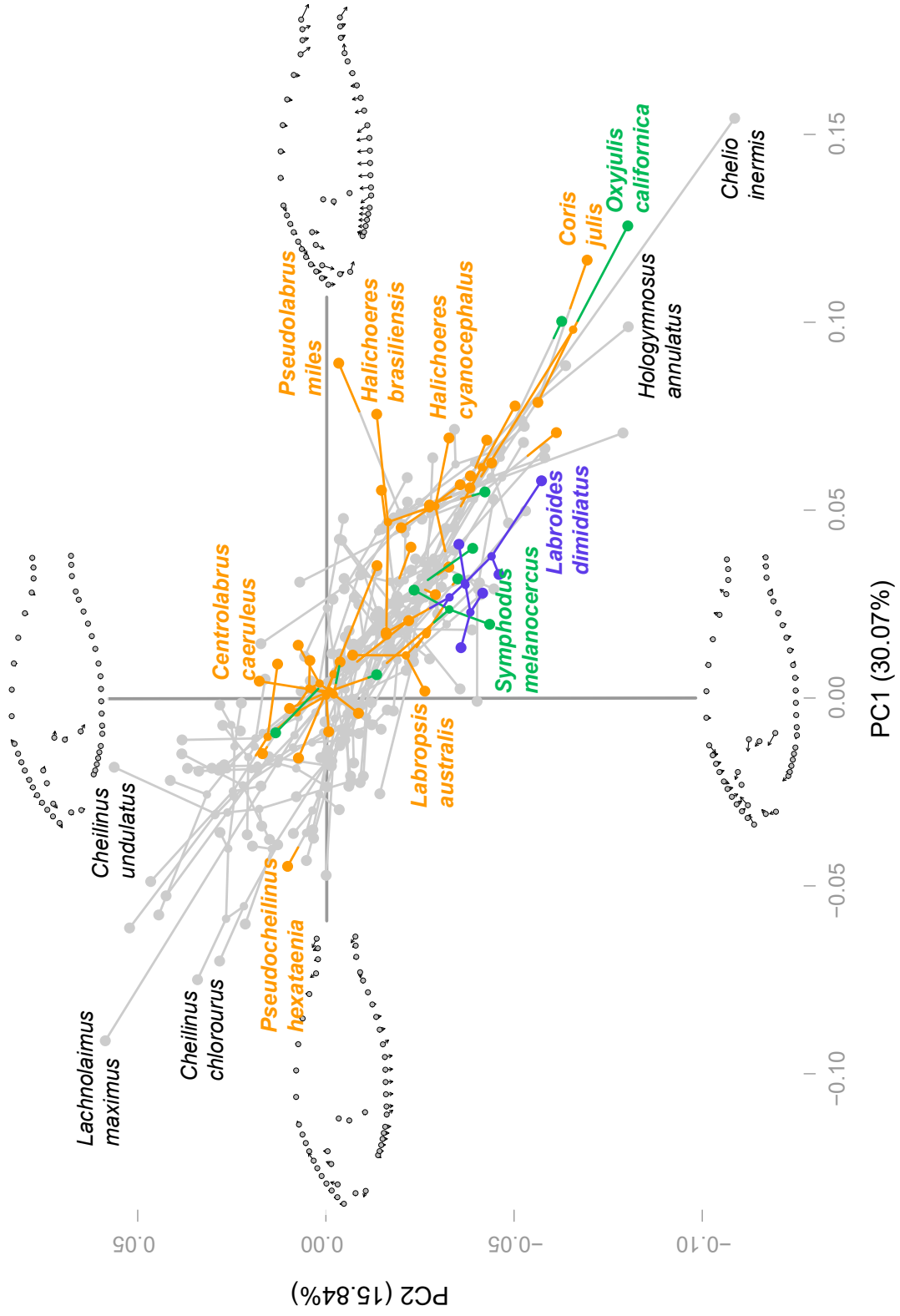
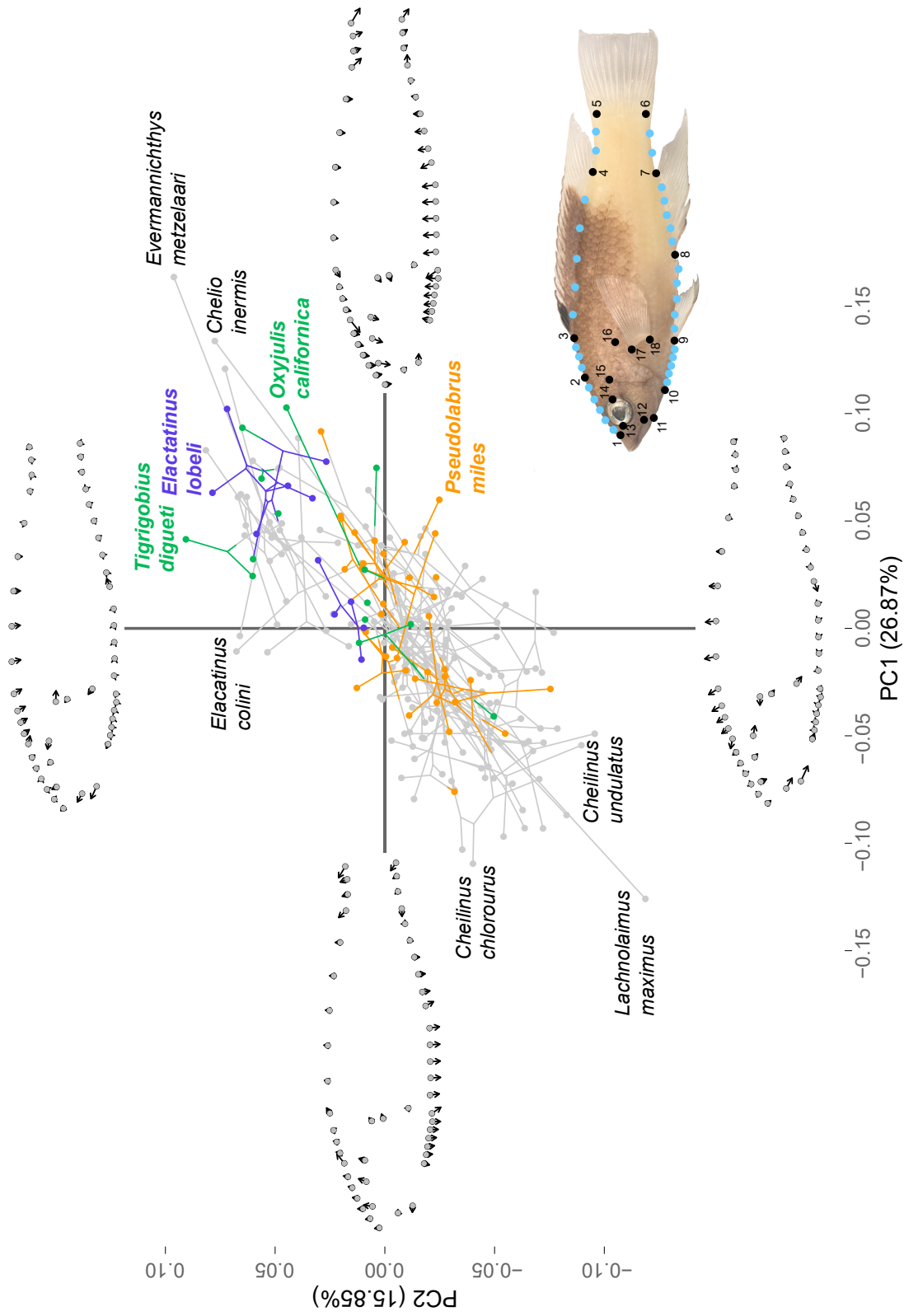


Fig. 2.8 – Combined phylomorphospace of gobiid and labrid taxa (on following page). The first two principal components of a phylogenetic PCA (Revell 2009) are shown, with MCC phylogeny and inferred ancestral character states. Shapes along the ends of each axis indicate displacements of landmarks (i.e. loadings) along that axis (see Methods for more details). For clarity, only species in peripheral regions of the phylomorphospace are labeled. For convenience, Fig. 2.2 is reproduced in the bottom right corner. Colors indicate dietary group: purple – obligate cleaner; green – facultative cleaner; orange – juvenile cleaner; grey – non-cleaner.



along the ventral aspects of the body. Along PC 2, species with higher positive scores possessed mouths that were more terminally-oriented along with additional reduction in body depth, predominately along the dorsal aspect of the body. In this phylomorphospace, gobies as a group had higher positive scores on PCs 1 and 2, indicating that members of this family tended to exhibit more extreme patterns of elongation than labrids. These PCs also showed significant correlation (Pearson's r : 0.75; $p < 0.001$), indicating that shape changes occurring along these axes are related.

Among gobiid taxa (Table 2.4, Figure 2.6), I found cleaner fishes as a group (12 species from 2 genera) did not show significant convergence (Stayton's C_4 : 0.0051; p -value: 0.105). Furthermore, facultative gobiid cleaners did not show significant convergence (Stayton's C_4 : 0.0052; p -value: 0.282).

Within the labrid phylomorphospace, I found that cleaner fishes as a group showed significant convergence (Stayton's C_4 : 0.0066; p -value: 0.002; Table 2.4, Figure 2.7). While juvenile cleaners similarly did not show significant convergence (Stayton's C_4 : 0.0030; p -value: 0.126), facultative taxa (8 species from 8 genera) did (Stayton's C_4 : 0.0066; p -value: 0.002).

Cleaner fishes (combined juvenile, facultative and obligate) in the Labridae and Gobiidae did not show significant convergence (Stayton's C_2 : 0.0450; p -value: 0.293) in a combined phylomorphospace for both groups (Table 2.4, Fig 2.8). When convergence was assessed among obligate taxa only (in *Labroides* and *Elacatinus*), I found significant convergence (Stayton's C_2 : 0.0696; $p < 0.001$). Among facultative

taxa (14 total species hailing from 8 labrid and 2 gobiid genera), I also found significant convergence (Stayton's C_2 : 0.050; $p < 0.001$).

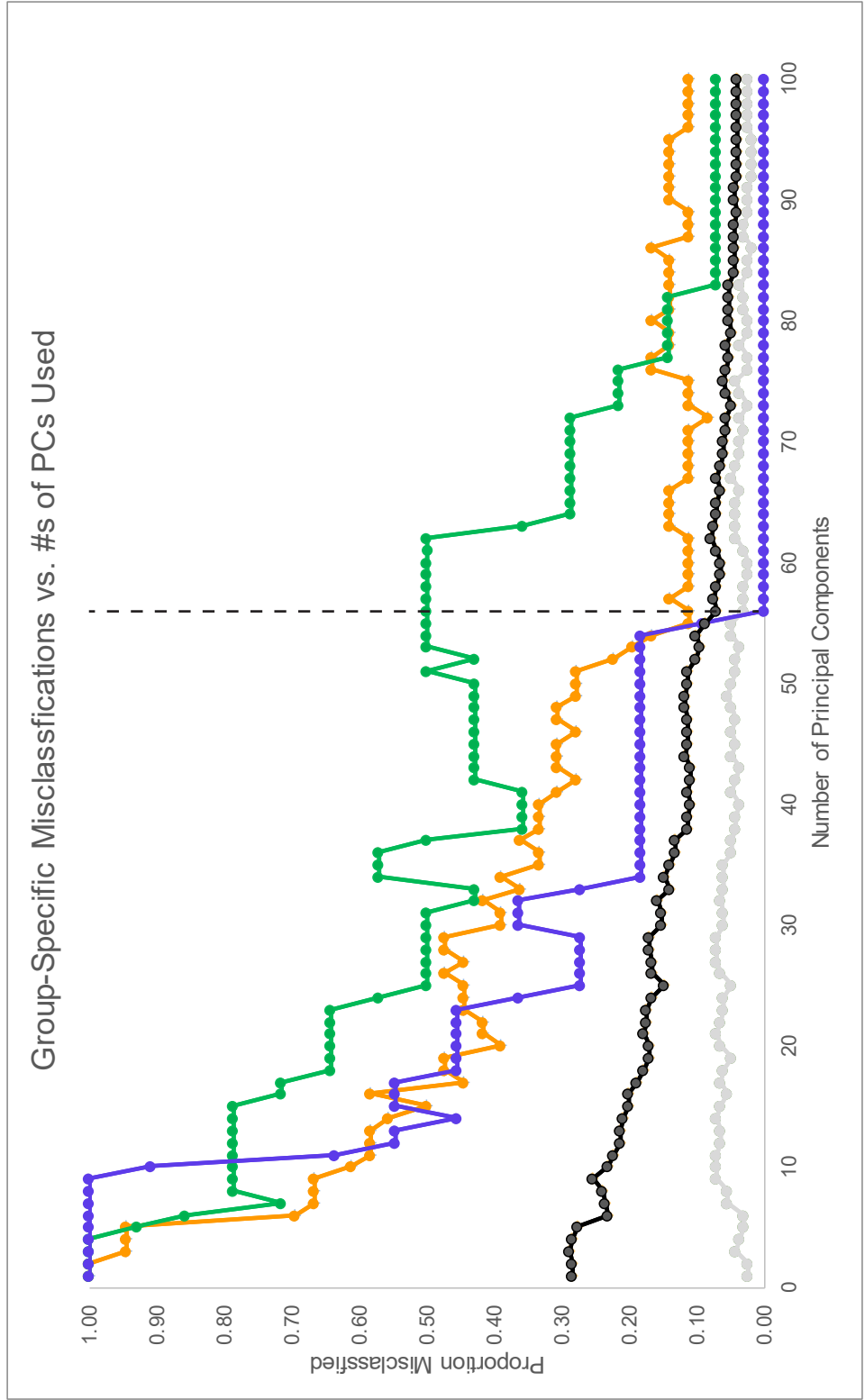
Table 2.4 Metrics of convergence among cleaners within each phylomorphospace

Phylomorphospace	Group	Stayton's C_2	C_2 p-value	Stayton's C_4	C_4 p-value
Gobiid	All Cleaners	-	-	0.0051	0.105
Gobiid	Facultative Cleaners	-	-	0.0052	0.282
Labrid	All Cleaners	-	-	0.0068	0.011
Labrid	Facultative Cleaners	-	-	0.0066	0.002
Labrid	Juvenile Cleaners	-	-	0.0030	0.126
Gobiid + Labrid	All Cleaners	0.0450	0.293	-	-
Gobiid + Labrid	Obligate Cleaners	0.0696	< 0.001	-	-
Gobiid + Labrid	Facultative Cleaners	0.0500	< 0.001	-	-

Definitions and procedure for hypothesis testing for Stayton's C_2 and C_4 follow Stayton (2014). Within each set of analyses for a particular phylomorphospace, p-values were adjusted for multiple hypothesis testing following Benjamini and Hochberg (1995).

Iteratively varying the number of principal component axes as inputs to pFDA allowed us to determine that 100% of obligate cleaner taxa could be correctly classified with a minimum of 56 pPCA axes (Figure 2.9). Thus, using the first 56 pPCA axes provided information on how obligate cleaners could be discriminated from taxa in other dietary groups. Correlations between the original pPCA axes and pFDA discriminant axes provide information on how shape changes along axes informed the discriminant function (Table 2.5). Obligate taxa were separated from all others along the third discriminant axis (DA3). Among the primary axes of variation in the dataset, PCs 2, 7, 8 and 9 were especially informative in discriminating obligate

Fig. 2.9 – Group-specific misclassifications (on following page). An iterative procedure, wherein the number of phylogenetic PCA axes used as input to phylogenetic FDA ranged from 1 to 100, was used to avoid over-parameterizing the final discriminant function. The overall misclassification (black) and the proportion of taxa within each dietary group that were misclassified by each discriminant analysis is shown. As no single set of PC axes minimized misclassifications in all dietary groups, the smallest set of PCs in which all obligate cleaners could be discriminated from each of the other groups (PCs 1-56; dashed vertical line) was used to generate the final model.



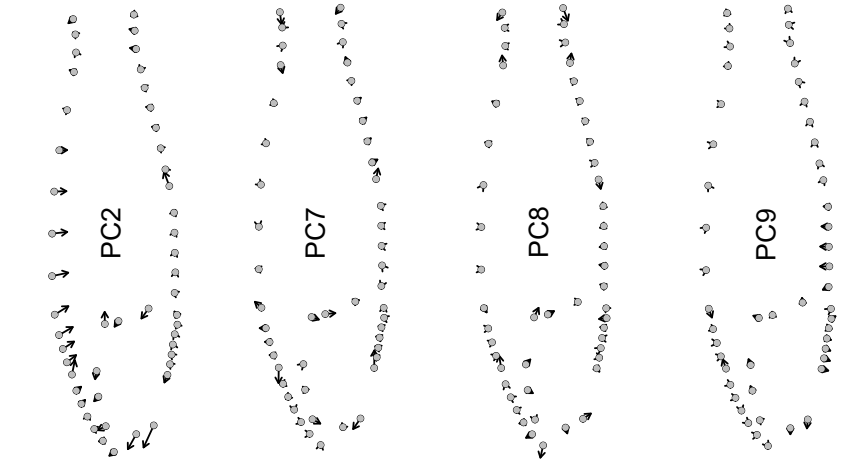
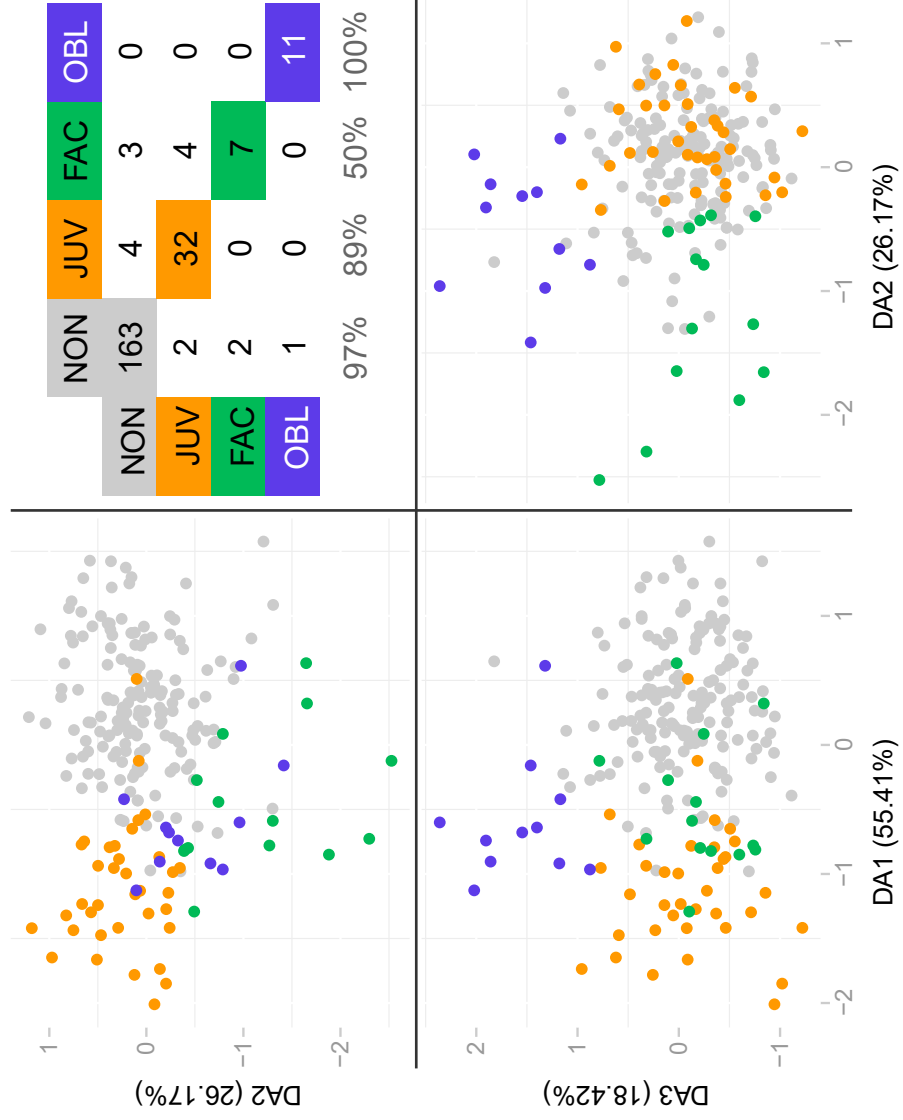
taxa from other cleaners and non-cleaners. Loadings of these PCs are plotted in Figure 2.10. Along these axes, obligate species tended to show more elongate bodies (predominately via a reduction in body depth), have more terminally-located mouths, and more elongate heads (by an increase in head length and a slight decrease in head depth).

Using pPCA axes 1 through 56, I also found that misclassifications among non-cleaner and juvenile cleaner taxa were low: among non-cleaners 5 of 168 species were misclassified (3.0% error) and among juvenile cleaners 4 of 36 were misclassified (11.1% error). Facultative cleaners experienced an elevated misclassification rate: 7 of 14 species were misclassified (50% error). Cleaner fishes (including obligate, facultative and juvenile cleaner taxa) could largely be discriminated from non-cleaners along DA1.

Table 2.5 Loadings of PC axes in pFDA (on following page). Correlations between original phylogenetic PCA axes and the axes of the phylogenetic Flexible Discriminant Analysis. The proportion of variance for which each discriminant axis accounts is listed in the column headings. Bolding indicates significant correlation ($\alpha = 0.05$). A heatmap effect has been added over cells with significant correlation: warmer colors indicate higher positive correlations, while cooler colors indicate stronger negative correlations.

	DA1 (55.41%)	DA2 (26.17%)	DA3 (18.42%)
PC1	-0.26	-0.40	0.24
PC2	-0.18	-0.50	0.31
PC3	-0.23	-0.05	0.11
PC4	0.09	-0.17	0.05
PC5	0.03	0.50	-0.15
PC6	0.33	-0.25	-0.21
PC7	-0.11	0.15	-0.30
PC8	-0.16	0.02	-0.25
PC9	-0.09	-0.06	0.26
PC10	-0.16	0.28	0.00
PC11	0.11	0.29	-0.24
PC12	0.09	-0.23	0.18
PC13	-0.02	0.04	0.01
PC14	0.25	-0.13	-0.14
PC15	-0.05	0.24	0.12
PC16	0.20	-0.24	0.02
PC17	0.18	-0.49	0.21
PC18	0.08	-0.24	0.11
PC19	0.06	-0.31	0.19
PC20	-0.12	-0.21	0.08
PC21	0.20	0.01	-0.05
PC22	0.17	0.08	-0.04
PC23	0.18	0.30	0.13
PC24	-0.30	-0.21	0.30
PC25	-0.18	0.04	-0.03
PC26	-0.16	-0.05	0.00
PC27	-0.19	0.24	-0.29
PC28	0.09	0.22	-0.22
PC29	-0.03	0.19	-0.07
PC30	0.27	0.09	-0.42
PC31	-0.03	0.11	-0.07
PC32	0.01	0.36	-0.19
PC33	-0.09	-0.36	0.25
PC34	0.03	-0.03	0.20
PC35	0.09	-0.28	0.22
PC36	-0.19	0.39	-0.17
PC37	0.16	0.34	-0.29
PC38	-0.05	0.15	-0.31
PC39	0.03	-0.28	0.23
PC40	0.15	-0.41	0.34
PC41	-0.21	0.01	-0.12
PC42	0.09	0.37	-0.23
PC43	-0.12	0.27	-0.21
PC44	0.22	0.08	-0.12
PC45	-0.03	-0.02	-0.13
PC46	0.24	0.07	-0.29
PC47	-0.13	-0.16	0.12
PC48	0.17	-0.12	0.20
PC49	-0.01	-0.26	0.12
PC50	-0.04	0.22	-0.20
PC51	0.07	0.34	-0.15
PC52	0.20	0.03	-0.11
PC53	-0.22	-0.20	0.21
PC54	-0.13	-0.25	0.29
PC55	-0.10	0.31	0.13
PC56	-0.12	0.30	-0.17

Fig. 2.10 – Phylogenetical Flexible Discriminant Analysis of geometric morphometric data (on following page). Using the first 56 axes from the phylogenetic PCA (pPCA) of gobiids and labrids, dietary group information, and the MCC phylogeny of these taxa, a phylogenetic Flexible Discriminant Analysis (pFDA; Motani and Schmitz 2011) was performed. The pFDA yielded three axes, which are plotted here. A confusion matrix is shown and indicates that most taxa were correctly classified. Obligate cleaners are clearly separated from the other dietary groups along DA3. Shape changes captured along the third discriminant axis (DA3) are plotted using representations of shape change along the pPCA axes that show strongest correlations with DA3.



2.4 Discussion

In the present study, I first inferred phylogenies for a set of Western Atlantic gobies and then a combined labrid and Western Atlantic gobiid taxon set. I used stochastic character mapping to infer how cleaning evolved within labrids and gobies. Using a phylogenetic comparative approach, we then analyzed whether the evolution of cleaning is associated with particular patterns of body size evolution. Finally, I examined body shape to understand the extent to which cleaner fishes in these families exhibit morphological convergence.

2.4.1 Phylogenetic Inference

The Western Atlantic gobiid maximum clade credibility (MCC) phylogeny is largely congruent with previously published phylogenies (Taylor and Hellberg 2005; Thacker 2015). The Bayesian phylogenetic analyses converged on divergence times among taxa that are similar to those in previous findings. Similarly, the combined labrid and Western Atlantic gobiid MCC phylogeny showed congruence with previously published phylogenies that have incorporated both families (Near et al. 2013; Rabosky et al. 2013).

Stochastic character mappings revealed that cleaning likely evolved three separate times in the Gobiidae, with two additional transitions back to non-cleaning. Obligate cleaning in *Elacatinus* appears to likely have arisen from a single evolutionary event, which is similar to the singular transition inferred in the evolution of obligate *Labroides* wrasses. Not only do these transitions occur in geographically distinct

areas (Figure 2.1), but they also appear to have evolved nearly concurrently: the transition to obligate cleaning likely occurred between 8 and 11 MYA in each group (Figure 2.3). Thus the evolution of obligate cleaning evolved in parallel in the Caribbean and Indo-Pacific within similar spans of time.

Unlike the labrid transition, however, obligate cleaning in *Elacatinus* is immediately preceded by non-cleaning; obligate cleaning in *Labroides* likely evolved from a juvenile cleaning state (Baliga and Law 2016; present study). Furthermore, obligate taxa in *Elacatinus* form a paraphyletic group, as there are three transitions to facultative cleaning and two transitions away from cleaning within the clade of obligate taxa. This is in stark contrast to the condition seen in *Labroides*, in which no secondary transitions to other states occur after the onset of obligate cleaning. Moreover, the pattern and process by which cleaning evolved in each family appears to be fundamentally different; no cleaner gobies are classified as juvenile cleaners, and thus transitions involving a juvenile cleaning state are not apparent. Whether non-cleaner gobies are perhaps “pre-adapted” to cleaning compared to non-cleaner labrids can be addressed by scrutinizing both size and shape among taxa.

2.4.2 *Cleaning and the evolution of maximum body size*

I found marginal evidence that the evolution of cleaning behavior influenced patterns of maximum body size for those species that clean, albeit to different degrees throughout their lives. In both the gobiid and labrid analyses, a single-optimum model was favored over diet-specific models, indicating that it was more likely that within

each family, the evolution of facultative and obligate cleaning is not associated with shifts in optimal body size. Because all known gobiid cleaners (14 taxa) and all labrid facultative and obligate cleaners (14 of 14 total species) were incorporated into the analyses, it is unlikely that incorporating body size data for additional species would affect my findings. On the other hand, nearly all facultative and obligate taxa are smaller than 23 cm total length, and occur in lineages in which body size trends are of a similar magnitude. The finding that the evolution of facultative and obligate cleaning itself does not affect body size optima, yet nearly all such species are nevertheless small indicates that these forms of cleaning are limited to arising in relatively smaller-bodied non-cleaner lineages.

Only in the case of *Labrus bergylta* do we find a facultative labrid cleaner that measures, at maximum, larger than 23 cm. *L. bergylta* presents a particularly interesting case, as observations of cleaning behavior in this species have largely involved their removal of sea lice (*Lepeophtheirus salmonis*) on farmed Atlantic salmon (Leclercq 2013). The extent to which this species cleans in nature is less established. Moreover, suites of traits which enhance sea lice removal may differ from those that are optimal for other forms of ectoparasitivism, as sea lice are substantially larger than gnathiid isopods found in the Indo-Pacific.

2.4.3 Shape diversity and the extent of convergence in cleaners

I found that the major axis of variation within the Labridae and Gobiidae involved elongation of the body, with gobiids as a group showing higher elongation than

labrids. This pattern of shape reinforces what has been shown in a larger dataset of marine fish taxa (Clavarié and Wainwright 2014). In using phylogenetic PCA, I found that pPCA axes often showed correlations, which is a recognized phenomenon when conducting these analyses (Revell 2009). These correlations capture an interesting facet of body shape evolution in labrids and gobiids: reductions in body and head depth appear to be evolutionary concordant with anterior shifts in pectoral fin attachment points and the possession of a more terminally-oriented mouth.

In a shared phylomorphospace, I found that labrid and gobiid cleaner fishes, as a group, did not exhibit morphological convergence. In scrutinizing patterns among juvenile, facultative, and obligate cleaners separately, my finding that facultative and obligate taxa each show convergence suggests that a lack of convergence among juvenile cleaner taxa drives the overall pattern. This hypothesis was confirmed by the labrid-specific phylomorphospace – juvenile cleaner fishes did not show significant convergence. Indeed, in both the labrid-specific phylomorphospace as well as the combined labrid and gobiid phylomorphospace, juvenile cleaners generally showed a diversity of body shapes, and in some cases occupied the most peripheral regions of each morphospace. While some labrid juvenile cleaners are extremely elongate (e.g. *Coris julis*) others (e.g. *Pseudocheilinus hexataenia*, *Centrolabrus caeruleus*) show an opposite trend: these taxa are more deep-bodied than their inferred ancestral states. Why the evolutionary patterns associated with these taxa do not conform to the patterns seen in the majority of other cleaners remains unknown.

Facultative cleaners in these families also show diverse patterns of convergence. Within the gobiid-specific phylomorphospace, facultative cleaners did not show significant convergence, which may be an important driver for the observation that gobiid cleaners (facultative + obligate) do not exhibit convergence. Facultative cleaning arose from disparate lineages and their starting points are diverse. Within labrids, however, facultative taxa showed significant convergence. In general, these taxa appear to have evolved towards a more elongate body shape, as the majority of these taxa show increases in scores along PC 1 of the labrid phylomorphospace.

Obligate cleaners show significant convergence in the shared labrid and gobiid phylomorphospace, indicating that the *Labroides* and *Elacatinus* lineages have evolved towards similar phenotypes over time. The discriminant analysis revealed that a reduction in body depth, elongation of the head, and a more terminal placement of the mouth are key hallmarks of obligate cleaner morphology. While the selection of PC axes as inputs to the discriminant analyses was informed by optimizing the classification of obligate cleaners, distinctions between all cleaners and non-cleaners could still largely be discerned along DA 1. Along this axis, species with more negative scores (i.e. cleaners) showed reductions in body depth, more terminal mouth positions, and slight elongation of the head. Together, these findings suggest that selection for cleaning largely operates on similar axes, regardless of whether taxa perform the behavior obligately. High phenotypic convergence in obligate cleaners that have evolved around the same evolutionary time scale but in different marine

clades suggests strong selection pressures on body features that are integrated with this tropic strategy.

2.5 Conclusions

In both the Gobiidae and Labridae, I found limited evidence that the evolution of facultative and obligate cleaning is associated with shifts in optimal body size. Generally, these taxa are relatively small, with nearly all species measuring less than 23 cm total length. Together, these results indicate that certain smaller-bodied lineages within these families may have been historically “pre-adapted” to evolve cleaning over ontogeny. Through phylogenetic inference, I also found that obligate cleaning in these families appears to have evolved contemporaneously (8 – 11 MYA) in separate geographic regions. These cleaners exhibited significant morphological convergence in a combined gobiid and labrid body shape phylomorphospace. While facultative and juvenile cleaner taxa showed varying patterns of convergence, I found that the evolution of cleaning is generally associated with a reduction in body depth, elongation of the head, and a more terminal orientation of the mouth. These traits may enhance a cleaner’s ability to remove ectoparasites that occupy vulnerable, tightly-confined, and hard to reach places such as the gills and oral cavity of their clients.

2.6 References

- Alfaro ME, Brock CD, Banbury BL, Wainwright PC. 2009. Does evolutionary innovation in pharyngeal jaws lead to rapid lineage diversification in labrid fishes? *BMC Evol. Biol.* 9, 255. doi:10.1186/1471-2148-9-255
- Baliga VB, Law CJ. 2016. Cleaners among wrasses: Phylogenetics and evolutionary patterns of cleaning behavior within Labridae. *Mol. Phyl. Evol.* 94, 424-435. (doi:10.1016/j.ympev.2015.09.006)
- Baliga VB, Mehta RS. 2016 (*In review*). Ontogeny and flexibility: Shape changes underlie life history patterns of cleaning behaviour. *Integ. Comp. Biol.*
- Bannikov A, Carnevale G. 2010. *Bellwoodilabrus landinii* n. gen., n. sp., a new genus and species of labrid fish (Teleostei, Perciformes) from the Eocene of Monte Bolca. *Geodiversitas.* 33, 201–220. doi:10.5252/g2010n2a2
- Bannikov AF, Sorbini L. 1990. *Eocoris bloti*, a new genus and species of labrid fish (Perciformes, Labroidei) from the Eocene of Monte Bolca, Italy. *Studie Ricerche sui Giacimenti Terziari di Bolca, Museo Civico di Storia Naturale, Verona.* 6, 133–148.
- Barber PH, Bellwood DR. 2005. Biodiversity hotspots: evolutionary origins of biodiversity in wrasses (*Halichoeres*: Labridae) in the Indo-Pacific and new world tropics. *Mol. Phylogenet. Evol.* 35: 235–253. doi:10.1016/j.ympev.2004.10.004
- Beaulieu JM, Jhwueng DC, Boettiger C, O'Meara BC. 2012. Modeling stabilizing selection: Expanding the Ornstein-Uhlenbeck model of adaptive evolution. *Evolution* 66:2369-2383.
- Benjamini Y, Hochberg Y. 1995. Controlling the false discovery rate: a practical and powerful approach to multiple testing. *J. Roy. Stat. Soc. B.* 57, 289–300.
- Bellwood DR. 1990. A new fossil fish *Phyllopharyngodon longipinnis* gen. et sp. nov. (family Labridae) from the Eocene, Monte Bolca, Italy. *Studie Ricerche sui Giacimenti Terziari di Bolca, Museo Civico di Storia Naturale, Verona.* 6, 149–160.
- Bellwood DR, Schultz O. 1991. A review of the fossil record of the parrotfishes (Labroidei: Scaridae) with a description of a new *Calotomus* species from the Middle Miocene (Badenian) of Austria. *Ann. Naturhist. Mus. Wien.* 92, 55–71.
- Bellwood DR, Wainwright PC, Fulton CJ, Hoey AS. 2006. Functional versatility supports coral reef biodiversity. *Proc. R. Soc. B Biol. Sci.* 273, 101–107. doi:10.1098/rspb.2005.3276

- Boettiger C, Coop G, and Ralph P. 2012. Is your phylogeny informative? Measuring the power of comparative methods, *Evolution* 66 (7) 2240-51. doi:10.1111/j.1558-5646.2011.01574.x
- Bollback JP. 2006. SIMMAP: stochastic character mapping of discrete traits on phylogenies. *BMC Bioinformatics* 7, 88. doi:10.1186/1471-2105-7-88
- Bouckaert R, Heled J, Kühnert D, Vaughan T, Wu C-H, Xie D, Suchard MA, Rambaut A, Drummond AJ. 2014. BEAST 2: A Software Platform for Bayesian Evolutionary Analysis. *PLoS Comp. Biol.* 10, e1003537. doi:10.1371/journal.pcbi.1003537
- Burgess WE, Axelrod HR, Hunziker R. 1991. *Atlas of Marine Aquarium Fishes*. Neptune City, NJ: T.F.H. Publications, Inc.
- Claverie T, Wainwright PC. 2014. A morphospace for reef fishes: Elongation is the dominant axis of body shape evolution. *PLoS One*. 9:e112732.
- Coates AG, Obando JA. 1996. The Geologic Evolution of the Central American Isthmus. p. 21. In: Jackson, J.B.C., Budd, A.F. and Coates, A.G. (eds.) *Evolution and environment in Tropical America*. University of Chicago Press, Chicago.
- Collar DC, Wainwright PC, Alfaro ME. 2008. Integrated diversification of locomotor and feeding in labrid fishes. *Biol Lett* 4: 84-86.
- Côté IM. 2000. Evolution and Ecology of Cleaning Symbioses in the Sea. *Oceanogr. Mar. Biol. an Annu. Rev.* 38, 311–355.
- Côté IM, Soares MC. 2011. Gobies as Cleaners. In *The Biology of Gobies*. New York, NY. CRC Press: 525-551.
- Cowman PF, Bellwood DR. 2011. Coral reefs as drivers of cladogenesis: expanding coral reefs, cryptic extinction events, and the development of biodiversity hotspots. *J. Evol. Biol.* 24, 2543–62. doi:10.1111/j.1420-9101.2011.02391.x
- Darriba D, Taboada GL, Doallo R, Posada D. 2012. jModelTest 2: more models, new heuristics and parallel computing. *Nat. Methods*. 9, 772. doi:10.1038/nmeth.2109
- Evans MEK, Smith SA, Flynn RS, Donoghue MJ. 2009. Climate, niche evolution, and diversification of the "bird-cage" evening primroses (*Oenothera*, sections *Anogra* and *Kleinia*). *Am. Nat.* 173, 225-240.
- Feder HM. 1966. Cleaning symbiosis in the marine environment. In *Symbiosis*, S.M. Henry (ed.). New York: Academic Press, 327-380.
- Froese R, Pauly D. 2016. FishBase, Version (5/2015). www.fishbase.org.

- GBIF. 2016. Labroides and Elacatinus. 4078 records, accessed on 3 March 2016.
GBIF IDs: 2383728 and 2376682.
- Gower JC. 1975. Generalized Procrustes analysis. *Psychometrika* 40:33-51.
- Grutter AS. 1996. Parasite removal rates by the cleaner wrasse *Labroides dimidiatus*.
Mar. Ecol. Prog. Ser. 130, 61–70.
- Grutter AS. 2010. Cleaner fish. *Curr. Biol.* 20, 547–549.
doi:10.1016/j.cub.2010.04.013
- Higham TE, Hulsey CD, Rican O, Carroll AM. 2007. Feeding with speed: prey capture evolution in cichlids. *J. of Evol. Biol.* 20, 70-78.
- Huelsenbeck JP, Nielsen R, Bollback JP. 2003. Stochastic Mapping of Morphological Characters. *Syst. Biol.* 52, 131–158. doi:10.1080/10635150390192780
- Kazancıoğlu E, Near TJ, Hanel R, Wainwright PC. 2009. Influence of sexual selection and feeding functional morphology on diversification rate of parrotfishes (Scaridae). *Proc. R. Soc. B Biol. Sci.* 276, 3439–46.
doi:10.1098/rspb.2009.0876
- Leclercq E, Davie A, and Migaud H. 2013. Delousing efficiency of farmed ballan wrasse (*Labrus bergylta*) against *Lepeophtheirus salmonis* infecting Atlantic salmon (*Salmo salar*) post-smolts. *Pest. Manag. Sci.* 2014; 70: 1274–1282.
doi:10.1002/ps.3692
- Montes C, Cardona A, Jaramillo C, Pardo A, Silva JC, Valencia V, Ayala C, Perez-Angel LC, Rodriguez-Parra LA, Ramirez V, Nino H. 2015. Middle Miocene closure of the Central American Seaway. *Science.* 348, 5–8.
- Motani R, Schmitz L. 2011. Phylogenetic versus functional signals in the evolution of form-function relationships in terrestrial vision. *Evolution.* 65, 2245-2257.
(doi:10.1111/j.1558-5646.2011.01271.x)
- Myers RF. 1999. Micronesian reef fishes: a comprehensive guide to the coral reef fishes of Micronesia, 3rd revised and expanded edition. Coral Graphics, Barrigada, Guam.
- Near TJ, Dornburg A, Eytan RI, Keck BP, Smith WL, Kuhn KL, Moore JL, Price SA, Burbrink FT, Friedman M, Wainwright PC. 2013. Phylogeny and tempo of diversification in the superradiation of spiny-rayed fishes. *Proc. Nat. Acad. Sci.* 101:12738-21743. doi:10.1073/pnas.1304661110
- Nielsen R. 2002. Mapping mutations on phylogenies. *Syst. Biol.* 51, 729–39.
doi:10.1080/10635150290102393

- Rabosky DL, Santini F, Eastman J, Smith SA, Sidlauskas B, Chang J, Alfaro ME. 2013. Rates of speciation and morphological evolution are correlated across the largest vertebrate radiation. *Nat. Commun.* 4, 1-8. doi:10.1038/ncomms2958
- Rambaut A, Suchard MA, Xie D, Drummond AJ. 2014. Tracer v1.6, Available from <http://beast.bio.ed.ac.uk/Tracer>
- Randall JE, Allen GR, Steene RC. 1997. *Fishes of the Great Barrier Reef and Coral Sea*. Crawford House Publishing, Bathurst, Australia.
- Revell LJ. 2009. Size-correction and principal components for interspecific comparative studies. *Evolution* 63, 3258-3268. (doi:10.1111/j.1558-5646.2009.00804.x)
- Revell LJ. 2012. phytools: an R package for phylogenetic comparative biology (and other things). *Methods Ecol. Evol.* 3, 217–223. doi:10.1111/j.2041-210X.2011.00169.x
- Rice AR, Wesncoat MW. 2005. Coordination of feeding, locomotor and visual systems in parrotfishes (Teleostei: Labridae). *J. Exp. Biol.* 208: 3503-3518.
- Rohlf FJ. 2006. tpsDig, version 2.10. Department of Ecology and Evolution, State University of New York, Stony Brook.
- Schultz O, Bellwood DR. 2004. *Trigonodon oweni* and *Asima jugleri* are different parts of the same species *Trigonodon juleri*, a Chiseltooth Wrasse from the lower and middle Miocene in the Central Europe (Osteichthyes, Labridae, Pseudodacninae). *Ann. Naturhist. Mus. Wien.* 105, 287–305.
- Sidlauskas B. 2008. Continuous and arrested morphological diversification in sister clades of characiform fishes: a phylomorphospace approach. *Evolution* 62, 3135–3156. (doi:10.1111/j.1558-5646.2008.00519.x)
- Stayton CT. 2014. convevol: Quantifies and assesses the significance of convergent evolution. R package version 1.0. Available at <http://cran.r-project.org/web/packages/convevol/index.html>.
- Stayton CT. 2015. The definition, recognition, and interpretation of convergent evolution, and two new measures for quantifying and assessing the significance of convergence. *Evolution* 69, 2140-2153. (doi:10.1111/evo.12729)
- Taylor MS, and Hellberg ME. 2005. Marine radiations at small geographic scales: speciation in neotropical reef gobies (*Elacatinus*). *Evolution*, 59(2):374-385. doi:10.1554/04-590

- Thacker CE. 2015. Biogeography of goby lineages (Gobiiformes: Gobioidae): origin, invasions and extinction throughout the Cenozoic. *J. Biogeogr.* 42, 1615–1625.
- Vaidya G, Lohman DJ, Meier R. 2011. Cladistics multi-gene datasets with character set and codon information. *Cladistics.* 27, 171–180.
- Wainwright PC, Bellwood DR, Westneat MW, Grubich JR, Hoey AS. 2004. A functional morphospace for the skull of labrid fishes: patterns of diversity in a complex biomechanical system. *Biol. J. Linn. Soc.* 82, 1–25. doi:10.1111/j.1095-8312.2004.00313.x
- Westneat MW, Alfaro ME. 2005. Phylogenetic relationships and evolutionary history of the reef fish family Labridae. *Mol. Phylogenet. Evol.* 36, 370–90. doi:10.1016/j.ympev.2005.02.001
- White JW, Grigsby CJ, Warner RR. 2007. Cleaning behavior is riskier and less profitable than an alternative strategy for a facultative cleaner fish. *Coral Reefs.* 26: 87–94 doi:10.1007/s00338-006-0161-2

**Chapter 3 – An evolutionary approach to scaling: Phylo-
allometric analyses indicate concordance between
morphology and the ontogeny of cleaning behavior in
wrasses**

Vikram B. Baliga^a, Rita S. Mehta^a

^aDepartment of Ecology and Evolutionary Biology, Long Marine Laboratory,
University of California Santa Cruz, 100 Shaffer Road, Santa Cruz, CA 95060, USA

Abstract

Recent studies comparing ontogenetic trajectories of closely-related taxa provide evidence that ontogenetic processes evolve. The evolution of these processes is what produces diversity in adult phenotypes. Comparative studies of scaling, however, must be placed in a phylogenetically-informed context, as phylogenetic information is inherently present in ontogeny. Using the evolution of cleaning behavior in the Labridae as a case study, we provide a phylogenetic framework in which the ontogenetic trajectories of multiple taxa can be compared. We first show that in the juvenile phase, cleaner fishes exhibit convergence in body, fins, and cranial traits. We then show evidence that taxa that transition away from cleaning during ontogeny exhibit phenotypic trajectories that are distinct from those of other wrasses. On the other hand, obligate and facultative species who continue to clean over ontogeny maintain characters that are conducive to cleaning in the juvenile phase. Overall, labrids exhibit a variety of ontogenetic trajectories, highlighting the diversity of ways in which phenotypic variation is generated over ontogeny.

3.1 Introduction

Ontogeny is fundamentally important to studies of evolutionary morphology. Juvenile animals are often ecologically distinct from their adult counterparts: they typically do not face the same functional demands. Accordingly, ecological opportunity may present itself only in particular life history phases, which could drive the scaling of traits over an organism's lifetime. Metamorphosis provides perhaps the most tangible examples of strong concordance between ecological and morphological shifts over ontogeny. Yet, ontogenetic shape change need not be drastic. Even subtle shifts in the scaling of traits can allow species to capitalize on new biomechanical grounds. For example, positive allometry of the jaw-closing in-lever in the lizard *Anolis equestris* produces disproportionately large bite forces in the adult form, allowing harder prey to be incorporated into the diet (Herrel and O'Reilly 2006). In the bluegill sunfish (*Leopomis macrochirus*), positive allometry of the jaw-opening in-lever is associated with faster jaw opening times and enhanced suction pressures (Wainwright and Shaw 1999; Carrol et al. 2004), enabling larger bluegill to reduce handling times on prey such as *Daphnia* (Mittelbach 1981). Emergent phenomena (which result from combinations of underlying traits), such as bite force or suction pressure, may be significantly affected by differential scaling of the individual traits that determine them.

Comparisons of the ontogenetic trajectories of traits across closely related species provide evidence that such trajectories are diverse, labile, and often correspond to

ecology (Mitteroecker et al. 2004; Frédérick and Sheets 2009; Wilson and Sánchez-Villagra 2010). Adams and Nistri (2010) provide evidence that ontogenetic scaling patterns of closely-related taxa are not necessarily static constraints that channel variation into fixed directions in phenotypic space, but that scaling processes themselves can evolve. The idea that closely related species can vary tremendously in their underlying developmental processes supports the idea that the course of ontogeny is a proximate origin of variation in traits (Klingenberg 1998).

Phenotypic evolution results from the tinkering of ancestral developmental patterns (Gould 1977). Evolutionary changes to morphological traits require alterations to the underlying developmental processes that shape them. Thus, phylogenetic information is inherently present in development, making it vital that comparisons among species' ontogenetic scaling patterns be placed in a phylogenetically-informed framework. Although examinations of ontogenetic allometry across closely-related species have been made (Wilson and Sánchez-Villagra 2010), the confound of phylogenetic influence remains untreated. Thus, to fully understand the selective regimes under which scaling patterns may be driven, an approach in which species' ontogenetic patterns can be compared while accounting for phylogenetic influence is necessary.

Here, we employ such a method and use the evolution of cleaning behavior in the Labridae (wrasses, parrotfishes, and weed-whitings) as a case study. The evolution of cleaning behavior in fishes presents a model system in which to explore the relationship between morphology and ecology. Cleaning behavior in fishes involves

the removal and consumption of ectoparasites, and is often characterized as a mutualistic relationship between a cleaner fish and its client(s) (Hobson 1969; Coté 2000). While over 130 species of teleost fishes have been observed to engage in cleaning other organisms, the Labridae contains the highest species diversity of cleaner fishes (Coté 2000). Notably, among the 58 species of labrid cleaners, 43 species (74.1%), are reported to clean predominantly as juveniles (Baliga and Law 2016). Less common are species that engage in cleaning facultatively throughout ontogeny (11 species; 19.0%), while the rarest strategy is obligate cleaning (8.6%), which is exclusively found the monophyletic *Labroides* genus.

The measure of a species' ontogenetic trajectory is defined by the traits from which it is composed. In order to compare such trajectories and test hypotheses related to ecological trends, an informative suite of traits first needs to be determined. Recent studies have identified the morphological and kinematic characters associated with cleaning behavior in some labrid taxa (Baliga and Mehta 2014; Baliga and Mehta 2015). These studies provide preliminary evidence that the evolution of cleaning in the Labridae involves an ontogenetic process by which the cranial skeleton is modified to reduce excursions and displacements in the jaws, providing a speed-driven albeit weak bite. Furthermore, Baliga and Mehta (*in review*) provide evidence that cleaner fishes from a variety of labrid lineages exhibit more elongate bodies than closely-related non-cleaners. In order to perform informed comparative allometric analyses, the extent to which cleaner fishes are convergent in cranial, body, and fin morphology must first be established.

We used phylogenetic comparative methods to assess whether the ontogeny of cleaning behavior in wrasses is concordant with ontogenetic patterns of morphology. We sought to discover 1) the extent to which cleaner fishes exhibit morphological convergence, 2) whether ontogenetic patterns in cleaning behavior are associated with a particular suite of ontogenetic changes in morphology, and 3) whether taxa that exhibit ontogenetic transitions away from cleaning show more extreme changes in morphology over ontogeny than other species.

3.2 Methods

3.2.1 Collection of Specimens and Data

We collected an ontogenetic size series of 15-29 individuals for each of 33 species (Fig. 3.1). The smallest specimens for each species were generally around 40 mm standard length (SL), and the largest specimens attained the adult common or maximum SL reported for the species (Froese and Pauly 2016). We chose to use approx. 40 mm SL as a minimum size to safely assure that all specimens were in a post-recruitment phase. We acquired specimens from museum collections and our personal collections of specimens gathered from the aquarium trade (see Table S1 in the Supporting Information for more on specimen acquisition).

All specimens were initially fixed in 10% formalin and then preserved in 60-70% ethanol. We took morphological measurements of body shape on ethanol-preserved specimens (Fig. 3.2 A); definitions of these measurements (Motta 1984; Wainwright et al. 2002) are listed in Table S2. We dissected the adductor mandibulae (AM) from

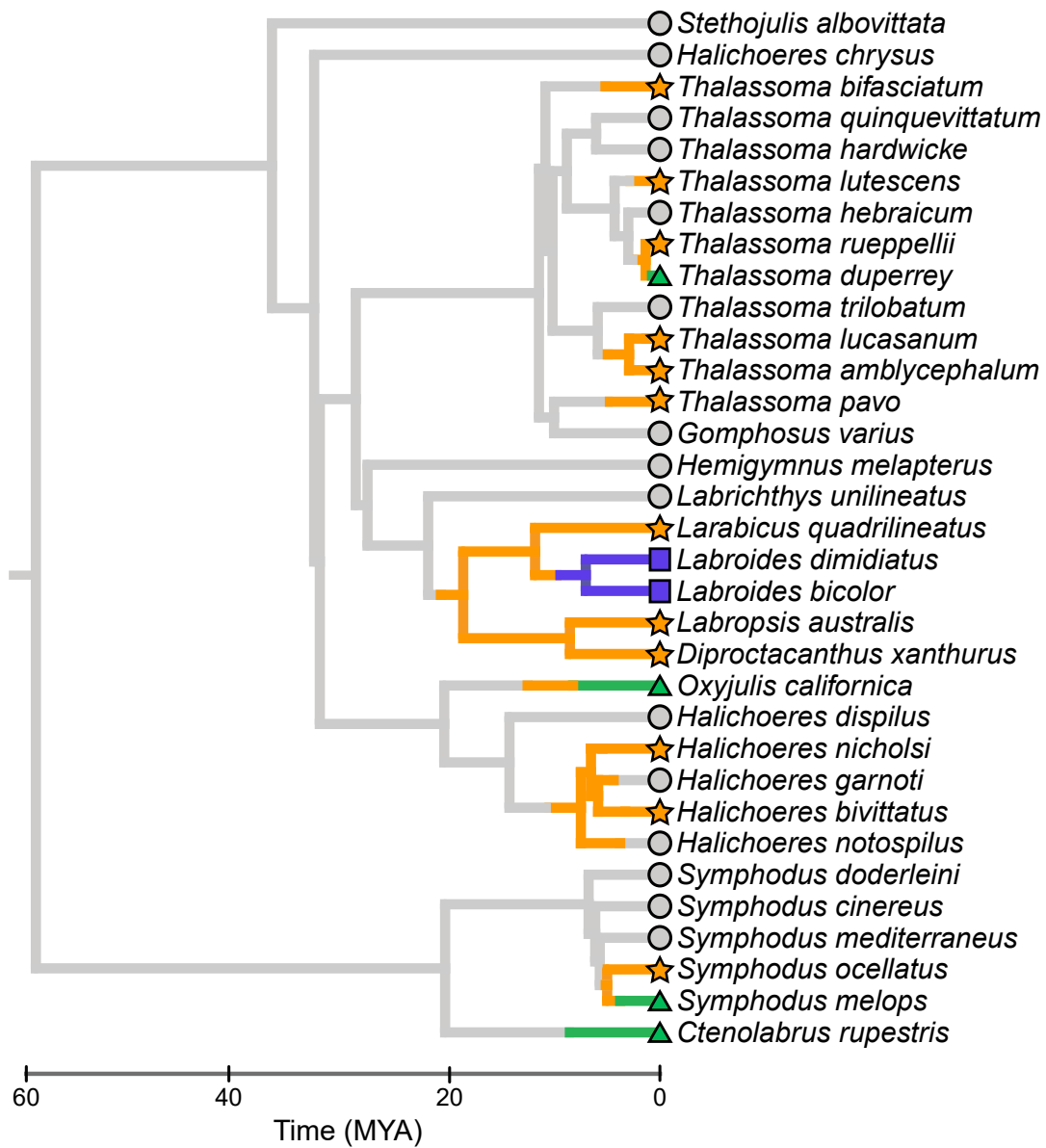


Fig. 3.1 - Phylogenetic relationships between species sampled in the present study. This tree is pruned from the Bayesian MCC phylogeny in Baliga & Law (2016). A single (but representative) stochastic character map has been overlaid. On each node, a pie chart indicates the distribution of mappings for the node across 1000 character maps. Stochastic character mapping was first performed on the full MCC tree from Baliga & Law (2016) and then pruned to the taxa shown here. Tip shapes and pie chart and branch colors indicate dietary group membership: obligate cleaners are purple squares, facultative cleaners are green triangles, juvenile cleaners are orange stars, and non-cleaners are grey circles.

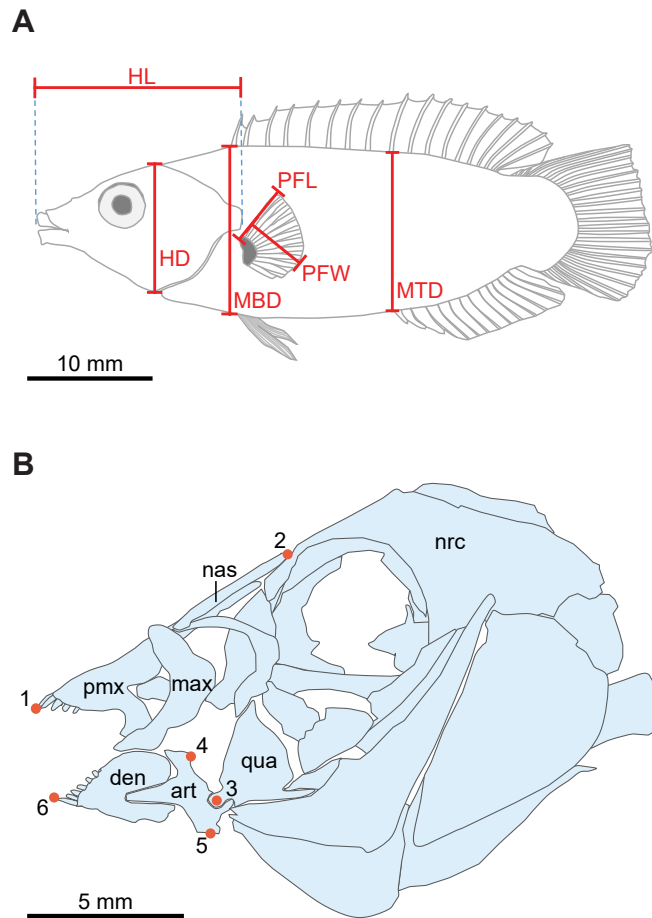


Fig. 3.2 - Measurements used in the present study. A) Line drawing of *Labrichthys unilineatus*, with body shape measurements. Abbreviations for traits follow those used in Table S2. Maximum body width, maximum tail width, and adductor mandibulae mass are not shown. B) Cranial skeleton of *Hemigymnus melapterus*, with landmarks used to measure cranial traits. Landmark definitions: 1 – the distal tip of the anteriormost tooth on the upper jaws, 2 – the articulation of the nasal and neurocranium, 3 – the quadrate-articular joint (jaw joint), 4 – insertion of the A2 section of the adductor mandibulae on the coronoid process, 5 – the point of attachment of the interoperculo-mandibular ligament on the articular, 6 – the distal tip of the anteriormost tooth on the lower jaws. Landmarks were used to measure the following cranial traits on cleared and double-stained specimens: premaxillary protrusion (distance between 1 and 2 when the jaws are fully closed subtracted from the distance when the jaws are open), vertical gape distance (distance between 1 and 6 when the jaws are open), jaw-closing in-lever length (distance between 3 and 4), jaw-opening in-lever length (distance between 3 and 5), jaw out-lever length (distance between 3 and 6). All traits were measured in millimeters. Bone abbreviations: art – articular, den – dentary, max – maxilla, nas – nasal, nrc – neurocranium, pmx – premaxilla, qua – quadrate.

one side of each specimen and weighed each muscle to the nearest 0.0001 g using a Secura 213-1S precision balance (Sartorius Stedim Biotech GmbH, Germany). The AM complex is a set of muscles that produces the forces involved in closing the jaws during behaviors such as biting. All sections of the AM (except A_{GD}) were removed and weighed together. Muscle identification followed descriptions by Winterbottom (1974). After dissections, we cleared and double-stained specimens for cartilage (using Alcian blue) and bone (using Alizarin red S) following a modification of Dingerkus and Uhler (1977). From these specimens, we measured additional traits of the cranial skeleton (Fig. 3.2 B) as defined in Table S2 (Motta 1984; Westneat 1990; Wainwright et al. 2004). Before all analyses, measurements of linear traits were natural log-transformed; measurements of mass were both cube-rooted and natural log-transformed.

Using information compiled by Baliga and Law (2016), we identified each species as belonging to one of the following dietary groups: non-cleaner, juvenile cleaner, facultative cleaner, or obligate cleaner (Fig. 3.1). For two species, our categorizations differ from those of Baliga and Law (2016). Recent observations provide evidence that *Thalassoma amblycephalum* engages in cleaning as a juvenile (S. Gingins, personal communication). Second, while *T. klunzingeri* had been documented as a juvenile cleaner (Randall 1986), the synonymy of this species and *T. rueppellii* was missed. Thus, in the present study, both *T. amblycephalum* and *T. rueppellii* were categorized as juvenile cleaners. Given these new data, stochastic character mapping was re-done on a larger (320 species) Bayesian MCC phylogeny

following methods available in Baliga and Law (2016). Trees with stochastic character maps were then pruned to the focal taxa of the present study using the `drop.tip.simmap()` function available in *phytools* (Revell 2012). Across these pruned stochastic character mappings, we computed summaries of states at each node. The pruned phylogeny, with information on node mappings and dietary grouping for extant taxa, is shown in Fig. 3.1.

One caveat of our approach is the straightforward assignment of species into dietary groups. Within a given category, species no doubt vary in the extent to which they clean. Without more refined data on the ontogeny of diets in all 33 species (which could allow for ordination of fish diets on continuous spectra), categorization was the best available option.

3.2.2 Assessment of Morphological Convergence

To understand the extent to which the evolution of cleaning involved morphological convergence, we constructed a phylogenetically-informed morphospace. Since a substantial portion of the taxa in the present study exhibit an ontogenetic shift away from cleaning behavior, we used juvenile specimens only in this analysis. We identified 3-5 juvenile specimens of each species by size and colour pattern (Burgess et al. 1991; Randall et al. 1997; Myers 1999). We then ran a phylogenetically-informed principal components analysis (PCA) (Revell 2009) using the pruned tree and the correlation matrix of the 12 cranial and body traits.

Using scores from each principal component, we estimated ancestral character states via maximum likelihood methods (Schluter et al. 1997). We then assessed the strength of convergence in cleaner fish morphology following recommendations in Stayton (2015). We quantified convergence among all cleaner fishes; species from all three cleaner dietary groups were together identified as a group of putatively convergent taxa. We explored the extent of convergence among cleaners using one of Stayton's (2015) distance-based measures, C_2 , which quantifies the amount that lineages evolve to be more similar. Stayton's C_2 is measured by subtracting D_{tip} (the distance, here Euclidean, between putatively convergent taxa in phenotypic space) from D_{max} (the maximum distance between any pair of taxa in the lineages). Larger values of C_2 indicate greater amounts of convergence. We used simulation procedures available in Stayton (2014) to test for significant convergence ($\alpha = 0.05$) among cleaners, with 1000 simulations per test. We used scores from all 12 principal components to avoid losing power in significance tests of convergence via data reduction (Stayton 2015; Adams 2014a,b).

We also ran a phylogenetically-informed PCA on the correlation matrix of traits from the largest 3-5 adult specimens of each species to understand if juvenile patterns of convergence were apparent in the adult form. Because juvenile cleaner taxa show ontogenetic shifts away from cleaning in adulthood, we assessed convergence at two different levels: 1) among all cleaner taxa (including juvenile cleaners), and 2) among facultative and obligate cleaner taxa only (i.e. species who clean throughout ontogeny). We again applied each of the aforementioned convergence assessment

metrics and hypothesis testing procedures, and adjusted p-values for multiple hypothesis testing following Benjamini and Hochberg (1995).

3.2.3 Phylogenetically-Informed Allometric Analyses

To compare and visualize multivariate patterns in ontogenetic scaling among species in a phylogenetically-informed context, we generated a “phylo-allometric space”. As detailed below, we achieved this by first inferring the multivariate allometric trajectory of each species following Klingenberg and Froese (1991), and then using methods in Revell (2009) to account for shared history between taxa in a PCA.

Following Jolicoeur (1963), when a PCA is computed using a non-size-corrected dataset, the first principal component (PC1) represents the line of best fit to the multivariate data (Pearson 1901), and size is considered a latent variable that affects all variables simultaneously. Thus, PC1 represents a multivariate generalization of allometry (Klingenberg and Froese 1991). We performed a separate PCA for each species on a correlation matrix of all traits. Our investigations of the relationships between the 12 traits showed that they all exhibited linear relationships with each other within every species’ dataset. Because the distribution of allometric growth can be visualized in the space defined by the normalized vector coefficients (of PC1) of the original traits (Klingenberg and Froese 1991; Gerber et al. 2008), we next used the 33 originally calculated PC1 eigenvectors as new observations for a second PCA.

This interspecific PCA was phylogenetically-informed following methods from Revell (2009) and using the pruned labrid tree, resulting in a phylo-allometric space.

To identify linear combinations of traits that best separate dietary group trajectories while simultaneously minimizing bias due to shared phylogenetic history, we used a phylogenetic Flexible Discriminant Analysis (pFDA) (Motani and Schmitz 2011). In this analysis, we used the 33 intraspecific PC1 eigenvectors (normalized to unit length) as the independent variables in order to predict dietary group membership. This “allometric pFDA” was performed using a modification of code provided in Motani and Schmitz (2011). This approach allowed us to explore the extent to which each of the dietary group’s ontogenetic scaling patterns could be distinguished from those of the others. We used scores from the discriminant axes as the independent variables and dietary group membership as the dependent variable in a phylogenetically-informed MANOVA (10,000 simulations) to test for significance in group differences (Garland et al. 1993).

3.2.4 Assessing Patterns of Ontogenetic Scaling

To further understand each species’ ontogenetic scaling patterns and help us interpret the interspecific patterns and loadings of traits we observed in phylo-allometric space, we performed standardized major axis (SMA) regressions on the ontogenetic trait data. Within each species and for each of the 12 traits, we performed an SMA regression of the natural log-transformed trait against the natural log-transformed standard length of specimens. We then tested whether regression slopes

were indicative of allometry by testing whether they differed significantly from 1.0, i.e. the hypothesized slope under isometric growth. Within each set of p-values for a species, we applied adjustments to account for multiple hypothesis testing following Benjamini and Hochberg (1995).

3.2.5 Comparing the Amount of Ontogenetic Change across Groups

To test whether certain dietary groups exhibit more extreme deviations from the average allometric trajectory, we computed the distance of each species' trajectory from the phylo-allometric centroid. This centroid represents the phylogenetic average ontogenetic trajectory of all taxa. We used both the “absolute distance” and “standardized distance” measures in morphospace employed by Bellwood et al. (2006). First, we extracted the scores from the principal components of phylo-allometric space that accounted for 85% of the variation in ontogenetic scaling (the first seven principal components in the present case). We then calculated each species' absolute distance (D_a) from the PCA centroid as:

$$D_a = \sqrt{\sum_{i=1}^n (S_i)^2}$$

where n is the number of retained principal components, and S_i is the score on the i^{th} PC. Similarly, we calculated the standardized distance (D_s) from the PCA centroid as:

$$D_s = \sqrt{\sum_{i=1}^n (S_i * V_i)^2}$$

where V_i is the proportion of total variance explained by the i^{th} PC. The D_s metric simply weighs each score in proportion to the variance for which its respective principal component accounts before computing distance from the centroid via the Pythagorean Theorem.

We then used each distance as the independent variable and dietary group membership as the dependent variable in separate phylogenetically-informed ANOVAs (10,000 simulations) to test for significance in group differences (Garland et al. 1993), and adjusted p-values for multiple hypothesis tests following Benjamini and Hochberg (1995).

3.3 Results

3.3.1 Juvenile and Adult Morphospaces

Through a phylogenetically-informed PCA on juvenile wrasses, we determined the major axes of juvenile morphological variation (Table 3.1). Nearly all traits loaded strongly and all eigenvectors were in the same direction on PC 1, which matches Jolicoeur's (1963) characterization of a "size axis". This size axis accounted for 44.09% of the variance in the data. Nine of the 12 traits loaded strongly on at least one of the first four axes of shape variation (PCs 2-5); the first two axes of shape variation (PCs 2 and 3) are depicted in Fig. 3.3.

For the adult dataset, a phylogenetically-informed PCA yielded axes of variation that differed from those of the juveniles (Fig. S1, Table S3). Again, on PC 1 all 12 traits loaded strongly and all eigenvectors were in the same direction. Unlike the PCA

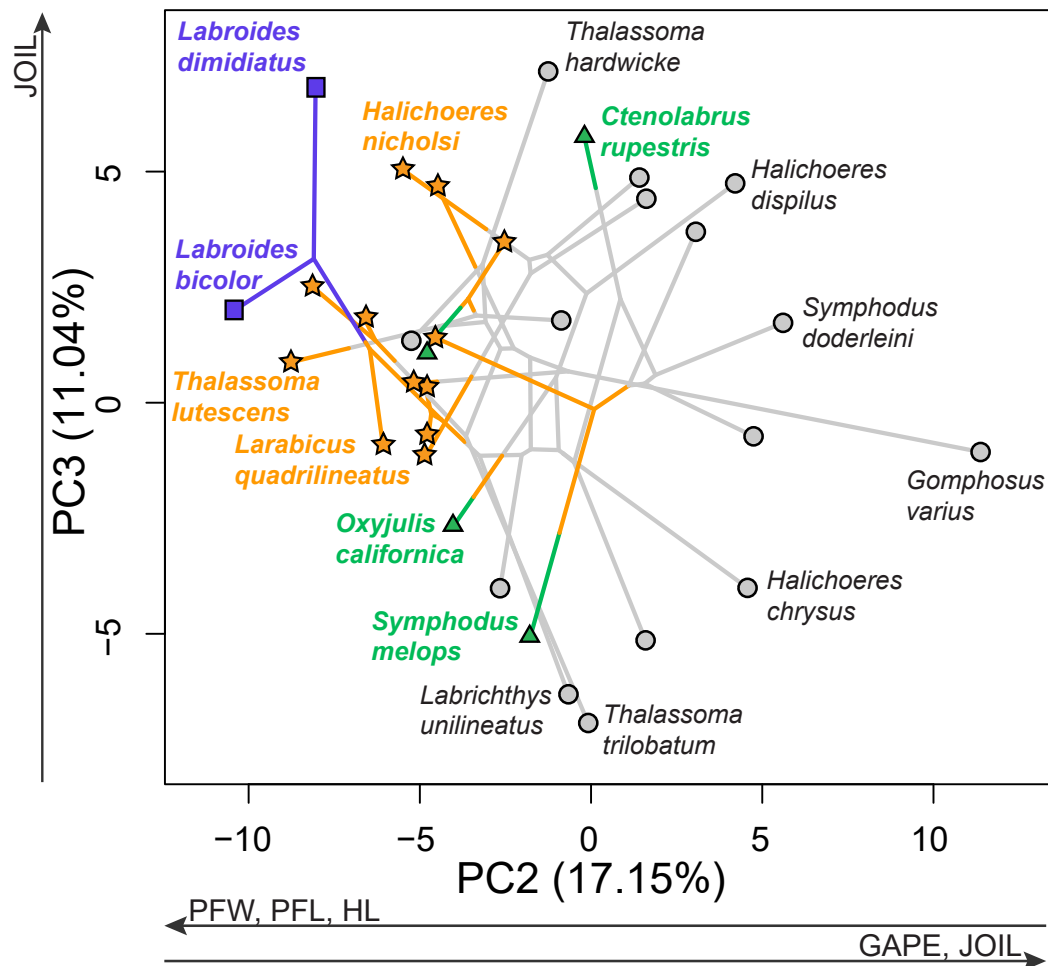


Fig. 3.3 - Juvenile phylomorphospace. A phylomorphospace (Sidlauskas 2008) was generated for the juvenile dataset using a phylogenetically-informed PCA (Revell 2009) and the tree shown in Fig. 1. Trait data were averaged within each species from the 3-5 smallest juvenile specimens. A single stochastic character map has been superimposed on the phylogeny; shapes and colors indicate dietary group membership: obligate cleaners are purple squares, facultative cleaners are green triangles, juvenile cleaners are orange stars, and non-cleaners are grey circles. The PCA was performed on the correlation matrix of traits. In the PCA, PC1 captured the effects of size on traits (see text for more details); PC2 and PC3 capture the primary axes of shape variation and are shown here. Traits that loaded strongly on each axis are represented by arrows that indicate the direction in which trait magnitudes increase along the axis. See Table 1 for additional details on the PCA.

on juvenile data, in the adult phylomorphospace, PC 1 accounted 77.32% of the variance. In addition, only 5 traits loaded strongly on PCs 2-5.

Among juvenile specimens, cleaner fish taxa showed morphological convergence in shape (Stayton's C_2 : 1.02; p-value: 0.02). Among adult wrasses, however, cleaner fish species as a group did not continue to show convergence (Stayton's C_2 : 0.29; p-value: 0.66). When we assessed convergence among only facultative and obligate taxa, (i.e. species who continue to clean in adulthood) we found that these species did exhibit significant convergence (Stayton's C_2 : 1.91; p-value < 0.01).

3.3.2 *Phylo-Allometric Space*

The phylo-allometric space yielded the major axes of scaling variation in wrasses (Table 3.2). All 12 traits loaded strongly on PC 1 and PC 2. A plot of the first two principal components (Fig. 3.4), shows that juvenile cleaners tend to have positive scores on PC 1, indicating that many of these species tend to show stronger positive scaling of the traits that load positively on this axis.

The first seven principal components of phylo-allometric space collectively accounted for 87.20% of the variance and were retained for further analyses on the amount of ontogenetic change in taxa. Scores from each of these axes were used to compute D_a and D_s (Fig. S2) for each species. A phylogenetic ANOVA run on each metric indicated that dietary groups did not exhibit significant differences (D_a : F-ratio: 0.74, p-value: 0.63; D_s : F-ratio: 3.04, p-value: 0.08). For each metric, post-hoc

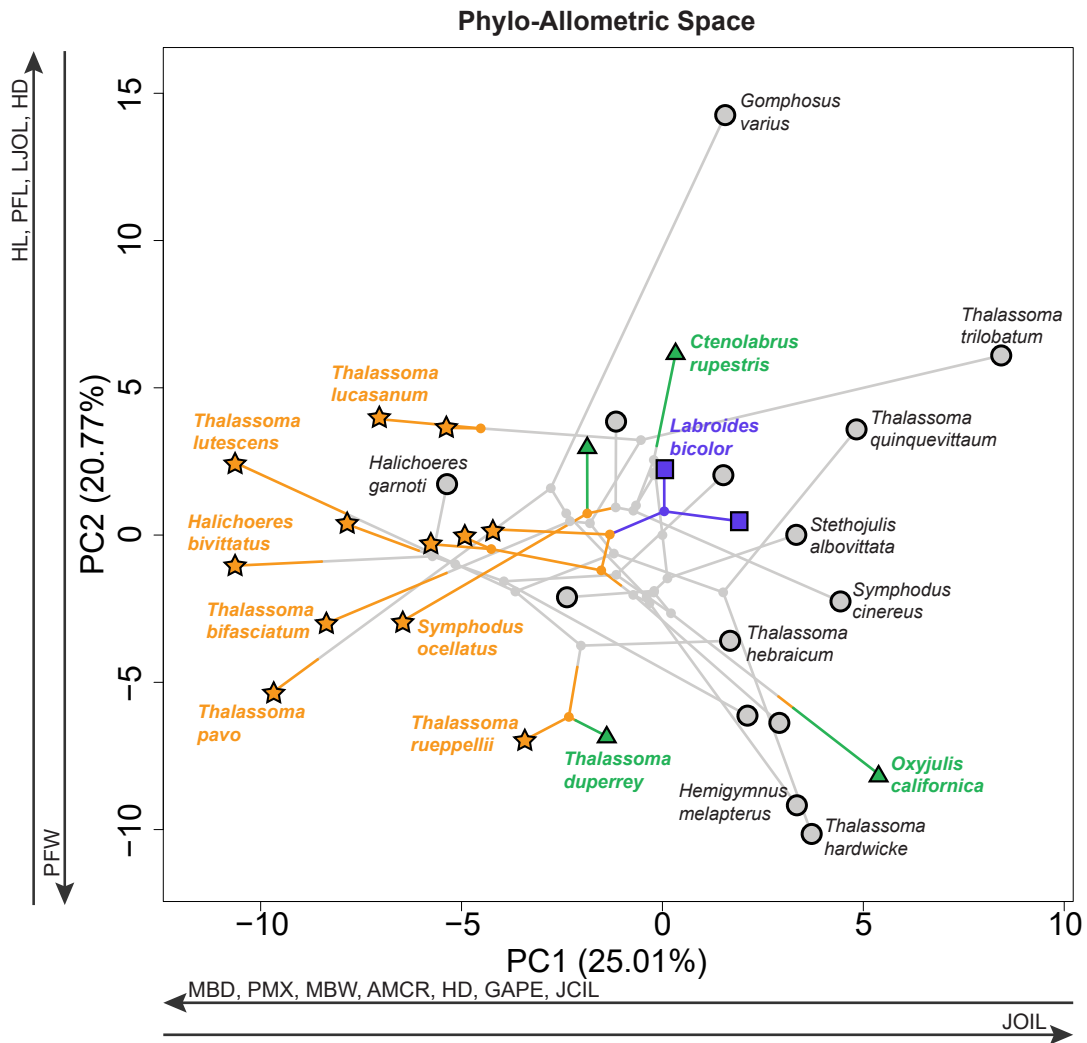


Fig. 3.4 - Phylo-allometric space for 33 species of wrasses. A visualization of the primary axes of ontogenetic variation for species in the present study, after accounting for shared history among taxa. A phylo-allometric space was generated using a phylogenetically-informed PCA (Revell 2009) on the set of intraspecific PC1 eigenvectors and the tree shown in Fig. 1 (see text for additional details). Traits that loaded strongly on each axis are represented by arrows that indicate the direction in which stronger positive allometry for the trait increase along the axis. See Table 2 for additional details on the phylo-allometric PCA. A single stochastic character map has been superimposed on the phylogeny; symbols and colors indicate dietary group membership: obligate cleaners are purple squares, facultative cleaners are green triangles, juvenile cleaners are orange stars, and non-cleaners are grey circles.

tests (with adjustments for multiple hypothesis testing) confirmed each pair of dietary group comparisons showed no significant differences (Table S4).

Table 3.1 - Loadings of traits in the juvenile morphospace

	PC1 (44.09%)	PC2 (17.15%)	PC3 (11.04%)	PC4 (8.71%)	PC5 (5.68%)
Adductor Mandibulae Mass	-0.569	0.303	0.301	0.612	0.271
Head Length	-0.736	-0.437	0.222	0.220	-0.099
Head Depth	-0.861	-0.222	-0.162	-0.146	-0.294
Maximum Body Width	-0.818	-0.168	-0.280	-0.053	0.216
Maximum Body Depth	-0.837	0.194	-0.046	0.060	-0.150
Pectoral Fin Length	-0.723	-0.512	-0.034	-0.050	0.359
Pectoral Fin Width	-0.213	-0.911	-0.107	0.047	-0.158
Lower Jaw Outlever Length	-0.517	0.363	0.369	-0.519	-0.049
Jaw-Closing In-Lever Length	-0.326	-0.145	0.862	-0.188	-0.118
Jaw-Opening In-Lever Length	-0.634	0.422	-0.340	0.128	-0.418
Vertical Gape Distance	-0.782	0.429	0.028	0.212	0.049
Premaxillary Protrusion Distance	-0.599	0.229	-0.266	-0.473	0.308

A phylogenetically-informed PCA was run using the correlation matrix of 12 traits. For each species, data were taken from the 3-5 smallest juvenile specimens. Loadings for the first 5 principal components are shown. The percent of the variance for which each PC accounts is listed in parentheses in the column headings. Traits that load strongly on each PC (i.e. |loading| > 0.4) are bolded.

Table 3.2 - Loadings of traits in phylo-allometric space

	PC1 (25.01%)	PC2 (20.77%)	PC3 (13.62%)	PC4 (9.53%)	PC5 (8.35%)
Adductor Mandibulae Mass	-0.573	0.237	0.547	0.228	0.146
Head Length	-0.373	0.641	0.112	0.043	-0.295
Head Depth	-0.471	0.501	-0.275	0.229	0.181
Maximum Body Width	-0.652	-0.375	0.172	-0.310	0.225
Maximum Body Depth	-0.801	0.119	0.223	0.002	0.401
Pectoral Fin Length	0.044	0.625	0.282	-0.256	-0.554
Pectoral Fin Width	-0.002	-0.733	-0.104	-0.336	-0.063
Jaw Outlever Length	0.164	0.600	-0.522	-0.308	0.316
Jaw-Closing In-Lever Length	-0.408	-0.384	-0.179	0.631	-0.318
Jaw-Opening In-Lever Length	0.622	-0.195	0.411	0.363	0.178
Vertical Gape Distance	-0.461	-0.126	-0.765	0.166	-0.131
Premaxillary Protrusion Distance	-0.671	-0.359	0.137	-0.333	-0.297

A phylogenetically-informed PCA was run using the set of intraspecific PC1 eigenvectors and the tree shown in Fig. 3.1. Loadings for the first 5 principal components are shown. The percent of the variance for which each PC accounts is listed in parentheses in the column headings. Traits that load strongly on each PC (i.e. $|\text{loading}| > 0.4$) are bolded.

The pFDA yielded three discriminant axes, with the first axis accounting for the vast majority of variance in the data (86.87%, Table S5). The traits with the largest coefficients on the first discriminant axis were maximum body depth and jaw-closing in-lever length; on the second discriminant axis, maximum body width, jaw-closing in-lever length and vertical gape distance had relatively large coefficients. Predictions from the pFDA showed that nearly all juvenile cleaners were correctly classified (Table 3.3). Classification for the other dietary groups was less successful, and the pFDA model had trouble discriminating between these groups (Fig. 3.5). A phylogenetically-informed MANOVA on the pFDA scores showed there were significant differences between the mean score of at least one pair of groups (F-ratio: 27.52; $p\text{-value} < 0.001$). Post-hoc tests showed that juvenile cleaners exhibit significant differences in mean score compared to the other groups (Table S6). Non-cleaners, facultative cleaners, and obligate cleaners did not show significant differences from each other's mean pFDA score.

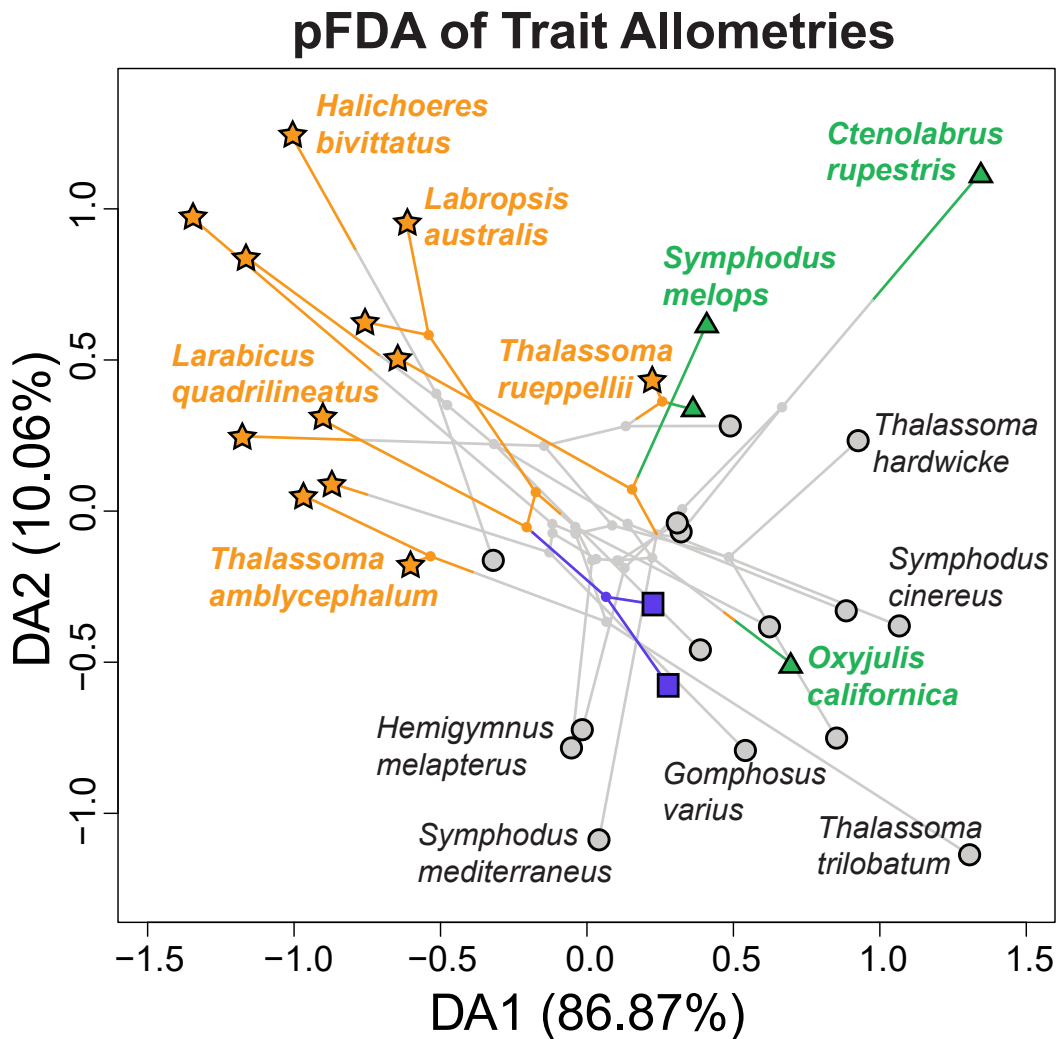


Fig. 3.5 - Discriminant axes for 33 species of wrasses. A phylogenetically-informed flexible discriminant analysis (pFDA) (Motani and Schmitz 2011) identifies combinations of trait allometries that separate dietary groups. Using the phylogeny shown in Fig 1, a pFDA was run on the set of intraspecific PC1 eigenvectors. Each taxon was assigned to a dietary group, and pFDA was able to discriminate between the ontogenetic scaling patterns of juvenile cleaners and all other groups, but could not further differentiate between the other groups. See Tables S5 and S6 for additional details on the pFDA. A single stochastic character map has been superimposed on the phylogeny; symbols and colors indicate dietary group membership: obligate cleaners are purple squares, facultative cleaners are green triangles, juvenile cleaners are orange stars, and non-cleaners are grey circles.

Table 3.3 - Confusion matrix from pFDA performed on ontogenetic scaling vectors

	Non-Cleaner	Juvenile Cleaner	Facultative Cleaner	Obligate Cleaner
Non-Cleaner	13	0	2	1
Juvenile Cleaner	0	11	0	0
Facultative Cleaner	1	1	2	0
Obligate Cleaner	1	0	0	1
% correct	86.67	91.6	50	50

Row names list the predicted groups while columns indicate true group membership; entries along the diagonal are thus correctly classified. The percent of taxa accurately identified within each dietary group is recorded in the final row. Overall, 81.8% of all predictions were correct, including 91.6% correct classifications of all juvenile cleaners.

3.3.3 Intraspecific Scaling Patterns

Performing SMA regressions of each trait against standard length in each species provided additional insights on the diversity of scaling patterns seen in wrasses (Table S7). Some traits showed a variety of scaling patterns. For instance, the scaling of lower jaw out-lever length showed negative allometry in 11 species, isometry in 14 species, and positive allometry in 8 species. Other traits showed relatively less diversity, e.g., for maximum body width, species only showed positive allometry (15 species) or isometry (18 species). The SMA regressions also allowed us to further characterize species' scaling patterns. To showcase this general diversity, four species (*Ctenolabrus rupestris*, *Halichoeres notospilus*, *Symphodus cinereus*, *S. doderleini*)

exhibited isometry for all 12 traits, while *Thalassoma hardwicke* and *T. lutescens* showed allometry in all but two traits.

Although each of these regressions was performed against log-standard length, the patterns captured through the SMA slopes should generally correspond with the trends captured by phylo-allometric analyses. We found that species with the most extreme scores on each axis of phylo-allometric space showed the most extreme SMA slopes for the traits that loaded strongly on the axis.

3.4 Discussion

In the present study, we investigated the extent to which labrid cleaner fishes exhibit concordance between the ontogeny of cleaning behavior and morphological trends in the body, fins and cranial skeleton. Because all labrids that clean do so in the juvenile phase, our construction of a juvenile phylomorphospace allowed us to first determine the extent to which cleaners show morphological convergence, and whether our traits of interest were informative of cleaning. Our creation of a phylogenetically-informed allometric space revealed the primary axes of ontogenetic variation of our traits. Species' distances from the centroid of 'phylo-allometric space' were used to determine whether certain dietary groups exhibited larger deviations from the phylogenetic average allometric trajectory. Finally, our use of pFDA on ontogenetic scaling vectors enabled us to determine the extent to which

each dietary group's trajectories could be discriminated from those of the other groups.

3.4.1 Patterns of Convergence in Cleaners

In a juvenile morphospace defined by a mix of body shape and cranial traits related to feeding, we found evidence of morphological convergence among cleaner fishes in the Labridae. In fact, cleaners could largely be differentiated from closely related non-cleaners along the primary axis of shape variation among juveniles (PC2). In the juvenile phase, cleaner fishes tended to show relatively wider and longer pectoral fins, little premaxillary protrusion, small gape, and elongate bodies compared to non-cleaners.

These findings support previous studies showing that cleaner fishes in the genera *Thalassoma* (Baliga and Mehta 2014), *Labroides*, and *Larabicus* (Baliga and Mehta 2015) exhibit little premaxillary protrusion, small gapes, and little displacement of the jaws during feeding behaviors. Collectively, these data indicate that the evolution of cleaning might involve selection for biting behaviors that can be characterized by a series of rapid, low-displacement, and often cyclical jaw movements. Instead of taking large, forceful bites to pry off ectoparasites or other prey attached to a surface, cleaners in these three genera appear to employ a more delicate approach via fast, multiple bites (coupled with the generation of suction). The observation that cleaners in diverse genera including *Halichoeres*, *Oxyjulis*, *Symphodus*, *Ctenolabrus*, *Labropsis*, and *Diproctacanthus* also share morphological characteristics (in the

juvenile phase) that similarly reduce displacement and gape provides evidence that cleaning in wrasses may involve selection for a common suite of traits. A generalized pattern of repeated evolutionary trends in the juvenile phase of labrid cleaner fishes is apparent in the present study.

The need to maneuver may be tied to the elongate body plan and relatively wide pectoral fins we observed in cleaners. Body elongation in cleaner wrasses is associated with low moment of inertia in the vertebral column (Baliga and Mehta, *in review*), affording cleaners with relatively flexible bodies. Wainwright et al. (2002) documented the diversity of pectoral fin aspect ratios in 143 species of labrids (calculated as the square of the length of the leading edge divided by the area of the fin), and then assessed the relationships between this trait, the angle of pectoral fin attachment to the body, and field measures of typical swimming speeds in 43 species. Species with higher aspect ratio fins tended to have faster size-specific swimming speeds, and used a “flapping” motion of the fins. Those with lower aspect ratio fins were documented to generate thrust more efficiently at low swimming speeds, and employed a “rowing” motion of the fins. This rowing mechanism may increase maneuverability in these taxa, especially at low swimming speeds (Blake 1981; Vogel 1994; Drucker and Lauder 2000; Walker and Westneat 2000). This indicates that there may be a trade-off between the efficiency of fast swimming and maneuverability in labrids. Our observation of increased pectoral fin width in cleaners (and thus, relatively lower pectoral fin aspect ratios) and body elongation provides evidence that selection for cleaning in labrids might push taxa towards the more

maneuverable end of the spectrum. Additionally, Wainwright et al. observed that slow swimming species typically swam closer to the reef while faster species dominated the water column and shallow, high-flow habitats. Given that cleaning stations are typically found in habitats closer to the reef (Hobson 1971), cleaner fishes' lower aspect ratio fins may afford them an advantage in capitalizing on resources in this calmer-water habitat (Fulton and Bellwood 2002).

Although cleaner taxa show significant convergence in this juvenile morphospace, the degree of convergence is not strong. A visualization of the primary axes of shape variation (PCs 2 and 3; Fig. 3.1) shows that facultative cleaners such as *Symphodus melops* and *Ctenolabrus rupestris* are on the periphery of the space occupied by cleaners. These peripheral species are particularly interesting as observations of cleaning behavior in both have largely involved their removal of sea lice (*Lepeophtheirus salmonis*) on farmed Atlantic salmon (Bjordal 1988, 1990). The extent to which each of these two species cleans in nature is less established. Moreover, suites of traits which enhance sea lice removal may differ from those that are optimal for other forms of ectoparasitivory, as sea lice are substantially larger than gnathiid isopods found in the Indo-Pacific.

In the adult phase, we find evidence that facultative and obligate species continue to exhibit morphological convergence. Again, these cleaner fishes (who still engage in cleaning as adults) show relatively modest values for traits such as gape size, maximum body depth, and the length of the pectoral fins. Juvenile cleaner species, however, appear to show a diverse array of morphological traits in adulthood, and do

not share convergence with the other cleaner groups. In fact, juvenile cleaner taxa, as adults, occupy some of the most extreme regions of the adult morphospace (Fig. S1). Thus, not only do juvenile cleaner species exhibit ontogenetic shifts away from cleaning, but also they undergo substantial morphological change over ontogeny.

Additionally, body size may be an important character in the evolution of cleaning. Obligate cleaners are generally relatively small; the largest *Labroides* species, *L. bicolor* typically attains a maximum length of just 15 cm (Kuitert and Tonozuka 2001). The only other obligate cleaner species are in the genus *Elacatinus* in the Gobiidae, who are all typically under 6 cm (Robins and Ray 1986). Furthermore, the majority of cleaner fishes perform the behavior predominately in the juvenile phase (Coté 2000). Thus, overall, cleaners can be expected to show small body size, which may enhance their ability to inspect the buccal cavity and/or gills of their clientele, where parasites are known to be found (Hobson 1969; Coté 2000). Only in the case of facultative cleaners, among whom cleaning may also be performed in adult stages, may the size of a cleaner exceed these thresholds. Since these species engage in cleaning relatively infrequently compared to obligates and even juvenile cleaners (Hobson 1969; Bjordal 1990; Coté 2000), the strength of selection in reducing body size in these taxa may not be pronounced.

3.4.2 The Ontogenetic Scaling of Cleaners

Our study provides evidence that juvenile cleaner species consistently show a fundamentally different pattern of ontogenetic scaling than non-cleaners and even

other cleaner fishes. The patterns of change exhibited by juvenile cleaners can be discriminated from those of the other groups (non-cleaner, facultative, and obligate). Allometric patterns of four traits (maximum body depth, jaw-closing in-lever length, vertical gape distance and maximum body width) were key in distinguishing the ontogenetic scaling of juvenile cleaners. For each of these traits, juvenile cleaners showed either positive allometry or isometry (vs standard length) over ontogeny; none of these traits exhibited negative allometry in this dietary group. On the other hand, obligate and facultative cleaners did not systematically show patterns of ontogenetic change that could be discriminated from those of non-cleaners. These two groups of cleaners, however, showed significant convergence in both the juvenile and adult morphospaces. Together, these results imply that facultative and obligate cleaners possess a suite of characteristics in the juvenile phase that are conducive to cleaning and maintain them over ontogeny. These species do generally exhibit ontogenetic shape change (only *Ctenolabrus rupestris* showed isometry in all 12 traits), but this change is not distinct in magnitude or direction compared to that shown by non-cleaners.

Previous workers have generated “allometric space” for other clades, e.g. rodents (Wilson and Sánchez-Villagra 2010), fishes (Klingenberg and Froese 1991), and ammonites (Gerber et al. 2008), in order to view the primary axes of ontogenetic scaling among focal taxa. To date, however, accounting for phylogenetic non-independence (due to common ancestry of taxa) has been missing. It is well documented that phylogenetic information should be incorporated into interspecific

analyses (Felsenstein 1985; Harvey and Pagel 1991; Martins and Hansen 1997; Garamszegi 2014). Revell (2009) demonstrates that incorporating phylogenetic information into multivariate analyses such as PCA reduces Type I error, indicating interspecific studies which ignore phylogeny could potentially produce spurious results. Computation of phylo-allometric space in the present study provides the major axes of ontogenetic change while accounting for phylogenetic relatedness among the taxa. Similar to analyses based on other forms of phylogenetic PCA, subsequent analysis using scores from phylo-allometric space should also use phylogenetic comparative methods (Revell 2009), such as the phylogenetic ANOVAs we employed herein.

Our finding that all 12 measured traits loaded strongly on at least one of the first few principal axes of phylo-allometric space speaks volumes on the diversity of ontogenetic patterns observed in the Labridae. Investigations of SMA slopes of each trait against standard length provide further evidence of this diversity. The substantial morphological diversity of the feeding apparatus (Wainwright et al. 2004), diversity of traits related to locomotion (Wainwright et al. 2002), and functional diversity of taxa (Bellwood et al. 2006) have been well documented in this group, but studies have generally focused on adult phenotype and ecology. The role of ontogenetic scaling in evolution is increasingly being recognized as a factor that potentially can influence evolutionary processes, promoting morphological and functional diversity (Gould 1966; Klingenberg 1998; Gerber et al. 2008). We suggest that evolutionary mechanisms that promote the diversity of ontogenetic patterns among the Labridae

could be a crucial force in generating functional and morphological diversity in this speciose group.

3.4.3 Conclusions

We provide an approach in which the ontogenetic trajectories of species can be analyzed in a phylogenetic comparative framework. Cleaning in the Labridae appears to correspond with both juvenile morphology and the direction of trait change over ontogeny. We find evidence of a suite of traits that unifies cleaners in the juvenile phase; cleaners show characteristics that enhance maneuverability in locomotion and decreased displacement of the jaws. Over ontogeny, some of these taxa (facultative and obligate cleaners) largely maintain these characters. Other taxa (juvenile cleaners) show consistent patterns of change in traits while also showing ontogenetic shifts away from cleaning.

3.5 Acknowledgements

We thank K Pelon, M Mac, S Baumgart, and K Galloway for assistance in collecting morphological data. We give special thanks to museum curators and staff for providing specimen loans: JT Williams (Smithsonian), R Feeny (LA County Museum), D Catania (California Academy of Sciences), and G Zora (Paris Museum). P Wainwright, B Lyon, and P Raimondi provided valuable discussion. The study was supported by the Society for Integrative and Comparative Biology (SICB) Grant-in-Aid of Research Award to V.B.B. Travel to museums was supported by the UC Santa

Cruz Graduate Student Association Travel Grant to V.B.B. The authors have no conflict of interest to declare.

3.6 References

- Adams, D.C. 2014a. Quantifying and comparing phylogenetic evolutionary rates for shape and other high-dimensional phenotypic data. *Syst. Biol.* 63, 166–177. (doi:10.1093/sysbio/syt105)
- Adams, D.C. 2014b. A generalized K statistic for estimating phylogenetic signal from shape and other high-dimensional multivariate data. *Syst. Biol.* 63, 685–697. (doi:10.1093/sysbio/syu030)
- Adams, D.C., and A. Nistri. 2010. Ontogenetic convergence and evolution of foot morphology in European cave salamanders (Family: Plethodontidae). *BMC Evol. Biol.* 10, 216. (doi:10.1186/1471-2148-10-216)
- Baliga, V.B., and R.S. Mehta. 2014. Scaling patterns inform ontogenetic transitions away from cleaning in *Thalassoma* wrasses. *J. Exp. Biol.* 217, 3597-3606. (doi:10.1242/jeb.107680)
- Baliga, V.B., and R.S. Mehta. 2015. Linking Cranial Morphology to Prey Capture Kinematics in Three Cleaner Wrasses: *Labroides dimidiatus*, *Larabicus quadrilineatus*, and *Thalassoma lutescens*. *J. Morphol.* 276, 1377–91. (doi:10.1002/jmor.20425)
- Baliga, V.B., and C.J. Law. 2016. Cleaners among wrasses: Phylogenetics and evolutionary patterns of cleaning behavior within Labridae. *Mol. Phyl. Evol.* 94, 424-435. (doi:10.1016/j.ympev.2015.09.006)
- Baliga, V.B., and R.S. Mehta. 2016 (*In review*). Ontogeny and flexibility: Shape changes underlie life history patterns of cleaning behaviour. *Integ. Comp. Biol.*
- Bellwood, D.R., Wainwright, P.C., Fulton, C.J., and A.S. Hoey. 2006. Functional versatility supports coral reef biodiversity. *Proc. R. Soc. B.* 273, 101–107. (doi:10.1098/rspb.2005.3276)
- Benjamini, Y, and Y. Hochberg. 1995. Controlling the false discovery rate: a practical and powerful approach to multiple testing. *J. Roy. Stat. Soc. B.* 57, 289–300.

- Bjordal, Å. 1988. Cleaning symbiosis between wrasse (Labridae) and lice infested salmon (*Salmo salar*) in mariculture. *Int. Counc. Explor. Sea, Maricu. Comm. F.* 17.
- Bjordal, Å. 1990. Sea lice infestation on farmed salmon: possible use of cleaner-fish as an alternative method for de-lousing. *Can. Tech. Rep. Fish. Aqu. Sci.* 1761, 85-89.
- Blake, R.W. 1981. Influence of pectoral fin shape on thrust and drag in labriform locomotion. *J Zool.* 194, 53-66. (doi:10.1111/j.1469-7998.1981.tb04578.x)
- Burgess, W.E., Axelrod, H.R., and R. Hunziker. 1991. *Atlas of Marine Aquarium Fishes.* Neptune City, NJ: T.F.H. Publications, Inc.
- Carroll A.M., Wainwright P.C., Huskey S.H., Collar D.C., and R.G. Turingan. 2004. Morphology predicts suction feeding performance in centrarchid fishes. *J. Exp. Biol.* 207, 3873-3881. (doi:10.1242/jeb.01227)
- Coté, I.M. 2000. Evolution and Ecology of Cleaning Symbioses in the Sea. *Oceanogr. Mar. Biol. Annu. Rev.* 38, 311–355.
- Dingerkus, G., and L. D. Uhler. 1977. Enzyme clearing of alcian blue stained whole small vertebrates for demonstration of cartilage. *Stain. Technol.* 52, 229–232. (doi:10.3109/10520297709116780)
- Drucker, E.G., and G.V. Lauder. 2000. A hydrodynamic analysis of fish swimming speed: wake structure and locomotor force in slow and fast labriform swimmers. *J. Exp. Biol.* 203, 2379-2393.
- Felsenstein, J. 1985. Phylogenies and the comparative method. *Am. Nat.* 125, 1-15. (doi:10.1086/284325)
- Frédérich, B., and H.D. Sheets. 2009. Evolution of ontogenetic allometry shaping giant species: a case study from the damselfish genus *Daschyllus* (Pomacentridae). *Bio. J. Linn. Soc.* 99, 99-117. (doi:10.1111/j.1095-8312.2009.01336.x)
- Fulton, C.J., and D.R. Bellwood. 2002. Ontogenetic habitat use in labrid fishes: an ecomorphological perspective. *Mar. Ecol. Prog. Ser.* 226, 135-142. (doi:10.3354/meps236255)
- Froese R., and D. Pauly, eds. 2016. *FishBase.* World Wide Web electronic publication. www.fishbase.org, version (1/2016).

- Garamszegi, L.Z, ed. 2014. *Modern Phylogenetic Comparative Methods and Their Application in Evolutionary Biology*. Springer-Verlag Berlin Heidelberg. (doi:10.1007/978-3-662-43550-2)
- Garland Jr., T., Dickerman, A.W., Janis, C.M., and J.A. Jones. 1993. Phylogenetic analysis of covariance by computer simulation. *Sys. Biol.* 42, 265-292. (doi:10.2307/2992464)
- Gerber, S., Eble, G.J., and P. Neige. 2008. Allometric space and allometric disparity: a developmental perspective in the macroevolutionary analysis of morphological disparity. *Evolution* 62, 1450-1457. (doi:j.1558-5646.2008.00370.x)
- Gould, S.J. 1966. Allometry and size in ontogeny and phylogeny. *Biol. Rev.* 41, 587-640. (doi:10.1111/j.1469-185x.1966.tb01624.x)
- Gould, S.J. 1977. *Ontogeny and Phylogeny*. Cambridge, Massachusetts: The Belknap Press of Harvard University Press. ISBN 0-674-63940-5.
- Harvey, P.H., and M.D. Pagel. 1991. *The Comparative Method in Evolutionary Biology*. Oxford University Press, Oxford.
- Herrel, A., and J.C. O'Reilly. 2006. Ontogenetic scaling of bite force in lizards and turtles. *Physiol Biochem. Zool.* 79, 31-42. (doi:10.1086/498193)
- Hobson, E.S. 1969. Comments on Certain Recent Generalizations Regarding Cleaning Symbioses in Fishes. *Pac. Sci.* 23, 35-39.
- Hobson, E.S. 1971. Cleaning symbiosis among California inshore fishes. *Fish. Bul. Nat. Ocean. Atmos. Admin.* 69, 491
- Jolicoeur, P. 1963. The multivariate generalization of the allometry equation. *Biometrics* 19, 497-499. (doi:10.2307/2527939)
- Klingenberg, C.P. 1998. Heterochrony and allometry: the analysis of evolutionary change in ontogeny. *Biol. Rev.* 73, 79-123. (doi:10.1111/j.1469-185x.1997.tb00026.x)
- Klingenberg, C.P., and R. Froese. 1991. A multivariate comparison of allometric growth patterns. *Syst. Zool.* 40, 410-419. (doi:10.2307/2992236)
- Kuiter, R.H., and T. Tonozuka. 2001. *Pictorial guide to Indonesian reef fishes. Part 2. Fusiliers - Dragonets, Caesionidae - Callionymidae*. Zoonetics, Australia.
- Martins, E.P., and T.F. Hansen. 1997. Phylogenies and the comparative method: A general approach to incorporating phylogenetic information into the analysis of interspecific data. *Am. Nat.* 149, 646-667. (doi:10.1086/286013)

- Mittelbach, G.G. 1981. Foraging Efficiency and Body Size: A Study of Optimal Diet and Habitat Use by Bluegills. *Ecology* 62, 1370–86. (doi:10.2307/1937300).
- Mitteroecker, P., Gunz, P., Bernhard, M., Shaefer, K., and F.L. Bookstein. 2004. Comparison of cranial ontogenetic trajectories among great apes and humans. *J. Hum. Evol.* 46, 679-698. (doi:10.1016/j.jhevol.2004.03.006)
- Motani, R., and L. Schmitz. 2011. Phylogenetic versus functional signals in the evolution of form-function relationships in terrestrial vision. *Evolution*. 65, 2245-2257. (doi:10.1111/j.1558-5646.2011.01271.x)
- Motta, P.J. 1984. Mechanics and Functions of Jaw Protrusion in Teleost Fishes: A Review. *Copeia*. 1984, 1. (doi:10.2307/1445030)
- Myers, R.F. 1999. Micronesian reef fishes: a comprehensive guide to the coral reef fishes of Micronesia, 3rd revised and expanded edition. Coral Graphics, Barrigada, Guam.
- Pearson, K. 1901. On lines and planes of closest fit to systems of points in space. *Phil. Mag.* 6, 559–572. (doi:10.1080/14786440109462720)
- Quignard, J-P, and A. Pras. 1986. Labridae. p. 919-942. In P.J.P. Whitehead, M.-L. Bauchot, J.-C. Hureau, J. Nielsen and E. Tortonese, eds. *Fishes of the north-eastern Atlantic and the Mediterranean*. UNESCO, Paris. Vol. 2.
- Randall, J.E. 1986. *Red Sea fishes*. London: Immel.
- Randall, J.E., Allen, G.R., and R.C. Steene. 1997. *Fishes of the Great Barrier Reef and Coral Sea*. Crawford House Publishing, Bathurst, Australia.
- Revell, L.J. 2009. Size-correction and principal components for interspecific comparative studies. *Evolution* 63, 3258-3268. (doi:10.1111/j.1558-5646.2009.00804.x)
- Revell, L.J. 2012. phytools: An R package for phylogenetic comparative biology (and other things). *Methods Ecol. Evol.* 3, 217-223. (doi:10.1111/j.2041-210x.2011.00169.x)
- Robins, C.R., and G.C. Ray. 1986. *A field guide to Atlantic coast fishes of North America*. Houghton Mifflin Company, Boston, U.S.A.
- Schluter, D., Price, T., Mooers, A.O., and D. Ludwig 1997. Likelihood of ancestor states in adaptive radiation. *Evolution* 51, 1699-1711. (doi:10.2307/2410994)
- Sidlauskas, B. 2008. Continuous and arrested morphological diversification in sister clades of characiform fishes: a phylomorphospace approach. *Evolution* 62, 3135–3156. (doi:10.1111/j.1558-5646.2008.00519.x)

- Stayton, C.T. 2015. The definition, recognition, and interpretation of convergent evolution, and two new measures for quantifying and assessing the significance of convergence. *Evolution* 69, 2140-2153. (doi:10.1111/evo.12729)
- Stayton, C.T. 2014. *convevol*: Quantifies and assesses the significance of convergent evolution. R package version 1.0. Available at <http://cran.r-project.org/web/packages/convevol/index.html>.
- Vogel, S. 1994. *Life in moving fluids*. Princeton University Press, Princeton, NJ
- Walker, J.A., M.W. Westneat. 2000. Mechanical performance of aquatic rowing and flying. *Proc. R. Soc. B.* 267, 1875–1881 (doi:10.1098/rspb.2000.1224)
- Wainwright, P.C., Bellwood, D.R., and M.W. Westneat. 2002. Ecomorphology of locomotion in labrid fishes. *Env. Biol. Fish.* 65, 47-62. (doi:10.1023/A:1019671131001).
- Wainwright, P.C., Bellwood, D.R., Westneat, M.W., Grubich J.R., and A. S. Hoey. 2004. A functional morphospace for the skull of labrid fishes: patterns of diversity in a complex biomechanical system. *Biol. J. Linn. Soc.* 82, 1-25. (doi:10.1111/j.1095-8312.2004.00313.x)
- Wainwright, P.C., and S.S. Shaw. 1999. Morphological basis of kinematic diversity in feeding sunfishes. *J. Exp. Biol.* 202, 3101-3110.
- Wilson, L.A.B., and M.R. Sánchez-Villagra. 2010. Diversity trends and their ontogenetic basis: an exploration of allometric disparity in rodents. *Proc. R. Soc. B.* 277, 1227-1234. (doi:10.1098/rspb.2009.1958)
- Westneat, M.W. 1990. Feeding mechanics of teleost fishes (Labridae; Perciformes): A test of four-bar linkage models. *J. Morphol.* 205, 269-295. (doi:10.1002/jmor.1052050304)
- Winterbottom, R. 1974. A descriptive synonymy of the striated muscles of the Teleostei. *Proc. Natl. Acad. Sci. Phil.* 125, 225–317.

SUPPORTING INFORMATION for:

An evolutionary approach to scaling: Phylo-allometric analyses indicate concordance between morphology and the ontogeny of cleaning behavior in wrasses

Vikram B. Baliga and Rita. S. Mehta

Contents:

1. Table S1: Specimens in the present study
2. Table S2: Traits measured on specimens in the present study
3. Table S3: Loadings of traits in the adult morphospace
4. Table S4: P-values from phylogenetically-informed ANOVA of D_a and D_s
5. Table S5: Coefficients from pFDA performed on ontogenetic scaling vectors
6. Table S6: Information regarding phylogenetically-informed MANOVA of pFDA scores
7. Table S7: Information regarding Standardized Major Axis regressions of each trait vs. standard length
8. Figure S1: Adult phylomorphospace
9. Figure S2: Absolute and standardized distances from the phylo-allometric centroid

Table S3.1 Specimens in the present study

Species (# of specimens)	Range of Standard Length	Catalog Numbers
<i>Ctenolabrus rupestris</i> (15)	41.27 – 108.32	MNHN 1977-0192, 1977-194
<i>Diproctacanthus xanthurus</i> (16)	39.21 – 82.21	CAS 201330, 201333, 201334, 201341; USNM 207468, 210232, 277107, 384516
<i>Gomphosus varius</i> (17)	39.89 – 185.29	LACM 37434-005, 57401-1, 57408-1; USNM 406991, 406992, 406994, 406995; VB
<i>Halichoeres bivittatus</i> (21)	40.95 – 186.34	CAS 8210, 18596, 37273; LACM 2479, 5560; VB
<i>Halichoeres chrysus</i> (24)	37.51 – 123.21	VB
<i>Halichoeres dispilus</i> (17)	38.56 – 180.93	LACM 8104; USNM 133078, 205447, 380926
<i>Halichoeres garnoti</i> (17)	40.24 – 179.20	USNM 133078, 410642, 410650; VB
<i>Halichoeres nicholsi</i> (18)	38.50 – 186.47	CAS 23751, 298374, 50009; LACM 32499-007, 43924-005
<i>Halichoeres notospilus</i> (16)	40.04 – 200.54	LACM 636, 48423-22, 48727-15
<i>Hemigymnus melapterus</i> (16)	39.15 – 165.03	VB
<i>Labrichthys unilineatus</i> (15)	38.95 – 137.41	CAS 35417, 65827, 93632; LACM 42489-26
<i>Labroides bicolor</i> (20)	39.00 – 135.51	CAS 39135, 89698, 989694; USNM 406998, 407845, 407846; VB
<i>Labroides dimidiatus</i> (23)	39.90 – 100.26	VB
<i>Labropsis australis</i> (15)	38.41 – 86.51	CAS 220169, 220206, 220614; USNM 235943; VB
<i>Larabicus quadrilineatus</i> (20)	37.67 – 93.61	CAS 233644, 235027, 235041; USNM 208450, 209719, 277504, 277518, 410647, 410648, 410649; VB
<i>Oxyjulis californica</i> (29)	45.15 – 218.00	VB
<i>Stethojulis albovittata</i> (16)	40.26 – 100.54	LACM 30859-67

<i>Symphodus cinereus</i> (15)	39.72 – 106.66	MNHN 1949-0071, 1977-0182; USNM 289684
<i>Symphodus doderleini</i> (17)	46.04 – 93.07	MNHN 1977-194, 1977-0195; VB
<i>Symphodus mediterraneus</i> (16)	45.23 – 116.54	MNHN 1962-0039, 1977-0196; VB
<i>Symphodus melops</i> (19)	43.53 – 171.64	MNHN 1960-390, 1960-389; USNM 10059
<i>Symphodus ocellatus</i> (15)	40.75 – 96.79	MNHN 1962-0038, 1977-0142
<i>Thalassoma amblycephalum</i> (15)	40.32 – 135.51	USNM 410644, 410645, 410646
<i>Thalassoma bifasciatum</i> (17)	39.65 – 180.34	LACM 54098-040, 56613-1; VB
<i>Thalassoma duperrey</i> (14)	44.90 – 181.58	CAS 21161, 29476; USNM 407843, 407844
<i>Thalassoma hardwicke</i> (22)	45.62 – 166.64	LACM 382104, 3998625, 51858-49; USNM 407842
<i>Thalassoma hebraicum</i> (18)	44.86 – 169.53	USNM 410655, 410656
<i>Thalassoma lucasanum</i> (16)	49.68 – 130.54	USNM 410653, 410654
<i>Thalassoma lutescens</i> (16)	34.19 – 180.94	CAS 20944, 215682; USNM 406996
<i>Thalassoma pavo</i> (18)	44.89 – 186.32	USNM 406999, 40784
<i>Thalassoma quinquevittatum</i> (16)	38.45 – 126.16	LACM 6674-74, 6679-32; VB
<i>Thalassoma rueppellii</i> (17)	45.58 – 180.32	USNM 410651, 410652
<i>Thalassoma trilobatum</i> (19)	43.02 – 114.31	USNM 410643; VB

Museum abbreviations: CAS – California Academy of Sciences (San Francisco, CA); LACM – Los Angeles County Museum of Natural History (Los Angeles, CA); USNM – Smithsonian National Museum of Natural History (Suitland, MD); MNHN – National Museum of Natural History (France). Other abbreviations: VB – personal collection of V.B. Baliga. Standard length ranges are reported in mm.

Table S3.2 Traits measured on specimens in the present study

Trait	Definition	Specimen Condition
Adductor Mandibulae Mass (AMCR)	Total mass of the adductor mandibulae complex (excluding A_{GD}); muscle identification followed Winterbottom (1974)	EtOH
Head Length (HL)	Distance between tip of closed mouth and posterior edge of operculum	EtOH
Head Depth (HD)	Distance between ventral edge of interopercle and dorsal edge of head (Motta 1984)	EtOH
Maximum Body Width (MBW)	Maximum distance between lateral edges of the body, measured perpendicular to the body axis	EtOH
Maximum Body Depth (MBD)	Maximum distance between the ventral and dorsal edges of the body, measured perpendicular to the body axis	EtOH
Pectoral Fin Length (PFL)	Length of the leading edge of the pectoral fin (Wainwright et al. 2002)	EtOH
Pectoral Fin Width (PFW)	Maximum width of the pectoral fin, measured perpendicular to the leading edge of the fin	EtOH
Lower Jaw Outlever Length (LJOL)	Distance between the quadrate-articular joint and the tip of the mandible (Westneat 1990)	C&S
Jaw-Closing In-Lever Length (JCIL)	Distance between the quadrate-articular joint and insertion point of adductor mandibulae onto the coronoid process (Westneat 1990)	C&S
Jaw-Opening In-Lever Length (JOIL)	Distance between the quadrate-articular joint and the insertion of the interoperculo-mandibular ligament (Westneat 1990)	C&S
Vertical Gape Distance (GAPE)	Distance between the distal edges of anteriormost teeth on the upper and lower jaws, with the mouth open (Motta 1984)	C&S
Premaxillary Protrusion Distance (PMX)	Excursion distance of the anteriormost tooth of the upper jaws as it travels rostrally when the jaws are protruded manually by depressing the lower jaw (Wainwright et al. 2004)	C&S

The Specimen Condition column indicates whether traits were measured on ethanol-preserved specimens (EtOH) or after specimens were cleared & double-stained (C&S). All traits were measured to the nearest 0.01mm, except adductor mandibulae mass, which was measured to the nearest 0.0001g. Before all analyses, measurements of all linear traits were first natural log-transformed, and measurements of mass were both cube-rooted and natural log-transformed.

References for Trait Definitions:

Winterbottom R. 1974 A descriptive synonymy of the striated muscles of the Teleostei. *Proc. Natl. Acad. Sci. Phil.* 125, 225–317.

Motta PJ. 1984 Mechanics and Functions of Jaw Protrusion in Teleost Fishes: A Review. *Copeia*. 1984, 1. (doi:10.2307/1445030)

Wainwright PC, Bellwood DR, Westneat MW. 2002 Ecomorphology of locomotion in labrid fishes. *Env. Biol. Fish.* 65, 47-62. (doi:10.1023/A:1019671131001).

Westneat MW. 1990 Feeding mechanics of teleost fishes (Labridae; Perciformes) : A test of four-bar linkage models. *J. Morphol.* 205, 269-295. (doi:10.1002/jmor.1052050304)

Wainwright PC, Bellwood DR, Westneat MW, Grubich JR, Hoey AS. 2004 A functional morphospace for the skull of labrid fishes: patterns of diversity in a complex biomechanical system. *Biol. J. Linn. Soc.* 82, 1-25. (doi:10.1111/j.1095-8312.2004.00313.x)

Table S3.3 Loadings of traits in the adult morphospace

	PC1 (77.32%)	PC2 (5.75%)	PC3 (3.51%)	PC4 (3.39%)	PC5 (2.98%)
Adductor Mandibulae Mass	-0.854	0.290	-0.033	-0.335	0.088
Head Length	-0.902	0.204	0.160	0.140	0.006
Head Depth	-0.935	-0.188	0.081	-0.028	-0.051
Maximum Body Width	-0.933	-0.148	0.040	-0.126	-0.020
Maximum Body Depth	-0.821	-0.433	0.246	-0.180	-0.146
Pectoral Fin Length	-0.838	-0.236	-0.400	0.032	0.052
Pectoral Fin Width	-0.865	0.004	-0.351	0.014	0.190
Jaw Outlever Length	-0.782	0.417	-0.099	0.028	-0.321
Jaw-Closing In-Lever Length	-0.914	0.177	0.001	-0.094	-0.212
Jaw-Opening In-Lever Length	-0.836	-0.230	0.160	-0.073	0.306
Vertical Gape Distance	-0.788	0.404	0.179	0.260	0.286
Premaxillary Protrusion Distance	-0.818	-0.305	0.010	0.406	-0.170

A phylogenetically-informed PCA was run using the correlation matrix of 12 traits. For each species, data were taken from 3-5 adult specimens. Loadings for the first 5 principal components are shown. The percent of the variance for which each PC accounts is listed in parentheses in the column headings. Traits that load strongly on each PC (i.e. |loading| > 0.4) are bolded.

Table S3.4A. P-values from phylogenetically-informed ANOVA of D_a

	Non-Cleaner	Juvenile Cleaner	Facultative Cleaner	Obligate Cleaner
Non-Cleaner	-			
Juvenile Cleaner	~1	-		
Facultative Cleaner	~1	~1	-	
Obligate Cleaner	~1	~1	~1	-

Table S3.4B. P-values from phylogenetically-informed ANOVA of D_s

	Non-Cleaner	Juvenile Cleaner	Facultative Cleaner	Obligate Cleaner
Non-Cleaner	-			
Juvenile Cleaner	0.776	-		
Facultative Cleaner	0.989	0.176	-	
Obligate Cleaner	0.776	0.176	0.697	-

A phylogenetically-informed ANOVA was run on species' a) absolute distances (D_a) and b) standardized distances (D_s) from the phylo-allometric centroid. Dietary groups did not exhibit significant differences (D_a : F-ratio: 0.74, p-value: 0.63; D_s : F-ratio: 3.04, p-value: 0.08). The above tables show p-values that have been adjusted for multiple hypothesis testing. Each table is symmetric across the diagonal; hence, only the elements below the diagonal are shown. In each of the metrics, each pair of groups do not show significant differences.

Table S3.5 Coefficients from pFDA performed on ontogenetic scaling vectors

	DA1 (86.87%)	DA2 (10.06%)	DA3 (3.07%)
Intercept	389.75	-167.73	123.03
Adductor Mandibulae Mass	-197.81	184.54	-189.65
Head Length	82.34	185.88	-11.15
Head Depth	-196.81	9.89	-0.69
Maximum Body Width	62.62	327.48	-121.03
Maximum Body Depth	-239.25	-178.11	48.59
Pectoral Fin Length	-135.52	-146.70	-190.81
Pectoral Fin Width	-32.75	37.56	-172.46
Jaw Outlever Length	-188.09	96.78	193.81
Jaw-Closing In-Lever Length	-373.39	-251.21	311.01
Jaw-Opening In-Lever Length	-2.05	18.25	-54.78
Vertical Gape Distance	65.16	231.00	-336.59
Premaxillary Protrusion Distance	-190.99	66.01	95.71

A total of three discriminant axes captured all of the variance in the dataset. Traits with especially large model coefficients are bolded.

Table S3.6A. T-values from phylogenetically-informed MANOVA of pFDA scores

	Non-Cleaner	Juvenile Cleaner	Facultative Cleaner	Obligate Cleaner
Non-Cleaner	-			
Juvenile Cleaner	-6.522	-		
Facultative Cleaner	-1.004	8.264	-	
Obligate Cleaner	-1.413	3.328	-0.875	-

Table S3.6B. P-values from post-hoc comparisons of pFDA scores

	Non-Cleaner	Juvenile Cleaner	Facultative Cleaner	Obligate Cleaner
Non-Cleaner	~1			
Juvenile Cleaner	0.003	~1		
Facultative Cleaner	0.402	0.003	~1	
Obligate Cleaner	0.402	0.024	0.535	~1

A phylogenetically-informed MANOVA was run on the scores from the pFDA to compare means among dietary groups. The MANOVA revealed significant differences between at least one set of groups ($F = 40.356$, $p < 0.001$). Listed above are A) t-values and B) p-values from post-hoc comparisons, with corrections for multiple hypothesis testing. Each table is symmetric across the diagonal; hence, only the elements below the diagonal are shown. Juvenile cleaners show significantly different mean scores from each of the other groups, while each of the other group comparisons does not show significant differences.

Table S7A. Slopes from Standardized Major Axis regressions of each trait vs. standard length (on following page)

Within each species and for each of 12 traits, we performed a standardized major axis regression of the trait against standard length. All traits, including standard length, were natural log-transformed before performing regressions. The slope from each regression is recorded above. We then tested whether regression slopes differed significantly from 1.0, i.e. the hypothesized slope under isometric growth. Within each set of p-values for a species, we applied adjustments to account for multiple hypothesis testing. In the above table, all slopes that exhibited significant allometry are bolded. Additionally, a heatmap effect is superimposed; warmer colors indicate more extreme positive allometry, while cooler colors represent more extreme negative allometry. Trait abbreviations: AMCR – cube root of adductor mandibulae mass; HL – head length; HD – head length; MBW – maximum body width; MBD – maximum body depth; PFL – pectoral fin length; PFW – pectoral fin width; LJOL – lower jaw out-lever length; JCIL – jaw closing in-lever length; JOIL – jaw opening in-lever length; GAPE – vertical gape distance; PMX – premaxillary protrusion distance.

Table S7A. Slopes from Standardized Major Axis regressions of each trait vs. standard length

	AMCR	HL	HD	MBW	MBD	PFL	PFW	LJOL	JCIL	JOIL	GAPE	PMX
<i>Ctenolabrus rupestris</i>	0.96	0.96	1.14	1.34	1.01	0.92	0.96	0.99	1.02	1.16	1.06	1.03
<i>Diproctacanthus xanthurus</i>	1.01	0.95	1.08	1.22	1.21	0.98	0.97	0.93	1.01	0.98	1.28	1.20
<i>Gomphosus varius</i>	0.98	1.31	0.97	1.04	1.01	1.15	1.04	1.15	0.99	0.61	1.12	0.76
<i>Halichoeres bivittatus</i>	1.07	1.00	1.10	1.22	1.36	1.11	1.00	1.06	1.14	1.19	1.34	1.48
<i>Halichoeres chrysus</i>	0.92	0.96	1.01	1.22	1.05	0.94	0.89	1.04	1.26	1.08	0.91	1.08
<i>Halichoeres dispilus</i>	0.95	0.99	1.16	1.26	1.01	0.96	0.97	0.98	0.99	1.18	0.90	0.87
<i>Halichoeres garnoti</i>	0.93	0.98	1.14	1.02	1.29	1.07	0.94	0.93	0.96	1.51	1.32	0.89
<i>Halichoeres nicholsi</i>	1.05	0.90	1.16	1.27	1.35	1.10	1.04	1.01	1.04	1.21	1.20	1.12
<i>Halichoeres notospilus</i>	0.99	0.94	0.97	1.03	1.04	1.01	1.10	0.93	1.00	1.09	0.96	1.02
<i>Hemigymnus melapterus</i>	0.81	0.97	1.00	1.10	1.05	0.97	0.94	1.01	0.85	1.03	1.23	1.38
<i>Labrichtys unilineatus</i>	0.85	0.89	0.97	0.97	0.98	1.06	0.89	0.94	1.12	1.07	1.09	0.97
<i>Labroides bicolor</i>	0.89	0.85	1.25	1.30	1.02	0.76	0.70	1.08	1.08	1.16	0.96	0.93
<i>Labroides dmidiatus</i>	0.86	0.91	1.03	1.17	1.32	1.24	1.18	0.79	0.88	0.80	0.94	1.01
<i>Labropsis australis</i>	0.94	0.94	1.09	1.21	1.24	0.98	1.00	0.85	1.09	1.12	1.28	1.40
<i>Larabicus quadrilineatus</i>	0.91	0.93	0.94	1.20	1.25	0.96	0.96	0.83	1.03	0.99	1.33	1.34
<i>Oxyjulis californica</i>	1.01	0.97	1.03	0.84	1.11	0.92	1.12	0.97	0.97	1.24	1.29	0.91
<i>Stethojulis albivittata</i>	0.98	0.82	1.07	1.07	1.08	0.82	0.87	0.77	0.79	0.59	1.43	1.21
<i>Symphodus cinereus</i>	0.93	0.95	1.19	1.12	1.10	1.11	1.21	1.02	1.14	1.18	1.05	0.85
<i>Symphodus doderleini</i>	0.98	1.01	0.97	1.05	1.12	1.14	1.08	0.95	1.19	1.07	1.11	1.13
<i>Symphodus mediterraneus</i>	0.99	1.07	1.14	1.23	1.05	1.06	1.23	0.70	0.73	1.27	0.94	0.84
<i>Symphodus melops</i>	1.01	1.04	1.09	1.17	1.10	1.09	1.10	0.81	0.98	0.96	1.34	1.08
<i>Symphodus ocellatus</i>	1.06	0.82	1.02	1.27	1.40	1.31	1.04	1.11	1.21	1.44	1.14	1.33
<i>Thalassoma amblycephalum</i>	0.91	1.06	1.06	0.86	1.22	1.04	0.73	0.64	0.94	1.13	0.96	1.08
<i>Thalassoma bifasciatum</i>	1.00	0.97	1.06	1.20	1.27	0.99	0.76	1.05	0.95	1.29	1.34	1.60
<i>Thalassoma duperrey</i>	0.96	1.02	1.04	1.17	1.16	1.06	0.81	0.92	1.10	1.23	1.09	1.32
<i>Thalassoma hardwicke</i>	0.83	0.79	1.03	1.15	0.92	0.99	0.90	0.86	0.87	1.11	0.75	1.25
<i>Thalassoma hebraicum</i>	0.96	0.98	1.11	1.04	0.98	1.05	0.72	1.10	1.24	1.23	0.92	1.13
<i>Thalassoma lucasanum</i>	1.01	0.85	1.25	1.11	1.25	1.00	0.91	0.92	1.09	1.09	1.26	1.51
<i>Thalassoma lutescens</i>	1.06	0.86	1.04	1.12	1.23	1.05	0.63	1.17	1.10	1.37	1.44	1.51
<i>Thalassoma pavo</i>	1.01	1.11	0.96	1.14	1.23	1.07	0.95	1.11	1.20	1.35	1.45	1.34
<i>Thalassoma quinquevittatum</i>	0.93	0.97	1.01	1.28	0.83	1.18	1.08	1.14	1.16	1.32	1.38	1.14
<i>Thalassoma rueppellii</i>	0.81	1.01	1.01	1.13	1.08	1.03	1.17	1.03	1.17	1.14	1.12	0.98
<i>Thalassoma trilobatum</i>	0.89	0.92	1.06	1.05	1.08	1.14	1.10	1.11	1.22	1.00	0.90	0.97

Table S7B. P-Values from Standardized Major Axis regressions of each trait vs. standard length (on following page)

Within each species and for each of 12 traits, we performed a standardized major axis regression of the trait against standard length. All traits, including standard length, were natural log-transformed before performing regressions. We then tested whether regression slopes differed significantly from 1.0, i.e. the hypothesized slope under isometric growth. Within each set of p-values for a species, we applied adjustments to account for multiple hypothesis testing. Adjusted p-values are recorded above, and those that are ≤ 0.05 are bolded. Trait abbreviations: AMCR – cube root of adductor mandibulae mass; HL – head length; HD – head length; MBW – maximum body width; MBD – maximum body depth; PFL – pectoral fin length; PFW – pectoral fin width; LJOL – lower jaw out-lever length; JCIL – jaw closing in-lever length; JOIL – jaw opening in-lever length; GAPE – vertical gape distance; PMX – premaxillary protrusion distance.

Table S7B. P-Values from Standardized Major Axis regressions of each trait vs. standard length

	AMCR	HL	HD	MBW	MBD	PFL	PFW	LJOL	JCIL	JOIL	GAPE	PMX
<i>Ctenolabrus rupestris</i>	0.889	0.889	0.220	0.220	0.416	0.416	0.889	0.889	0.889	0.889	0.889	0.889
<i>Diprotacanthus xanthurus</i>	0.224	0.004	0.026	0.001	0.007	0.536	0.359	0.002	0.899	0.714	0.020	0.006
<i>Gomphosus varius</i>	< 0.001	< 0.001	0.303	0.303	0.748	0.007	0.620	< 0.001	0.620	< 0.001	< 0.001	0.001
<i>Halichoeres bivittatus</i>	< 0.001	0.943	< 0.001	< 0.001	< 0.001	0.002	0.943	0.108	< 0.001	0.034	< 0.001	< 0.001
<i>Halichoeres chrysus</i>	< 0.001	0.002	0.300	< 0.001	0.040	0.040	0.098	0.003	< 0.001	0.153	0.005	0.093
<i>Halichoeres dispilus</i>	0.012	0.816	0.012	0.004	0.816	0.327	0.816	0.327	0.816	< 0.001	0.158	0.212
<i>Halichoeres garnoti</i>	0.212	0.421	0.001	0.817	< 0.001	0.265	0.476	0.001	0.300	< 0.001	< 0.001	0.189
<i>Halichoeres nicholsi</i>	0.001	< 0.001	0.009	< 0.001	< 0.001	0.066	0.691	0.733	0.225	< 0.001	< 0.001	0.018
<i>Halichoeres notospilus</i>	0.996	0.833	0.996	0.996	0.553	0.996	0.717	0.553	0.998	0.553	0.996	0.996
<i>Hemigymmus melapterus</i>	< 0.001	0.712	0.969	0.100	0.100	0.712	0.414	0.712	< 0.001	0.100	< 0.001	< 0.001
<i>Labrichthys unilineatus</i>	0.037	0.037	0.476	0.404	0.476	0.404	0.154	0.154	0.011	0.154	0.238	0.790
<i>Labroides bicolor</i>	0.025	0.003	0.003	0.003	0.681	0.003	0.005	0.113	0.113	0.113	0.519	0.121
<i>Labroides dimidiatus</i>	0.002	0.015	0.418	0.005	< 0.001	< 0.001	0.011	< 0.001	0.002	< 0.001	0.168	0.911
<i>Labropsis australis</i>	0.422	0.040	0.006	0.007	0.007	0.815	0.659	0.042	0.046	0.008	0.006	0.010
<i>Larabicus quadrilineatus</i>	0.002	0.004	0.056	0.002	0.001	0.154	0.590	< 0.001	0.590	0.771	< 0.001	< 0.001
<i>Oxyjulius californica</i>	0.695	0.450	0.695	0.064	0.172	0.029	0.033	0.106	0.172	< 0.001	< 0.001	0.064
<i>Stethojulis albovittata</i>	0.570	< 0.001	0.006	0.457	0.410	0.006	0.175	< 0.001	< 0.001	< 0.001	< 0.001	0.004
<i>Symphodus cinereus</i>	0.187	0.362	0.187	0.187	0.187	0.318	0.187	0.840	0.318	0.362	0.187	0.187
<i>Symphodus dodderleini</i>	0.847	0.847	0.847	0.847	0.847	0.847	0.847	0.847	0.847	0.414	0.847	0.847
<i>Symphodus mediterraneus</i>	0.701	0.114	0.114	0.143	0.009	0.376	0.204	0.009	0.007	0.017	0.555	0.204
<i>Symphodus melops</i>	0.733	0.566	0.501	0.091	0.142	0.517	0.582	< 0.001	0.582	0.582	< 0.001	0.582
<i>Symphodus ocellatus</i>	0.459	0.036	0.747	0.112	0.062	0.036	0.747	0.459	0.062	0.036	0.062	0.036
<i>Thalassoma amblycephalum</i>	0.001	0.267	0.446	0.267	0.014	0.446	0.003	< 0.001	0.091	0.261	0.461	0.446
<i>Thalassoma bifasciatum</i>	0.966	0.097	0.002	< 0.001	< 0.001	0.781	< 0.001	0.001	0.076	0.000	< 0.001	< 0.001
<i>Thalassoma duperrey</i>	0.095	0.417	0.110	< 0.001	< 0.001	0.146	< 0.001	0.002	< 0.001	0.002	< 0.001	< 0.001
<i>Thalassoma hardwicke</i>	< 0.001	< 0.001	0.424	< 0.001	0.002	0.683	0.001	< 0.001	< 0.001	0.004	< 0.001	< 0.001
<i>Thalassoma hebraicum</i>	0.392	0.677	0.194	0.677	0.677	0.537	0.001	0.004	< 0.001	< 0.001	0.016	0.016
<i>Thalassoma lucasanum</i>	< 0.001	0.008	< 0.001	0.071	< 0.001	0.996	0.258	0.181	0.258	0.394	0.004	0.003
<i>Thalassoma lutescens</i>	0.002	< 0.001	0.091	< 0.001	< 0.001	0.052	< 0.001	< 0.001	< 0.001	< 0.001	< 0.001	< 0.001
<i>Thalassoma pavo</i>	0.578	< 0.001	0.213	0.005	< 0.001	0.012	0.149	0.005	< 0.001	0.001	< 0.001	0.003
<i>Thalassoma quinquevittatum</i>	0.305	0.515	0.825	0.011	0.005	0.001	0.515	< 0.001	< 0.001	< 0.001	< 0.001	0.080
<i>Thalassoma rueppellii</i>	0.029	0.734	0.869	0.110	0.086	0.652	0.029	0.316	0.001	0.029	0.029	0.652
<i>Thalassoma trilobatum</i>	0.002	0.039	0.212	0.559	0.545	0.002	0.545	0.012	0.012	0.989	0.212	0.943

Conclusions

The evolution of cleaning behavior in the Labridae presented a model system to investigate how microevolutionary processes affect broad scale patterns of diversity. Ectoparasitivory, “cleaning”, in labrid fishes is a feeding strategy that involves varying degrees of morphological specialization. The overall goal of this dissertation was to understand how incorporating ontogenetic scaling patterns can contribute to understanding macroevolutionary patterns of morphological and ecological diversity, as the majority of labrid cleaners show ontogenetic transitions away from this feeding strategy.

While Côté (2010) summarized the ontogenetic patterns of cleaner fish ecology, the functional morphology of cleaning, as well as the morphological correlates of this trophic strategy, was little understood. Thus, I first sought to determine what morphological and kinematic characteristics may be used to discern cleaners from non-cleaners. Through my research in Chapter 1, I discovered that feeding in cleaners is associated with low-displacement, fast jaw movements that allow for rapid gape cycles on individually-targeted items (Baliga and Mehta 2015). These findings are further corroborated by additional kinematic data I have acquired for several other cleaner (8 sp.) and non-cleaner (9 sp.) labrids (Baliga, *unpublished*; Baliga and Mehta 2015). In a related study, I discovered that juvenile labrid cleaners of the genus *Thalassoma*, as juveniles, possess jaws with low mobility and exhibit low bite forces compared to non-cleaner congeners (Baliga and Mehta 2014). Upon reaching

adulthood, however, morphological and functional differences between cleaner species and non-cleaners begin to overlap in their growth trajectories for jaw traits.

While individual case studies of kinematic or morphological patterns provide valuable insights into the functional morphology of animal behavior, it can be challenging to make generalizations from these trends to comment on broader macroevolutionary patterns. My Chapter 2 complements these kinematic studies by examining macroevolutionary patterns of size and shape in relation to cleaning in both the Labridae and Gobiidae, two marine clades in which obligate cleaning has evolved. Therefore, Chapter 2 further advances our understanding of cleaning by first providing inference of phylogenetic relationships within each of the two families and then using stochastic character mapping to infer the evolution of cleaning in both the Gobiidae and the Labridae. These analyses then enabled me to observe that the evolution of obligate cleaning is associated with not just a small body size but also a reduction in body depth, elongation of the head, and a more terminal orientation of the mouth. While facultative and juvenile cleaner taxa showed more varying patterns of convergence, I found that the evolution of cleaning is generally associated with similar characteristics in both of these groups.

Completing Chapters 1 and 2 thus enabled me to identify general head and body characteristics that were associated with the evolution of cleaning: an elongate body paired with an elongate head, and a terminal mouth that allows jaws with low mobility to bite rapidly on individually-targeted prey items. These findings guided me to select an informative suite of traits in which to explore evolutionary patterns of

ontogenetic change. Although previous studies have examined ontogenetic allometry across closely-related species (e.g. Wilson and Sánchez-Villagra 2010), the confound of phylogenetic influence had been untreated. In Chapter 3, I developed an approach in which the ontogenetic trajectories of multiple taxa can be analyzed through a phylogenetic-comparative framework.

These “phylo-allometric” analyses enabled me to show evidence that the repeated evolution of facultative and obligate cleaning (in which taxa continue to clean as adults) is associated with the maintenance of characters over ontogeny that are conducive to cleaning in the juvenile phase. On the other hand, taxa that transition away from cleaning during ontogeny do not maintain such characters, and exhibit phenotypic trajectories that are distinct from those of other wrasses. This indicates that the recurring evolution of juvenile cleaning behavior in the Labridae has involved similar effects on developmental scaling patterns. The repeated evolution of each of these patterns shows that labrid scaling trajectories are fundamentally labile and appear to evolve adaptively to changing ecological pressures over ontogeny. Further studying the lability in the developmental patterns of the Labridae in a phylo-allometric framework may help us better understand how and why this group exhibits broad morphological and functional diversity.

Through my studies, I have found the evolution of cleaning behavior in marine fishes to present an ideal system in which to test hypotheses regarding the interplay between selection and the developmental processes that produce selectable variation. I have also contributed to our understanding of the diversity of feeding behavior in

bony fishes by describing the functional morphology of cleaning in a variety of taxa. One striking finding from some of my kinematics work is that cleaner fishes appear to show a markedly higher degree of integration (defined as the strength of the relationship between kinematic variables in Wainwright et al., 2008) in jaw movements during feeding than do closely-related, non-cleaner taxa. Thus the evolution of cleaning behavior also presents a model system in which we can examine the extent to which patterns of integration in feeding kinematics may correspond to patterns of integration in cranial morphology.

Analyses of morphological integration provide a framework for exploring general patterns of trait interactions, which are often shown to be a major influence on morphological diversity (Marroig et al. 2009; Drake and Klingenberg 2010). But, few broad-scale comparative studies on morphological integration exist; consequently, hypotheses on the role of integration in shaping morphological and functional diversity are relatively unexplored (but see Goswami et al. 2014; Collar et al. 2014).

Assessing phenotypic integration affords promising avenues of understanding morphological evolution and kinematic diversity. For example, evolutionary increases in phenotypic integration could constrain diversity in the skull. With strong phenotypic integration (exhibited throughout ontogeny), lineages could become “stuck” at phenotypic optima. Given that cleaning has evolved multiple times in the Labridae, this study system affords the ability to test the hypothesis that the evolution of cleaning is associated with diminished levels of integration in ancestral conditions, allowing lineages to occupy new optima.

5.2 References

- Baliga VB and Mehta RS. 2014. Scaling patterns inform ontogenetic transitions away from cleaning in *Thalassoma* wrasses. *J Exp. Biol.* 217, 3597-3606.
- Baliga VB and Mehta RS. 2015. Linking Cranial Morphology to Prey Capture Kinematics in Three Cleaner Wrasses: *Labroides dimidiatus*, *Larabicus quadrilineatus*, and *Thalassoma lutescens*. *J Morphol.* 276, 1377–91.
- Collar D.C., Wainwright P.C., Alfaro M.E., Revell L.J., Mehta R.S. 2014. Biting disrupts integration to spur skull evolution in eels. *Nat. Comm.* 5: 5505.
- Côté I.M. 2000. Evolution and Ecology of Cleaning Symbioses in the Sea. *Oceanogr. Mar. Biol. Annu. Rev.* 38, 311–355.
- Côté I.M. 2010. Gobies as cleaners. In *The Biology of Gobies*. Patzner R. A. (editor). Boca Raton: CRC Press.
- Drake A.G., Klingenberg C.P. 2010. Large-scale diversification of skull shape in domestic dogs: Disparity and modularity. *Am. Nat.* 175: 289–301
- Goswami A. Smaers J.B., Soligo C., Polly P.D. 2014. The macroevolutionary consequences of phenotypic integration. *Phil. Trans. Roy. Soc. Lond., B*, 369: 20130254.
- Marroig G., Shirai L.T., Porto A., Oliveira F. B., Conto V. 2009. The Evolution of Modularity in the Mammalian Skull II: Evolutionary Consequences. *Evol. Biol.* 36:136-148
- Wainwright P.C., Mehta R.S., Higham T.E. 2008. Stereotypy, flexibility and coordination: central concepts in behavioral functional morphology. *J Exp. Biol.* 211:3523-3528.
- Wilson L.A.B., Sánchez-Villagra M.R. 2010. Diversity trends and their ontogenetic basis: an exploration of allometric disparity in rodents. *Proc. R. Soc. B.* 277, 1227-1234. (doi:10.1098/rspb.2009.1958)

Appendix

Contents

A.1 Tables S2.1 – S2.5

A.2 Permission for Published Material

Table S2.1: GenBank Accession IDs of sequences used in this study for 45 gobiid species

Name	CYTB	RAG1	RHOD	COI	12S	TRNT	GPR85	ZIC1
<i>Aruma histrio</i>	KF41550 5.1	AY84656 4.1	AY84663 1.1		AF49105 4.1		KF41611 6.1	KF41590 5.1
<i>Barbulifer ceuthoecus</i>	KF41551 0.1	KF415705 .1	HQ53689 1.1		AF49105 6.1	AF49105 5.1	KF41612 1.1	KF41591 0.1
<i>Elacatinus atronasus</i>		AY84652 7.1	AY84659 4.1			AY84647 5.1		
<i>Elacatinus cayman</i>				KM98726 7.1				
<i>Elacatinus centralis</i>				KM89416 9.1				
<i>Elacatinus chancei</i>	DQ25058 1.1	AY84651 5.1	AY84658 2.1	KM89417 0.1	AF49106 9.1	AY84646 4.1		
<i>Elacatinus colini</i>				KM89417 4.1				
<i>Elacatinus evelynae</i>	AY84642 7.1	AY84653 3.1	AY84660 0.1	KM98726 6.1	AF49107 0.1	AY84648 3.1		
<i>Elacatinus figaro</i>	KF41554 5.1	AY84654 4.1	AY84661 2.1	KM98726 5.1	AF49107 1.1		KF41616 1.1	KF41595 1.1
<i>Elacatinus genie</i>	AY84642 3.1	AY84652 9.1	AY84659 6.1	KM98724 4.1	AF49107 2.1	AY84648 5.1		
<i>Elacatinus horsti</i>	KF92900 8.1		JF261565 .1	KM89417 3.1	AF49107 3.1	AY84647 0.1		
<i>Elacatinus illecebrosus</i>		AY84654 1.1	AY84660 8.1	KM98726 1.1		AY84648 6.1		
<i>Elacatinus lobeli</i>				KM98725 0.1				

<i>Elacatinus lori</i>	KF92902 0.1	AY84651 9.1	AY84658 6.1	KM89416 8.1			AY84646 8.1		
<i>Elacatinus louisae</i>	KF41554 6.1	KF415744 .1		KM89416 1.1	AF49107 5.1	AF49107 5.1	AY84647 1.1	KF41616 2.1	KF41595 2.1
<i>Elacatinus oceanops</i>			JF261558 .1	KM98724 2.1	AF49107 6.1	AF49107 6.1	AY84647 8.1		KC83076 3.1
<i>Elacatinus panamensis</i>				GU90815 3.1					
<i>Elacatinus phthiophagus</i>				KM98726 8.1					
<i>Elacatinus prochilos</i>	AY84643 6.1	AY84654 3.1	AY84661 0.1	KM98726 9.1	AF49107 7.1	AF49107 7.1	AY84649 1.1		
<i>Elacatinus puncticulatus</i>	AY84644 3.1	AY84654 8.1	AY84661 6.1		AF49107 8.1	AF49107 8.1			
<i>Elacatinus randalli</i>		AY84654 7.1	AY84661 4.1	KM98726 0.1			AY84649 5.1		
<i>Elacatinus rubrigenis</i>				GU90815 4.1					
<i>Elacatinus xanthiprora</i>	AY84641 9.1	AY84652 5.1	AY84659 2.1		AF49108 0.1	AF49108 0.1	AY84647 3.1		
<i>Evermannichthys metzelaari</i>	KF41555 5.1	KF415755 .1			AF49106 5.1	AF49106 5.1		KF41617 3.1	KF41596 1.1
<i>Ginsburgellus novemlineatus</i>	KF41556 4.1	KF415765 .1	KF23553 1.1	KF415564 .1	AF49106 7.1	AF49106 7.1	AY84649 7.1	KF41618 3.1	KF41597 0.1
<i>Gnatholepis thompsoni</i>	DQ16738 1.1			JQ842870 .1					
<i>Gobionellus oceanicus</i>				KF461183 .1					

<i>Gobiosoma bosch</i>	KF41557 9.1	KF415782 .1		KM07782 9.1	AF49109 5.1	KF41619 9.1	KF41598 6.1
<i>Gobiosoma chiquita</i>	KF41558 0.1	KF415783 .1	JF261564 .1	HQ90946 7.1	AF49108 1.1	KF41620 0.1	KF41598 7.1
<i>Gobiosoma ginsburgi</i>				KP254065 .1	AF49109 6.1		
<i>Gobiosoma paradoxum</i>	KF41558 1.1	KF415784 .1				KF41620 1.1	KF41598 8.1
<i>Gobiosoma yucatanum</i>	KF41558 2.1	KF415785 .1				KF41620 2.1	KF41598 9.1
<i>Gobiosoma robustum</i>			KF23553 4.1	KP254957 .1			
<i>Risor ruber</i>	KF41565 5.1	KF415859 .1	AY84662 7.1		AF49111 6.1	KF41628 3.1	KF41606 7.1
<i>Tigrigobius digueti</i>	AY84639 3.1	AY84649 8.1	AY84656 6.1				
<i>Tigrigobius dilepis</i>	KF41567 4.1	KF415877 .1	AY84661 8.1	GU22440 8.1	AF49109 8.1	KF41630 1.1	KF41608 7.1
<i>Tigrigobius gemmatus</i>	AY84645 1.1	AY84655 6.1	AY84662 4.1		AF49109 9.1		
<i>Tigrigobius harveyi</i>				KM89414 6.1			
<i>Tigrigobius janssi</i>	AY84640 0.1	AY84650 6.1	AY84657 4.1				
<i>Tigrigobius limbaughi</i>	AY84639 9.1	AY84650 5.1	AY84657 2.1		AF49110 0.1	AY84649 6.1	
<i>Tigrigobius macrodon</i>	AY84644 6.1	AY84655 3.1	HQ53688 9.1				

<i>Tigrigobius multifasciatus</i>	AY84640 2.1	KF415878 .1	AY84657 5.1	GU90815 8.1	AF49110 2.1	KF41630 2.1	KF41608 8.1
<i>Tigrigobius nesiotetes</i>	AY84639 6.1	AY84650 2.1	AY84657 0.1				
<i>Tigrigobius pallens</i>	AY84645 3.1	AY84655 8.1	AY84662 6.1	GU22440 9.1	AF49110 3.1		
<i>Tigrigobius saucrus</i>	AY84644 9.1	AY84655 4.1	AY84662 2.1		AF49110 4.1		

Table S2.2: GenBank Accession IDs of sequences used in this study for 10 gobiid outgroup species

Name	CYTB	RAG1	RHOD	COI	12S	TRNT	GPR85	ZIC1
<i>Amblyeleotris periphalma</i>			HQ536926 .1	HQ536651. 1				
<i>Bathygobius saporator</i>	AY781105 .1			HM748426 .1				
<i>Coryphopterus glaucofraenum</i>		KF235437 .1	KF235511. 1					
<i>Lythrypnus nesiotes</i>	JX024770. 1	JX024823. 1						
<i>Microgobius microlepis</i>	KF415610. 1	KF415817 .1	JF261576. 1	HQ909478. 1	AF491112 .1		KF416235 .1	KF416021 .1
<i>Notropis lutipinnis</i>	FJ605094. 1							
<i>Ophiogobius jenynsi</i>	KF415621. 1	KF415827 .1	JF261580. 1	HQ909482. 1			KF416248 .1	KF416033 .1
<i>Ptereleotris calliura</i>	AB560894 .1							
<i>Ptereleotris helene</i>		KF235477 .1	KF235553. 1	JQ840666. 1				
<i>Zosterisessor ophiocephalus</i>	KF415684. 1	KF415889 .1	JF261594. 1		KF415492 .1		KF416314 .1	KF416100 .1

Table S2.3: GenBank Accession IDs of sequences used in this study for 320 labrid species

Name	12S	16S	COI	CYTB	RAG2	RAG1	ZIC1
<i>Acantholabrus palloni</i>		AF517587. 1	GQ341585. 1	DQ197923. 1			
<i>Achoerodus viridis</i>	AY279574	AY279677	EF609278. 1		AY279883		
<i>Anampses caeruleopunctatus</i>	AY279575	KJ866392. 1	AY850746	JF457907.1	AY279884		
<i>Anampses chrysocephalus</i>	JN935299. 1	KJ866393. 1	JQ839400.1				
<i>Anampses cuvier</i>	JN935301. 1	KJ866394. 1	JN935329.1				
<i>Anampses elegans</i>	JN935304. 1	KJ866395. 1	JN935330.1				
<i>Anampses femininus</i>	JN935305. 1	KJ866396. 1	JN935332.1				
<i>Anampses geographicus</i>	AJ810125	KJ866397. 1	DQ164156				
<i>Anampses lennardi</i>		KJ866398. 1	JN935335.1				
<i>Anampses lineatus</i>	JN935310. 1	KJ866399. 1	KF929597. 1	JF457908.1			KC830920. 1
<i>Anampses meleagrides</i>	DQ164139	KJ866401. 1	DQ164157				
<i>Anampses neoguinaicus</i>	AY279576	AY279679	FJ582843.1		AY279885		
<i>Anampses twistii</i>	AY850807	KJ866403. 1	AY850745	JF457914.1			

<i>Anchichoerops natalensis</i>					HQ945819.1				
<i>Austrolabrus maculatus</i>	AY279577	AY279680				AY279886			
<i>Bodianus anthioides</i>		JF457246.1		JF457916.1					
<i>Bodianus axillaris</i>		JF457252.1		JF457923.1					KC830925.1
<i>Bodianus bilunulatus</i>					KF929662.1				
<i>Bodianus bimaculatus</i>					JF492963				
<i>Bodianus diana</i>		JF457254.1		JF457927.1					
<i>Bodianus dictynna</i>					KC684982.1				
<i>Bodianus diplotaenia</i>					KC684987.1				
<i>Bodianus eclancheri</i>					JQ839404.1				
<i>Bodianus mesothorax</i>	AY279578	AY279681			KF929664.1	AY279887			KC830880.1
<i>Bodianus oxycephalus</i>					FJ237632.1				
<i>Bodianus perditio</i>		JF457259.1		JF457929.1					
<i>Bodianus pulchellus</i>					FJ582902.1				
<i>Bodianus rufus</i>	AY279579	AY279682.1			AY850741	AY279888	JQ353050.1		JQ353159.1
<i>Bodianus scrofa</i>		AF517582		DQ197931					
<i>Bodianus solatus</i>					KC684997.1				
<i>Bodianus speciosus</i>					GQ341587.1				

<i>Bodianus tanyokidus</i>					FJ237633.1							
<i>Bodianus trilineatus</i>					JF492970.1							
<i>Bodianus unimaculatus</i>					EF609299.1							
<i>Bolbometopon muricatum</i>	EU601178	AY081091				AY081126	EU601307					
<i>Calotomus carolinus</i>	EU601179	AY081092			JQ349815.1	EU601358	EU601308		KF141195.1			
<i>Calotomus spinidens</i>	EU601180				JF493012.1	EU601359	EU601309					
<i>Centrolabrus caeruleus</i>	AF414194	AY092034										
<i>Centrolabrus exoletus</i>	EU601224	EU601260			GQ341588.1	EU601403	EU601353					
<i>Centrolabrus trutta</i>	AY092046	AY092035										
<i>Cetoscarus bicolor</i>	EU601181	AY081088			KF929705.1	AY081123	EU601310		JX189899.1			
<i>Cheilinus chlorourus</i>	AJ810127	JF457348.1			KF929728.1						KC830910.1	
<i>Cheilinus fasciatus</i>	AY279580	AF517580			KF929729.1	JF458021.1	AY279889				KC830866.1	
<i>Cheilinus oxycephalus</i>	AY279581	AY279684			KF929730.1	JF458023.1	AY279890					
<i>Cheilinus trilobatus</i>	AJ810128	JF457359.1			JQ431607.1	JF458025.1						
<i>Cheilinus undulatus</i>	EU601220	AY279685			EF609322.1	EU601399	AY279891.1					
<i>Cheilito inermis</i>	AY279583	AY279686.1			AY850742	JF458028.1	AY279892					
<i>Chlorurus bleekeri</i>	EU601182	JX026458.1				EU601361	EU601311					

<i>Chlorurus bowersi</i>	EU601183	JX026459. 1		EU601362	EU601312		
<i>Chlorurus capistratoides</i>	EU601184	JX026460. 1		EU601363	EU601313		
<i>Chlorurus japonensis</i>	EU601209	EU601250		EU601388	EU601338		
<i>Chlorurus microrhinos</i>	EU601185	JX026466. 1		EU601364	EU601314		
<i>Chlorurus oedema</i>	EU601186	AY081090		AY081125	EU601315		
<i>Chlorurus sordidus</i>	AY279584	AY279687	KF929743. 1	AY081124	AY279893	JX189878. 1	KC830906. 1
<i>Choerodon anchorago</i>	AY279585	AY279688			AY279894		
<i>Choerodon azurio</i>	AB121235	KP219774. 1	JN242484.1	JN212026.1			
<i>Choerodon cauteroma</i>		KP219779. 1	KM224701. 1		KP219825. 1		
<i>Choerodon cephalotes</i>		KP219781. 1	KM224702. 1		KP219826. 1		
<i>Choerodon fasciatus</i>	AY081079	AY081097		AY081132	KP219828. 1		
<i>Choerodon monostigma</i>		KP219797. 1			KP219833. 1		
<i>Choerodon oligacanthus</i>	AF121218	KP219798. 1			KP219834. 1		
<i>Choerodon rubescens</i>		KP219806. 1	EF609330. 1		KP219836. 1		
<i>Choerodon schoenleinii</i>	AY279586	AY279689	EF609331. 1		AY279895		
<i>Choerodon venustus</i>		KP219815. 1	EF609332. 1		KP219839. 1		

<i>Cirrhilabrus cyanopleura</i>				FJ583220.1					
<i>Cirrhilabrus exquisitus</i>		JF457424.1		JF434935.1					
<i>Cirrhilabrus flavidorsalis</i>				FJ583232.1					
<i>Cirrhilabrus lubbocki</i>	AY279587	AY279690		FJ583238.1		AY279896			
<i>Cirrhilabrus rubrimarginatus</i>				FJ583240.1					
<i>Cirrhilabrus rubriventralis</i>				FJ583241.1					
<i>Cirrhilabrus scottorum</i>		JF457426.1		JQ839410.1	JF458096.1				
<i>Clepticus parrae</i>	AY279588	AY279691		KF929770.1		AY279897	JX189879.1	JX189105.1	
<i>Coris atlantica</i>				GQ341590.1					
<i>Coris aurilineata</i>	AY850839	AY850902		AY850777					
<i>Coris aygula</i>	AY279589	JF457428.1		JQ839415.1	JF458098.1	AY279898			
<i>Coris batuensis</i>	AY279591	AY279694.1		AY850793		AY279900		JX189106.1	
<i>Coris bulbifrons</i>				EF609338.1					
<i>Coris caudimacula</i>		JF457432.1		JF434940.1	JF458102.1			KC830900.1	
<i>Coris cuvieri</i>		JF457436.1		JQ839416.1	JF458106.1				
<i>Coris dorsomacula</i>	AY850830	AY850893		AY850768					
<i>Coris flavovittata</i>	AY850832	AY850895		AY850770					
<i>Coris formosa</i>				KF929780.1				KC830922.1	

<i>Coris gaimard</i>	AY279590	JF457437.1	AY850764	JF458107.1	AY279899	JX189880. 1	KC830921. 1
<i>Coris julis</i>	AJ810130	AY092044	GQ341591. 1	AY328856		EU167885. 1	
<i>Coris picta</i>	AY850829	AY850892	AY850767. 1				
<i>Coris pictoides</i>	AY850840	AY850903	AY850778				
<i>Cryptotomus roseus</i>	EU601188	AY279695	JQ840469.1	AY081131	AY279901	KF141213. 1	
<i>Ctenolabrus rupestris</i>	AJ810131	AF517586	GQ341592. 1	HM049943. 1			
<i>Cymolutes praetextatus</i>	AY279593	AY279696	JQ839423.1		AY279902		
<i>Cymolutes torquatus</i>	AY279594	AY279697	JQ839424.1		AY279903		
<i>Decodon melasma</i>		HQ127654. 1	JQ839425.1				
<i>Decodon puellaris</i>			KF929812. 1				
<i>Diproctacanthus xanthurus</i>	AY279595	AY279698			AY279904	JX189881. 1	JX189108. 1
<i>Doratonotus megalepis</i>			JQ840471.1				
<i>Epibulus insidiator</i>	EU601222	EU601259	KF929847. 1	EU885925	AY279905	JX189883. 1	KC830891. 1
<i>Eupetrichthys angustipes</i>	AB121250						
<i>Gomphosus caeruleus</i>		AY328984	JF434979.1	AY328857			
<i>Gomphosus varius</i>	AY279597	AY279700	JQ431774.1	AY328858	AY279906	JX189884. 1	KC830876. 1
<i>Haletta semifasciata</i>	AY279656	AY279759	EF609368. 1		AY279965		
<i>Halichoeres adustus</i>			JQ839442.1				

<i>Halichoeres argus</i>	AY279598	AY850910	AY850785	AY279907		
<i>Halichoeres binotopsis</i>	AY850845	AY850908	AY850783			
<i>Halichoeres biocellatus</i>	AY850852	AY850915	AY850790			KC830892. 1
<i>Halichoeres bivittatus</i>	AY279599	AY850880	AY850755	AY279908	JX189885. 1	JX189111. 1
<i>Halichoeres brasiliensis</i>						
<i>Halichoeres brownfieldi</i>	AY850860	AY850923	AY850798			
<i>Halichoeres chloropterus</i>	AY850861	AY850924	KC970477. 1			
<i>Halichoeres chrysus</i>	AF285919	AY850916	AY850791			
<i>Halichoeres claudia</i>						
<i>Halichoeres cosmetus</i>		JF457472.1	JQ724929.1			
<i>Halichoeres cyanocephalus</i>			JF434986.1		JF458140.1	
<i>Halichoeres dispilus</i>	AY850813	AY850876	HM389563. 1		AY591379	
<i>Halichoeres garnoti</i>	AY850819	AY850882	AY850751		EF185122. 1	
<i>Halichoeres hartzfeldii</i>	AY279600	AY850873	JQ842153.1		AY591375	
<i>Halichoeres hortulanus</i>	AJ810133	AY850886	AY850748	AY279909		
<i>Halichoeres iridis</i>			JQ839472.1	AY279910	KC187972. 1	
<i>Halichoeres lapillus</i>	DQ164143	DQ164178	JF493597.1			KC830923. 1
<i>Halichoeres leucoxanthus</i>	DQ164144	DQ164179	DQ164160			
<i>Halichoeres leucurus</i>	AY850848	AY850911	DQ164161			
<i>Halichoeres maculipinna</i>	AY850811	AY850874	AY850786			
			AY850749		AY591354	

<i>Halichoeres margaritaceus</i>	AJ810134	AY850921	AY850796		AY279911		JX189112. 1
<i>Halichoeres marginatus</i>	AJ810135	AY850906	AY850780	JF458147.1	AY279912		
<i>Halichoeres melanurus</i>	AY850844	AY850907	AY850782	AY208614. 1		AY208617. 1	
<i>Halichoeres melasmapomus</i>	AY850850	AY850913	AY850788				
<i>Halichoeres miniatus</i>	AY279604	AY850920	AY850795		AY279913		
<i>Halichoeres nebulosus</i>	AY850859	AY850922	AY850797				
<i>Halichoeres nicholsi</i>	AY279605	AY850879	AY850754	EF185125. 1	AY279914		
<i>Halichoeres nigrescens</i>	AY850854	AY850917	AY850792				
<i>Halichoeres notospilus</i>	AY279606	AY850884	AY850759		AY279915		
<i>Halichoeres ornatus</i>	AY850851	AY850914	AY850789				
<i>Halichoeres papilionaceus</i>	AY279609	AY850909	AY850784		AY279918		
<i>Halichoeres pictus</i>	AY850815	AY850878	AY850753	EF185123. 1			
<i>Halichoeres podostigma</i>	AY850856	AY850919	AY850794				
<i>Halichoeres poeyi</i>	AY850820	AY850883	AY850758	AY823581			
<i>Halichoeres prosopion</i>	AY850838	AY850901	AY850776				
<i>Halichoeres radiatus</i>	AY279607	AY850881	AY850756	AY823575	AY279916		
<i>Halichoeres richmondi</i>	AY850849	AY850912	AY850787				
<i>Halichoeres scapularis</i>	AY279608	AY850887	AY850762	JF458148.1	AY279917		
<i>Halichoeres semicinctus</i>	AY850822	AY850885	KF929956. 1	AY328859			

<i>Halichoeres socialis</i>	AY850814	AY850877	AY850752	EF185120. 1			
<i>Halichoeres solorensis</i>	AY279610	AY850904	AY850779		AY279919		
<i>Halichoeres tenuispinis</i>	AB121236		HM180599. 1				
<i>Halichoeres trimaculatus</i>	AY850825	AY850888	AY850763				
<i>Hemigymnus fasciatus</i>	AJ810136	JF457502.1	JF435016.1	JF458151.1			
<i>Hemigymnus melapterus</i>	AY279611	DQ076707	JF435018.1	JF458154.1	AY279920. 1		
<i>Heteroscarus acroptilus</i>	AY279658	AY279761			AY279967		
<i>Hipposcarus longiceps</i>	EU601189	AY081093	KF929973. 1	AY081128	EU601318		
<i>Hologymnosus annulatus</i>	AY850834	JF457522.1	AY850772	JF458174.1			
<i>Hologymnosus doliatus</i>	AY279612	AY279715. 1	AY850771		AY279921		
<i>Iniistius aneitensis</i>	AY279654	AY279757			AY279963		
<i>Iniistius pavo</i>			JQ839541.1				
<i>Iniistius verrens</i>		JN211472. 1	JN242508.1				
<i>Labrichthys unilineatus</i>	AY279613	AY279716. 1	AY850750		AY279922	JX189886. 1	JX189113. 1
<i>Labroides bicolor</i>	AY279614	AY279717	JF435039.1		AY279923		
<i>Labroides dimidiatus</i>	AJ810139	AY279718	JQ431878.1	JF458175.1	AY279924		KC830919. 1
<i>Labroides pectoralis</i>			JQ839545.1				
<i>Labroides phithiophagus</i>			DQ521031. 1				
<i>Labroides rubrolabiatus</i>	AY279616	AY279719			AY279925		

<i>Labropsis australis</i>	AY279617	AY279720			AY279926	JX189887. 1	JX189114. 1
<i>Labropsis polynesiaca</i>		JF457531.1	JF435045.1				
<i>Labrus bergylta</i>	AF414201	AF517591	GQ341593. 1	EF427569. 1		EF0956669. 1	
<i>Labrus merula</i>	AJ810141	AF517592	GQ341595. 1	HM049949. 1			
<i>Labrus mixtus</i>		KJ128799. 1	JN231253.1	EU492296. 1			
<i>Labrus viridis</i>	AJ810142	AF517593	GQ341596. 1				
<i>Lachnolaimus maximus</i>	EU601225	AY279721. 1	JQ841241.1	EU601404	AY279927	FJ616724.1	KC830858. 1
<i>Lappanella fasciata</i>		AF517589	GQ341597. 1				
<i>Larabicus quadrilineatus</i>	AY279619	AY279722			AY279928		
<i>Leptojulius cyanopleura</i>	AY279620	AY850872	AY850747		AY279929		
<i>Leptoscarus vaigiensis</i>	EU601190	AY081094	FJ583627.1	AY081129	EU601319		
<i>Macropharyngodon bipartitus</i>	DQ164130	DQ164165	DQ164148				
<i>Macropharyngodon choati</i>	AY850836	DQ164166. 1	AY850774				
<i>Macropharyngodon cyanoguttatus</i>	DQ164132	DQ164167	DQ164150				
<i>Macropharyngodon geoffroy</i>	AY279621	DQ164168	DQ164151		AY279930		
<i>Macropharyngodon kuiteri</i>	DQ164134	DQ164169	DQ164152				

<i>Macropharyngodon meleagris</i>	AY279622	DQ164170. 1	AY850775	AY279931		
<i>Macropharyngodon negrosensis</i>	AY850835	DQ164171. 1	AY850773			
<i>Macropharyngodon ornatus</i>	DQ164137	DQ164172	DQ164155			
<i>Malapterus reticulatus</i>	AY279623	AY279726		AY279932		
<i>Neodax balteatus</i>	AY279657	AY279760		AY279966		
<i>Nicholsina denticulata</i>	U95761	U95762	JQ839551.1			
<i>Nicholsina usta</i>	EU601191	AY279727	GU224565. 1	AY279933		
<i>Notolabrus fucicola</i>		EU848435. 1				
<i>Notolabrus gymmogenis</i>	AY279625	AY279728	EF609418. 1	AY279934		
<i>Notolabrus parilus</i>	AB121240					
<i>Notolabrus tetricus</i>	AJ810143	EU848468. 1	EF609419. 1			
<i>Novaculichthys taeniourus</i>	AY279627	AY279730	KF930197. 1	AY279936		KC830913. 1
<i>Novaculoides macrolepidotus</i>	AY279626	AY279729	JQ839559.1	AY279935		
<i>Odax cyanoallix</i>	AY279659	AY279762		AY279968		
<i>Odax pullus</i>	AY279661	AY279764		AY279970		
<i>Olisthops cyanomelas</i>	AY279660	AY279763		AY279969		
<i>Ophthalmolepis lineolata</i>	AY279628	AY279731	JQ839560.1	AY279937		
<i>Oxycheilinus bimaculatus</i>	AY279629	AY279732	KF930214. 1	AY279938		

<i>Oxycheilinus celebicus</i>	AY279630	AY279733				AY279939	JX189888. 1	
<i>Oxycheilinus digramma</i>	EU601221	EU601258	KF930215. 1	EU601400	EU601400	EU885922		KC830912. 1
<i>Oxycheilinus unifasciatus</i>	AY279631	AY279734	KF930216. 1	JF458189.1	JF458189.1	AY279940		
<i>Oxyjulis californica</i>	AY279632	AY279735	JN582151.1	DQ132499. 1	DQ132499. 1	AY279941	JX189889. 1	JX189117. 1
<i>Paracheilinus angulatus</i>			KF709104. 1					
<i>Paracheilinus carpenteri</i>			FJ583815.1					
<i>Paracheilinus cyaneus</i>			KF709108. 1					
<i>Paracheilinus filamentosus</i>			KF709110. 1					
<i>Paracheilinus flavianalis</i>			KF709105. 1					
<i>Paracheilinus hemitaeniatus</i>			KF489688. 1					
<i>Paracheilinus mccoskeri</i>			KF709099. 1					
<i>Paracheilinus walton</i>			KF709097. 1					
<i>Parajulis poecilepterus</i>			HM180755. 1					
<i>Pictilabrus laticlavus</i>	AJ810144	AY279736				AY279942		
<i>Polyplepion russelli</i>		JF457577.1	JF435093.1					
<i>Pseudocheilinus evanidus</i>		JF457623.1	KF930329. 1					

<i>Pseudocheilinus hexataenia</i>		JF457625.1	KF930330.1				KC830898.1
<i>Pseudocheilinus ocellatus</i>		JF457626.1	JF435142.1				
<i>Pseudocheilinus octotaenia</i>	AY279634	AY279737	JQ432062.1			AY279943	
<i>Pseudocheilinus tetrataenia</i>		JF457631.1	FJ583975.1				
<i>Pseudocoris aurantiofasciata</i>		JF457632.1	JF435148.1				
<i>Pseudocoris bleekeri</i>			FJ583992.1				
<i>Pseudocoris heteroptera</i>	AY850827	AY850890	AY850765				
<i>Pseudocoris yamashiroi</i>	AY279635	AY279738.1	AY850766			AY279944	
<i>Pseudodax moluccanus</i>	EU601227	EU601262	JF435149.1	AY081133		AY279945	
<i>Pseudojuloides atavai</i>	AY279637	AY279740	JQ839569.1			AY279946	
<i>Pseudojuloides cerasinus</i>	AY279638	AY279741	KF489719.1			AY279947	
<i>Pseudojuloides severnsi</i>			JQ839574.1				
<i>Pseudolabrus biserialis</i>	AB121242	AB029288.1					
<i>Pseudolabrus eoethinus</i>	AB121243	AB029276.1					
<i>Pseudolabrus fuentesi</i>	AB121244						
<i>Pseudolabrus gayi</i>	AY279639	AY279742				AY279948	
<i>Pseudolabrus guentheri</i>	AB121245	AB029286.1					
<i>Pseudolabrus miles</i>	AB121246	AB029287.1					

<i>Pseudolabrus sieboldi</i>	AB121247	AB029285. 1	HM180806. 1				
<i>Pteragogus amboinensis</i>	AY279640	AY279743			AY279949		
<i>Pteragogus cryptus</i>	AY279641	AF517579	JQ839575.1		AY279950		
<i>Sagittalarva inornata</i>	JX684105. 1	JX684106. 1	JX034559.1		JX684103. 1		
<i>Scarus atipinnis</i>	EU601192	JX026473. 1	JQ432095.1	EU601371	EU601321		
<i>Scarus chameleon</i>	EU601193	JX026475. 1	FJ237917.1	EU601372	EU601322		
<i>Scarus coelestinus</i>	EU601194	AY081084		AY081119	EU601323		
<i>Scarus dimidiatus</i>	EU601195	AY279745		EU601374	AY279951		
<i>Scarus festivus</i>	EU601196	JX026483. 1		EU601375	EU601325		
<i>Scarus flavivectoralis</i>	EU601197	AY081086		AY081121	EU601326		
<i>Scarus forsteni</i>	EU601198		JQ432097.1	EU601377	EU601327		
<i>Scarus frenatus</i>	EU601199	AY279746	FJ237920.1	AY081122	AY279952		
<i>Scarus ghobban</i>	EU601200	EU601241. 1	EF609452	EU601379	EU601329		KC830907. 1
<i>Scarus globiceps</i>	EU601201	JX026492. 1	JQ432103.1	EU601380	EU601330	KF141352. 1	
<i>Scarus guacamaia</i>	EU601202	EU601243	JQ843039.1	AY081120	EU601331		
<i>Scarus hypselopterus</i>	EU601204	EU601245		EU601383	EU601333		
<i>Scarus iseri</i>	EU601203	EU601244	JQ841788.1	EU601382	EU601332		
<i>Scarus niger</i>	EU601205	EU601246	KF930375. 1	EU601384	EU601334	KF141353. 1	KC830905. 1
<i>Scarus oviceps</i>	EU601206	EU601247	JQ432106.1	EU601385	EU601335		
<i>Scarus prasiognathos</i>	EU601207	EU601248		EU601386	EU601336		

<i>Scarus psittacus</i>	EU601208	EU601249	JQ432113.1	EU601387	EU601337	EF095675.1	
<i>Scarus quoyi</i>	EU601210	EU601251	KF930376.1	EU601389	EU601339		
<i>Scarus rivulatus</i>	EU601211	EU601252		EU601390	EU601340		
<i>Scarus rubroviolaceus</i>	EU601212	EU601253	KF930377.1	EU601391	EU601341		KC830908.1
<i>Scarus schlegeli</i>	EU601213	EU601254	JQ432114.1	EU601392	EU601342		
<i>Scarus spinus</i>	EU601214	EU601255		EU601393	EU601343		
<i>Scarus taeniopterus</i>	EU601215	EU601256	JQ842302.1	EU601394	EU601344		
<i>Scarus tricolor</i>	EU601216	EU601257	JQ350335.1	EU601395	EU601345		
<i>Semicossyphus pulcher</i>	EU601226	AY920487	JQ934980.1	EU601405	AY279953	FJ616726.1	
<i>Siphonognathus argyrophanes</i>	AY279662	AY279765			AY279971		
<i>Sparisoma amplum</i>				DQ457024			
<i>Sparisoma atomarium</i>	U95767	U95768	JQ840705.1	DQ457029			
<i>Sparisoma aurofrenatum</i>	EU601217	AY081082	KF930448.1	EU601396	EU601346		
<i>Sparisoma axillare</i>	KC526954.1	KC526953.1		DQ457034			
<i>Sparisoma chrysopteron</i>	EU601218	AY279748	JQ839587.1	EU601397	AY279954	DQ457048.1	
<i>Sparisoma cretense</i>	U95777	AF517578	KC501552.1	DQ457026			
<i>Sparisoma frondosum</i>	JX645341.1	JX645342.1		DQ457032			
<i>Sparisoma radians</i>	U95771	U95772	JQ839591.1	DQ457028			

<i>Sparisoma rubripinne</i>	AF114483	U95774	JQ839592.1	EF456024		DQ457050. 1	
<i>Sparisoma strigatum</i>				DQ457027			
<i>Sparisoma tuiupiranga</i>				DQ457030			
<i>Sparisoma viride</i>	EU601219	AY081081	KF930449. 1	EU601398	EU601348	DQ457042. 1	
<i>Stethojulis albobittata</i>	AJ810145	JF457660.1	HQ561472. 1	JF458271.1			
<i>Stethojulis balteata</i>	DQ164146	DQ164181	DQ164163				KC830914. 1
<i>Stethojulis bandanensis</i>	AJ810146	JF457661.1	AY850744		AY279955		
<i>Stethojulis interrupta</i>			JQ839604.1				
<i>Stethojulis strigiventer</i>		JF457663.1	JQ839607.1	JF458274.1			KC830915. 1
<i>Stethojulis trilineata</i>	AY279647	AY279750. 1	AY850743		AY279956		
<i>Suezichthys gracilis</i>	AB121238						
<i>Symphodus bailloni</i>	AY092052	AY092037	GQ341601. 1				
<i>Symphodus cinereus</i>	AJ810147	AY092036	GQ341603. 1				
<i>Symphodus doderleini</i>		AF517602	GQ341606. 1				
<i>Symphodus mediterraneus</i>	AJ810148	AF517601	GQ341607. 1				
<i>Symphodus melanocercus</i>	AJ810149	AF517595	GQ341600. 1				
<i>Symphodus melops</i>	AY092049	AY092038	GQ341604. 1				

<i>Symphodus ocellatus</i>	AJ810150	AF517603						
<i>Symphodus roissali</i>	AJ810151	AY092039	GQ341605. 1					
<i>Symphodus rostratus</i>	AF414198	AY092040	GQ341608. 1					
<i>Symphodus tinca</i>	AJ810152	AF517596	GQ341602. 1					
<i>Tautoga onitis</i>	AY279648	AF517588	JN313932.1	EU601402	AY279957	JX189891. 1	JX189119. 1	
<i>Tautogolabrus adspersus</i>	AY279649	AF517585	KF930497. 1		AY279958	JX189892. 1		
<i>Thalassoma amblycephalum</i>		AY328987	KJ968295.1	AY328860			KC830917. 1	
<i>Thalassoma ascensionis</i>		AY328988		AY328861				
<i>Thalassoma ballieui</i>		AY328989	DQ521017. 1	AY328862				
<i>Thalassoma bifasciatum</i>	AJ810153	AY279753	FJ584173.1	AY328863	AY279959			
<i>Thalassoma cupido</i>		AY328991	JX034560.1	AY328864				
<i>Thalassoma duperrey</i>		AY328994	DQ443874	AY328865				
<i>Thalassoma genivittatum</i>		AY328992	DQ443875	AY328866				
<i>Thalassoma grammaticum</i>		AY328993	JQ839619.1	AY328867				
<i>Thalassoma hardwicke</i>	AY850802	AY850865	DQ443843	AY328868				
<i>Thalassoma hebraicum</i>		AY328996	JF435198.1	AY328869				
<i>Thalassoma janssenii</i>		AY328997	DQ443872. 1	AY328870				
<i>Thalassoma loxum</i>		AY328998		AY328871				
<i>Thalassoma lucasanum</i>		AY328999	JQ839621.1	AY328872				

<i>Thalassoma lunare</i>	AJ810154	AY850862	DQ443879	AY328873	AY279960	KC830918. 1
<i>Thalassoma lutescens</i>	AY850800	JF457688.1	DQ443877	AY328874		
<i>Thalassoma newtoni</i>		AY329002		AY328875		
<i>Thalassoma noronhanum</i>		AY329003	JQ839625.1	AY328876		
<i>Thalassoma pavo</i>		AF517583	GQ341611. 1	DQ198011		
<i>Thalassoma purpureum</i>		AY329005	JF435205.1	AY328878		
<i>Thalassoma quinquevittatum</i>	AY850801	JF457694.1	DQ443855	AY328879		KC830916. 1
<i>Thalassoma robertsoni</i>		AY329007	JQ839642.1	AY328880		
<i>Thalassoma rueppellii</i>		AY329008		AY328881		
<i>Thalassoma sanctaehelenae</i>		AY329009		AY328882		
<i>Thalassoma septemfasciata</i>		AY329010		AY328883		
<i>Thalassoma trilobatum</i>		AY329011	JQ839648.1	AY328884		
<i>Thalassoma virens</i>		AY329012	JQ839654.1	AY328885		
<i>Wetmorella albofasciata</i>			JQ432219.1			
<i>Wetmorella nigropinnata</i>	AY279652	AY279755	JF435214.1	JF458288.1	AY279961	KC830909. 1
<i>Xiphocheilus typus</i>	AY279653	AY279756			AY279962	
<i>Xyrichtys martinicensis</i>	AY279655	AY279758	GU225065. 1		AY279964	JX189121. 1
<i>Xyrichtys mundiceps</i>			JQ839662.1			
<i>Xyrichtys novacula</i>	KJ433962. 1	KJ433965. 1	GU225070. 1	EF439246		

<i>Xyrichtys splendens</i>					GU225071.1 1	U92004.1		
----------------------------	--	--	--	--	-----------------	----------	--	--

Table S2.4: GenBank Accession IDs of sequences used in this study for 20 species set as outgroup to the labrids

Name	12S	16S	COI	CYTB	RAG2	RAG1	ZIC1
<i>Abudefduf saxatilis</i>	AY279570	AY279673	AY662765	AY208553	AY27987 9		JX189122. 1
<i>Abudefduf vaigiensis</i>	AB121234	KF925346. 1	KF434769. 1	JF457889.1			
<i>Amblyglyphidodon leucogaster</i>	AY279568	AY279671	AY662764	AY208565	AY27987 7		
<i>Amphistichus argenteus</i>	AY279571	JN125228. 1	JX487273. 1	AF159327	AY27988 0		
<i>Dascyllus trimaculatus</i>	AY279569	AY279672	JQ431680. 1	AY208545	AY27987 8		
<i>Diagramma picta</i>	AY279563	AY279666	GU207326. 1	HQ676699. 1	AY27987 2	HQ676637. 1	
<i>Embiotoca jacksoni</i>	AY279573	AY279676	AY662763	AF159331	AY27988 2		JX189100. 1
<i>Epinephelus polyphekadion</i>	AY279560	AY279663		EF213716	AY27986 9		
<i>Etroplus maculatus</i>	AY279565	AY279668	DQ119221	AF370625	AY27987 4		
<i>Geophagus steindachneri</i>		DQ119188	DQ119217	AF370660	AY56673 0		
<i>Kyphosus vaigiensis</i>	AY279561	AY279664	JQ431874. 1		AY27987 0		

<i>Lepomis macrochirus</i>	AF150004. 1	AY742530	KF930037. 1	AY115975		AY430227. 1	
<i>Micropterus salmoides</i>	KM273840. 1	AY742550	KF930133. 1	AY116000		GU368833. 1	JQ353131. 1
<i>Perca flavescens</i>	JN655527.1	AY520099	AY662755	AF045357			GU368821. 1
<i>Percina maculata</i>	AY372801	AY520098	EU524259. 1	AF045353			
<i>Platax orbicularis</i>	AY279562	AY279665	KF930266. 1	FJ167721.1	AY27987 1		EF533903. 1
<i>Ptychochromis oligacanthus</i>	AY279564	AY279667	AY263873	AF370630	AY27987 3		
<i>Rhacochilus vacca</i>	AY279572	EF119281	KF930353. 1	AF159330	AY27988 1		JX189099. 1
<i>Thorichthys meeki</i>	AY279566	AY279669	EU751976. 1	U88860	AY27987 5		
<i>Variola louti</i>		DQ532981	DQ107957	AY786428			

Table S2.5: GenBank Accession IDs of sequences used in this study for 5 species set as outgroup to the gobiids and labrids

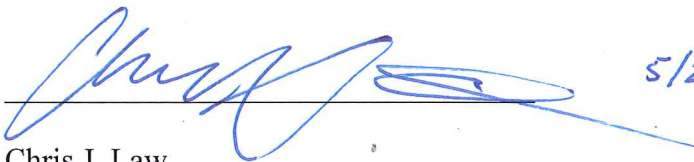
Name	12S	16S	COI	CYTB	RAG2	RAG1	ZIC1
<i>Pristiapogeton kallopterus</i>	AB206133 .1	AB206133. 1	KF489710. 1	KM455430 .1		KT266395. 1	KT266502. 1
<i>Phaeoptyx pigmentaria</i>	AB889662 .1	AB889662. 1	AB890090 .1			AB893442 .1	KC831144 .1
<i>Upeneus moluccensis</i>	FJ008156. 1	AF227681. 1	KC501834 .1	FJ008145.1		EU167747. 1	KC831119 .1
<i>Mullus surmuletus</i>	FJ008154. 1	FN688087. 1	FN688957. 1	FN688383. 1		EF095658. 1	
<i>Opsanus pardus</i>	AF165327. 1	DQ874745 .1	AF165337. 1	AF165347. 1	DQ874790 .1	JX190866. 1	

A.2 Permission for Published Material

The text of this dissertation includes portions of the following previously published material:

Baliga VB and Law CJ. 2016. Cleaners among wrasses: Phylogenetics and evolutionary patterns of cleaning behavior within Labridae. *Molecular Phylogenetics and Evolution*. 94A, 424-435.

The co-author listed in this publication, Chris J. Law, hereby provides permission to Vikram B. Baliga to use portions of the publication within the present dissertation.


Chris J. Law

5/23/16